



2008

A NOVEL CLASS OF IMMUNOPROTEASOME CATALYTIC SUBUNIT LMP2 INHIBITOR AND ITS THERAPEUTIC POTENTIALS IN CANCER

Yik Khuan (Abby) Ho
University of Kentucky

[Click here to let us know how access to this document benefits you.](#)

Recommended Citation

Ho, Yik Khuan (Abby), "A NOVEL CLASS OF IMMUNOPROTEASOME CATALYTIC SUBUNIT LMP2 INHIBITOR AND ITS THERAPEUTIC POTENTIALS IN CANCER" (2008). *University of Kentucky Doctoral Dissertations*. 686.
https://uknowledge.uky.edu/gradschool_diss/686

This Dissertation is brought to you for free and open access by the Graduate School at UKnowledge. It has been accepted for inclusion in University of Kentucky Doctoral Dissertations by an authorized administrator of UKnowledge. For more information, please contact UKnowledge@lsv.uky.edu.

ABSTRACT OF DISSERTATION

Yik Khuan (Abby) Ho

The Graduate School
University of Kentucky
2008

A NOVEL CLASS OF IMMUNOPROTEASOME CATALYTIC SUBUNIT LMP2
INHIBITOR AND ITS THERAPEUTIC POTENTIALS IN CANCER

ABSTRACT OF DISSERTATION

A dissertation submitted in partial fulfillment of the
requirements for the degree of the Doctor of Philosophy in the
College of Pharmacy
at the University of Kentucky

By

Yik Khuan (Abby) Ho

Lexington, Kentucky

Director: Dr. Kyung-Bo Kim, Associate Professor of Pharmaceutical Sciences
Lexington, Kentucky
2008

Copyright © Yik Khuan (Abby) Ho 2008

ABSTRACT OF DISSERTATION

A NOVEL CLASS OF IMMUNOPROTEASOME CATALYTIC SUBUNIT LMP2 INHIBITOR AND ITS THERAPEUTIC POTENTIALS IN CANCER

The immunoproteasome, known to play an important role in MHC class I antigen processing and presentation, have been linked to neurodegenerative diseases and hematological cancers. However, the pathophysiological functions of the immunoproteasome in these diseases are still not very well established. This can be attributed mainly to the lack of appropriate molecular probes that selectively target the immunoproteasome catalytic subunits. Herein, we report the development of a small molecular inhibitor (**AM**) that selectively targets the major catalytic subunit, LMP2, of the immunoproteasome. We show that the compound covalently modifies the LMP2 subunit with high specificity in human prostate cancer cell. **AM** was also shown to selectively inhibit the chymotrypsin-like activity of LMP2 subunit. More importantly, the anti-proliferative activity of **AM** is more pronounced in prostate cancer cells that highly express LMP2 without inducing toxicity in normal cells. These results implicate an important role of LMP2 in regulating cell growth of malignant tumors that highly express LMP2.

Subsequently, the modes of action of **AM** were investigated. Prostate cancer cells that highly express LMP were shown to induce G2/M cell cycle arrest and apoptosis via PARP cleavage when treated with the compound. Similar to epoxomicin, the treatment of **AM** induced the accumulation of poly-ubiquitination in prostate cancer cells, which indicates the inhibition of proteolysis. However, unlike epoxomicin, the treatment of **AM** did not appear to inhibit the activation of inflammation. In conclusion, these results suggest that the LMP2 inhibitor, **AM**, may induce cytotoxicity prostate cancer cells that highly express LMP2 catalytic subunit in similar modes of action as epoxomicin but it does not involve the inflammatory pathway.

KEYWORDS: immunoproteasome inhibitor, LMP2 catalytic subunit inhibitor, anti-tumor, apoptotic, prostate cancer

Yik Khuan (Abby) Ho

December 1st 2008

A NOVEL CLASS OF IMMUNOPROTEASOME CATALYTIC SUBUNIT LMP2
INHIBITOR AND ITS THERAPEUTIC POTENTIALS IN CANCER

By

Yik Khuan (Abby) Ho

Dr. Kyung-Bo Kim
Director of Dissertation

Dr. Janice Buss
Director of Graduate Studies

January 21, 2009
Date

DISSERTATION

Yik Khuan (Abby) Ho

The Graduate School
University of Kentucky
2008

A NOVEL CLASS OF IMMUNOPROTEASOME CATALYTIC SUBUNIT LMP2
INHIBITOR AND ITS THERAPEUTIC POTENTIALS IN CANCER

DISSERTATION

A dissertation submitted in partial fulfillment of the
requirements for the degree of the Doctor of Philosophy in the
College of Pharmacy
at the University of Kentucky

By

Yik Khuan (Abby) Ho

Lexington, Kentucky

Director: Dr. Kyung-Bo Kim, Associate Professor of Pharmaceutical Sciences
Lexington, Kentucky
2008

Copyright © Yik Khuan (Abby) Ho 2008

ACKNOWLEDGEMENTS

This dissertation would not have been possible without the guidance and support of several people. Thus I would like to take the opportunity to acknowledge those who have helped me tremendously in this journey. First and foremost, my long time mentor, Dr. Kyung Bo Kim who has provided me with tremendous inspiration, motivation, advice, assistance, patience and kindness throughout the years of my scientific career. While Dr. Royce Mohan was not a member of my committee, he has also played the role of a mentor. He has continuously provided me with much insight as well as guidance. Secondly, my committee members who have challenged me to become a better scientist during our meetings: Dr. Val Adams, Dr. Peter Crooks, and Dr. Hollie Swanson. I would also like to thank Dr. Daniel Noonan who served as an outside examiner on the defense of my dissertation.

I am also exceptionally fortunate to have worked with an extremely supportive group of colleagues, including Kedra Cyrus, Hyosung Lee, Marie Wehenkel, Sung Hee Park, Yang Eon Kim, and Hyeong Jun Han. I thank you all for your friendship, motivation, assistance and encouragement.

Finally, my parents, brother and husband have all been extremely patient, supportive, loving and caring during my graduate work and dissertation writing. I am truly grateful and blessed to have all of them there for me when I needed them.

TABLE OF CONTENTS

Acknowledgements.....	iii
List of Tables.....	vi
List of Figures.....	vii
List of Schemes.....	viii
Chapter One: Background To Research	
A. Ubiquitin Proteasome Pathway	
1. Introduction.....	1
2. Ubiquitin and Ubiquitin Related Enzymes.....	3
3. Proteasomes.....	10
4. Physiological Disorders	22
B. Proteasome Inhibitors	
1. Active Site-Directed Proteasome Inhibitors.....	26
2. Non Active Site-Directed Proteasome Inhibitors.....	37
3. Immunoproteasome Specific Inhibitors.....	40
4. Activity-Based Proteasome Probes.....	42
5. Conclusions.....	44
C. Hypothesis and Specific Aims.....	45
Chapter Two: Synthesis and Evaluation of Dihydroeponemycin Analogs	
A. Introduction.....	47
B. Development of Novel Synthetic Strategy.....	49
C. Synthesis of Dihydroeponemycin Analogs.....	53
D. Synthesis of Biotin Probes.....	60
E. Screening of Dihydroeponemycin Analogs.....	62
F. Conclusions.....	66
G. Methods and Materials.....	67
Chapter Three: Lead Optimization and Evaluation	
A. Introduction.....	78
B. Optimization of Lead Compound.....	79
C. Screening of the Second Generation of Dihydroeponemycin Analogs.....	80
D. Conclusions.....	82
E. Methods and Materials.....	84
Chapter Four: Biological Studies of analog AM in Human Cancer Cells	
A. Introduction.....	89

B. LMP2/LMP7 Subunit Profiling in Human Cancers.....	90
C. Characterization of Subunit Binding Specificity of AM in Human Prostate Cancer Cells.....	92
D. Selective Inhibition of Proteolytic Activity and Cytotoxicity of AM	99
E. Modes of Action of AM	104
F. Conclusions.....	113
G. Future Directions.....	116
H. Methods and Materials.....	117
References.....	121
Vita.....	137

LIST OF TABLES

Table 1: MTS Assay.....	102
-------------------------	-----

LIST OF FIGURES

Figure 1.1: The ubiquitin proteasome pathway.....	2
Figure 1.2: The proposed proteolytic mechanism of the proteasome.....	14
Figure 1.3: The formation of immunoproteasome.....	18
Figure 1.4: The assembly of the 20S proteasome.....	21
Figure 1.5: The Peptide aldehyde proteasome inhibitors.....	28
Figure 1.6: The vinyl sulfone proteasome inhibitors.....	29
Figure 1.7: The boronic acid proteasome inhibitors.....	30
Figure 1.8: The β -lactone proteasome inhibitors.....	31
Figure 1.9: The epoxyketone proteasome inhibitors.....	32
Figure 1.10: The macrocyclic proteasome inhibitors.....	33
Figure 1.11: Traditional Remedy.....	34
Figure 1.12: Subunit specific proteasome inhibitors.....	36
Figure 1.13: Non active site proteasome inhibitors I.....	38
Figure 1.14: Non active site proteasome inhibitors II.....	39
Figure 1.15: Immunoproteasome inhibitors.....	41
Figure 1.16: Proteasome inhibitors with fluorescent probes.....	43
Figure 2.1: Dihydroeponemycin.....	47
Figure 2.2: The first small library of dihydroeponemycin analogs.....	59
Figure 2.3: Competition Assay.....	63
Figure 2.4: Screening of dihydroeponemycin analogs using competition assay.....	64
Figure 2.5: Competition assay using different biotin-tagged probe.....	65
Figure 3.1: The second generation of dihydroeponemycin analogs.....	79
Figure 3.2: The screening of the second generation of dihydroeponemycin analogs.....	80
Figure 3.3: The mobility shift assay.....	81
Figure 4.1: Differential expression levels of LMP2/LMP7.....	91
Figure 4.2: Selective modification of LMP2 in PC3 cells.....	94
Figure 4.3: Characterization of AM -LMP2 binding properties.....	96
Figure 4.4: Thin layer chromatography analysis.....	97
Figure 4.5: Kinetic studies and 3D endothelial cell sprouting assay.....	100
Figure 4.6: Cell cycle analysis.....	105
Figure 4.7: Apoptosis analysis.....	106
Figure 4.8: Apoptosis analysis on a molecular level.....	107
Figure 4.9: Inhibition of poly-ubiquitination.....	109
Figure 4.10: The effect of AM on NF κ B activation.....	112

LIST OF SCHEMES

Scheme 2.1: The conventional synthetic scheme of dihydroeponemycin.....	49
Scheme 2.2: The improved synthetic strategy.....	51
Scheme 2.3: The mechanistic rationale of the improved synthetic strategy.....	52
Scheme 2.4: Synthesis of the left hand fragment of dihydroeponemycin analogs.....	54
Scheme 2.5: Modification of intermediate 3	56
Scheme 2.6: The final coupling of dihydroeponemycin analogs.....	57
Scheme 2.7: The synthetic scheme of biotin-dihydroeponemycin.....	60
Scheme 2.8: The synthetic scheme of biotin-epoxomicin.....	61

LIST OF ABBREVIATIONS

FDA	Food and Drug Administration
G76	Glycine 76
K48	Lysine 48
Ublp	Ubiquitin-like proteins
SCF complex	Skp, Cullin, F-box containing complex
ATP	Adenosine Triphosphate
AMP	Adenosine Monophosphate
E1	Ubiquitin Activating Enzyme
E2	Ubiquitin Conjugating Enzyme
E3	Ubiquitin Ligating Enzyme
DUB	Deubiquitinating Enzymes
HECT	Homologous to E6-AP Carboxyl Terminus
RING	Really Interesting New Gene
PHD	Plant Homeo-Domain
HPV	Human Papilloma Virus
UCH	Ubiquitin C-terminal Hydrolase
USP	Ubiquitin-Specific Proteases
OTU	Ovarian Tumor Proteases
MJD	Machado-Joseph Disease Proteases
CT-L	Chymotrypsin-like
C-L	Caspase-like
T-L	Trypsin-like
MHC	Major Histocompatibility Complex
Ntn	N-terminal nucleophilic
BrAAP	Branched-chain Amino Acid Preferring
SNAAP	Small Neutral Amino Acid Preferring
NUK	Nucleophilic Water Molecules
ER	Endoplasmic Reticulum
GRR	Glycine Rich Region
ODC	Ornithine Decarboxylase
LMP2	Low-molecular Mass Polypeptide 2
LMP7	Low-molecular Mass Polypeptide 7
MECL-1	Multicatalytic Endopeptidase Complex
IFN- γ	Interferon- γ
TNF- α	Tumor Necrosis Factor- α
POMP	Proteassemblin or hUmp1, homolog of yeast Ump1
VHL	Von Hippel-Lindau
HIF	Hypoxia-Inducible Transcription Factor
VEGF	Vascular Endothelial Growth Factor
Cdk	Cyclin-Dependent Kinase
APC	Adenomatous Polyposis Coli
AD	Alzheimer's Disease
HD	Huntington's Disease
TCR	T Cell Receptors

LIST OF ABBREVIATIONS

Thr1O ^γ	Hydroxyl side chain of the N-terminus threonine of proteasome
EGCG	Epigallocatechin-3-gallate
RIP-1	Regulatory Particle Inhibitor Peptoid-1
DMF	Dimethylformamide
BuLi	<i>n</i> -Butyllithium
TBDMSCl	<i>tert</i> -Butyl Dimethylchlorosilane
TLC	Thin Layer Chromatography
HBTU	O-Benzotriazole-N,N,N',N'-tetramethyluronium Hexafluorophosphate
HoBt	1-Hydroxybenzotriazole
CH ₂ Cl ₂	Methylene Chloride
DIPEA	N,N-Diisopropylethylamine
MeOH	Methanol
EtOAc	Ethyl Acetate
TBDPS	<i>tert</i> -Butyl Diphenylsilyl
MOM	Methoxy Methyl
MEM	Methoxyethoxy Methyl
THP	Tetrahydropyran
TFA	Trifluoroacetic Acid
NMR	nuclear magnetic resonance
HRP	Horseradish Peroxidase
THF	Tetrahydrofuran
CDCl ₃	Deuterated Chloroform
SDS-PAGE	Sodium Dodecyl Sulfate Polyacrylamide Gel Electrophoresis
PVDF	Polyvinylidene Fluoride
ECL	Enhanced Chemiluminescence
HATU	O-(7-Azabenzotriazole-1-yl)-N, N,N',N'-tetramethyluronium hexafluorophosphate
HoAt	1-Hydroxy-7-Azabenzotriazole
EDC	1-Ethyl-3-(3-dimethylaminopropyl)carbodiimide
ER	Estrogen Receptor
ATCC	American Type Culture Collection
3D-ECSA	Three Dimensional Endothelial Cell Sprouting Assay
VEGF	Vascular Endothelial Growth Factor
Epx	Epoxomicin
Epn	Dihydroepinomycin Substitute
PI	Propidium Iodide
PARP	Poly (ADP-ribose) Polymerase

CHAPTER ONE: BACKGROUND TO RESEARCH

A. Ubiquitin Proteasome Pathway

1. Introduction

The ubiquitin proteasome pathway was discovered fairly recently by Hershko, Rose and Ciechanover, whom were awarded the 2004 Nobel Prize in Chemistry, signifying the importance of this pathway. These Nobel Laureates were the pioneers in deciphering the mechanism of the ubiquitin proteasome pathway, following the discovery of ubiquitins. The ubiquitin proteasome pathway is very unique because it is a highly regulated energy-dependent protein degradation system that uses polyubiquitin chains as smoke signals to communicate with the 26S proteasome. In other words, the pathway employs an enzyme system that marks proteins destined for degradation with a chain of ubiquitins. These multi-ubiquitin-tagged proteins will then be recognized by 26S proteasome, which unfolds and degrades the proteins into smaller peptides (Figure 1.1).

Since the discovery of the ubiquitin proteasome pathway, there has been an exponential increase in the literature that demonstrates the importance of this pathway in a myriad of cellular functions such as cell cycle regulations, gene transcriptions, DNA repairs, apoptosis, signal transductions and immune responses. Consequently, the pathway has been widely recognized for its integral role in constitutive cellular functioning. Given the wide range of cellular processes that are regulated by the ubiquitin proteasome pathway, it is not surprising to find this pathway involved in the pathogenesis of a number of diseases. As a result, the ubiquitin proteasome pathway has become a valuable target for the development of therapeutic agents. The majority of the ubiquitin proteasome pathway inhibitors that are currently available directly target the proteolytic activity of the proteasome. Being the first Food and Drug Administration (FDA) approved proteasome inhibitor, bortezomib, also known as VelcadeTM, is the novel paradigm for therapeutic intervention. Not only has the number of proteasome inhibitors increased in recent years, but more sophisticated inhibitors such as catalytic subunit specific or non-catalytic subunit inhibitors have also been developed. In addition, inhibitors targeting non-proteolytic processes associated with the ubiquitin proteasome

pathway have also been reported. Consequently, the development of proteasome inhibitor for therapeutic purposes is gaining significant importance.

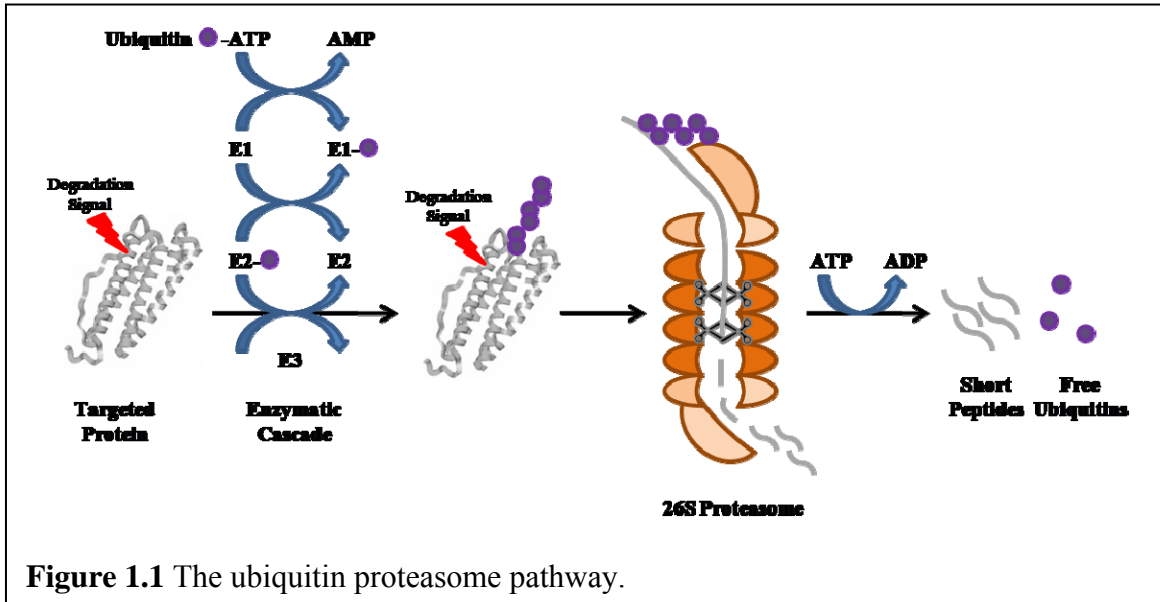


Figure 1.1 The ubiquitin proteasome pathway.

2. Ubiquitin and Ubiquitin Related Enzymes

a. Ubiquitins and Ubiquitin-Like Proteins

Ubiquitin is a 76 amino acid polypeptide that assumes a globular compact conformation with a very pronounced hydrophobic core, which confers it high thermal stability [3]. It has been shown to be evolutionary well conserved, which in turn underscores the biological importance of the ubiquitin proteasome pathway [4]. These remarkable polypeptides are usually present in the cell either as monomers or conjugated to protein substrates. Although ubiquitins lack intrinsic proteolytic activity, they have a few selective amino acid residues that serve as conjugating sites. These sites can be conjugated to another ubiquitins to form polyubiquitin chains as well as protein substrates for degradation. Specifically, glycine 76 (G76), located at the C terminus, forms conjugates with the ϵ -amino group of lysine 48 (K48) on the adjacent ubiquitin via an isopeptide bond to form polyubiquitin chain [5]. This C terminal G76 has been shown to be a crucial residue for the formation of covalent conjugates as its deletion renders ubiquitin inactive [6]. On the other hand, there are seven lysine residues within the ubiquitin where polyubiquitin chains of different topologies can form. The K48 linked polyubiquitin chain is typically associated with proteasomal degradation where as the other isopeptide linkages have been reported to participate in distinct biological processes, predominantly K6, K11, K29 and K63 linkages [5, 7]. For example, the K29 linkage can not only function as a proteolytic signal [8], but have also been shown to possibly mediate lysosomal degradation [9]. However, unlike K48 and K29, K63 linked polyubiquitin chains are believed to have non-proteolytic functions. Neurodegenerative diseases [10], DNA repair, stress response, endocytosis and translational regulations are a few among other functions that are associated to the K63 linked polyubiquitin chain [8].

In addition to the 76 amino acid ubiquitin, there are other similar proteins known as the ubiquitin-like proteins (Ublp). They undergo conjugation processes, similar to ubiquitination, which form isopeptide bonds between the C-terminal glycine and an amino group within the protein substrate [11]. Post-translational modifications by Ublp are known to induce a myriad of non-proteolytic cellular functions. Only a handful of Ublps has been identified thus far and two well known examples are Nedd8 and Sumo.

Sumo conjugation, also known as sumoylation, is involved in cellular processes such as nuclear transport, signal transduction, stress response and cell cycle regulation [12], while Nedd8 targets the cullin family proteins, which is part of the SCF complex (Skp, Cullin, F-box containing complex) involved in the ubiquitin enzymatic cascade. Neddylation plays an important role in SCF-mediated ubiquitination and proteolysis [13].

b. Ubiquitin Enzymatic Cascade

The defining characteristic of the ubiquitin proteasome pathway is the employment of a universal proteolytic signal, which is the polyubiquitin chain, to target protein substrates for degradation. This in turn allows the recognition of a wide array of substrates for degradation as the proteasome only needs to recognize this proteolytic signal and not proteins directly [14]. A well-established mechanism provides the attachment of ubiquitins to targeted proteins through the adenosine triphosphate (ATP) dependent sequential actions of three enzymes: ubiquitin activating E1, ubiquitin conjugating E2, and ubiquitin ligating E3. Briefly, the carboxyl terminal of G76 within the ubiquitin is first activated by ATP to form an ubiquitin adenylate intermediate. This activated ubiquitin is then transferred to a conserved cysteine residue on E1 to form a thiol ester linkage, with the concomitant release of adenosine monophosphate (AMP). The ubiquitin is subsequently linked to a catalytic cysteine residue on E2 via a transesterification reaction [15]. Finally, with the cooperation of the catalytic properties of E3, ubiquitin is ligated to its protein substrate by forming an isopeptide bond between the G76 of ubiquitin and the ϵ -amino group of a lysine residue within the targeted protein (Figure 1.1) [5]. This ubiquitination process is believed to reiterate itself until a chain of at least four ubiquitins are attached to the protein for efficient proteasomal degradation [14].

In addition to poly-ubiquitination, protein substrates can also be mono-ubiquitinated. This is a non-proteolytic process in the proteasome pathway as mono-ubiquitinated proteins are either activated to acquire a modulated cellular function or targeted to the lysosome for degradation. In recent years, mono-ubiquitinations have begun to emerge as regulators of the cellular distribution and activity of various proteins,

including endocytosis, histone regulation, virus budding, transcription regulation, cell signaling [16, 17], membrane trafficking [18, 19], and DNA repair [20].

c. Ubiquitin Related Enzymes

Ubiquitination is a highly selective process in large part due to the diversity of E2 conjugating enzymes and E3 ligases. Each E2 enzyme is specific to a few E3 ligases, which in turn are specific to a few protein substrates. The combination of specific E2-E3 complexes or E3 alone dictates the substrate specificity of proteasome. On the other hand, E1 activating enzymes are highly conserved. Ubiquitination of protein substrates are also negatively regulated by another class of enzymes referred to as deubiquitinating enzymes (DUB). These enzymes proofread and edit ubiquitinated proteins to prevent inappropriate degradation. This ubiquitinating enzyme hierarchy not only confers the ubiquitin proteasome pathway its high specificity but also allows it to tightly regulate the degradation of each protein in the cell.

Ubiquitin Activating Enzymes (E1)

Despite initial assumption that a single E1 ubiquitin activating enzyme (UBE1) is responsible for the activation of all ubiquitins, a novel E1 enzyme was very recently discovered by Jin *et al.* [21] and Pelzer *et al.* [22], independently. It remains to be determined whether this novel E1 enzyme is as vital as UBE1. Early proteasomal studies have shown that the deletion of the E1 enzyme in yeast is lethal [23] and subsequently, the mutation of its catalytic cysteine residue also renders it inactive in yeast [24]. In addition, a murine cell line which contained a thermolabile E1 gene failed to degrade otherwise short-lived proteins at non-permissive temperature [25, 26]. These results revealed the importance of ubiquitination in cell cycle progression and cell viability [27].

Ubiquitin Conjugating Enzyme (E2)

Compared to the ubiquitin activating enzyme, there are a greater number of E2 conjugating enzymes dedicated to ubiquitins. For example, the yeast genome encodes at least 13 ubiquitin conjugating enzymes (UBC1-13) [28] and more than 35 have been identified in the mammalian genome [29]. The reaction catalyzed by these E2 enzymes is

the first determining step of substrate specificity in the ubiquitination process. E2 enzymes commonly contain a conserved catalytic core domain of approximately 150 amino acids, known as the UBC domain [4]. Within this domain is a highly conserved catalytic cysteine residue that is essential for the formation of thiol ester conjugation with ubiquitin. Its deletion has been shown to abolish UBC activity [30]. In addition, a strictly conserved asparagine was recently demonstrated by Wu *et al.* to participate in the catalysis of isopeptide bond formation between ubiquitin and the protein substrate [31]. E2 enzymes can be categorized into two classes. The first class consists of smaller E2 enzymes that only contain the UBC domain. These E2 enzymes lack the ability to transfer ubiquitin to the substrate directly; hence they may require its cognate E3 enzyme for substrate recognition. On the other hand, the second type of E2 enzymes is larger with an extended C-terminal or N-terminal tail or both. These extensions may help mediate substrate specificity, intrinsic E2 activity, E3 interaction, and intracellular localization [32, 33].

Ubiquitin ligases E3

In addition to ubiquitin conjugating enzymes, there are an even larger number of ubiquitin E3 ligases by which the substrate specificity of ubiquitination is determined. It is estimated that the mammalian genome consists of at least a few hundred E3 ligases. This enormous diversity, in conjunction with E2 enzymes, permits the ubiquitin proteasome pathway to regulate the degradation of a myriad of protein substrates. All known E3 ligases are comprised of two separate domains, one that interacts with its cognate E2 enzyme and the other with its substrates. In spite of the countless numbers of proteins that are present in cells, each of these E3 ligases is able to recognize its cognate substrates for ubiquitination. Several modes of recognitions have been characterized and they include N-end rule, post-translational modifications in protein substrates as well as activation of E3 ligases. The N-end rule is based on the *in vivo* finding by Varshavsky that the half life of a protein is dependent on the identity of the amino acid residue at the N-terminal [34]. Nevertheless, most protein substrates utilize degradation signals to communicate with E3 ligases. These signals include post-translational modifications such as phosphorylation, oxidation and acetylation. Finally, some E3 ligases are synthesized as

inactive precursors which undergo post-translational modification or require auxiliary proteins to yield the active form when conditions permit.

Unlike E1 and E2 enzymes, E3 ligases are structurally more diverse. They can be divided into four major classes, which are characterized by their distinct domains. These domains have been identified as HECT (homologous to E6-AP carboxyl terminus), RING (really interesting new gene) finger, U-box and PHD (Plant Homeo-Domain) finger.

E6-AP was the first mammalian E3 ubiquitin protein ligase to be identified and characterized. It was found to promote the ubiquitination of p53 for proteasomal degradation in the presence of the E6 oncoprotein produced by human papilloma virus (HPV) [35]. It was later discovered that other non E3 ligase protein also share substantial homology with E6-AP at the C-terminal. This conserved domain of approximately 350 amino acids is now referred to as the HECT domain [36]. Within the HECT domain is a highly conserved cysteine residue that forms a thiol ester linkage between ubiquitin and the HECT E3 ligase. Mutation on this residue has been shown to completely abolish ubiquitination of its substrate [36]. HECT E3 ligases are truly unique because this is the only class of E3 ligase by which ubiquitin first forms a thiol ester intermediate with the conserved cysteine residue before being transferred to a lysine residue on the protein substrates. Substrate specificity is determined by the highly variable N-terminal extensions of HECT E3 ligases [37].

The next class of E3 ligase is the RING finger ligases, which is the largest class of E3 ligases. RING fingers are characterized by eight highly conserved cysteine and histidine residues that coordinate with two zinc ions to form a unique 'cross-braced' arrangement [38]. The RING E3 ligases are different from HECT E3 ligases in that they do not form a thiol ester intermediate with ubiquitin but mediate ubiquitination of substrate indirectly. The RING E3 ligases serve as a bridge to bring substrate and E2 into close proximity and position them optimally. This allows ubiquitin to be directly transferred from the E2 to the protein substrate without docking on E3. Mutation in the RING finger has been shown to result in the inability of the E3 to facilitate ubiquitination of its protein substrate [39, 40]. While the substrate binding domains are more variable, the RING finger domain is solely responsible for the recognition and binding of E2 conjugating enzymes.

The RING E3 ligases can be divided into two categories: the single subunit RING E3 ligase and the multi-subunit RING E3 ligase. The single subunit RING E3s are able to determine substrate specificity and recruit its cognate E2 enzyme without any ancillary proteins. One of the well studied examples is the oncogene Mdm2, which is responsible for ubiquitinating p53 [39, 41]. The other RING E3 ligases such as SCF and APC are more intricate as they consist of several protein subunits by which substrate specificity and E2 recruitment are individually carried out. All known multi-subunit RING E3 have a small RING finger protein and a member of the cullin protein family, among other protein subunits [42]. For example, in SCF E3 ligases, Rbx1/Roc1/Hrt1 functions as the RING finger component to which E2 enzyme binds [19]. The cullin protein family acts as the structural scaffold complex whereas F-box protein dictates substrate specificity. Lastly, Skp1 protein is the adaptor protein that links cullin to F-box protein. Within the F-box protein is a peptide motif referred to as WD40, which is mainly responsible for recognizing substrates in a phosphorylation-dependent manner [33].

The next two classes of E3 ligases, PHD and U-box proteins, are structurally similar to the RING E3 ligases as they do not form thiol ester intermediates with ubiquitin. The PHD E3 ligase is closely related to the RING finger in that it also has eight conserved zinc-ligating residues arranged in a cross-brace pattern [43]. An example of a PHD E3 ligase is the MEKK1, which has been shown to activate and ubiquitinate ERK1/2 [44]. U-box proteins do not contain the conserved zinc-chelating residues but are distantly related to RING E3 ligases in sequence [45]. The first U-box protein implicated in ubiquitination was UFD2, which was initially identified as a novel ubiquitination factor, E4 [46]. UFD2a, a mammalian homolog of yeast UFD2, has been implicated in the formation of polyubiquitin chain linkages that surprisingly do not participate in proteolysis [47]. Taken all together, the diversity of E3 ligases is truly astounding. Nature has provided us with such complexity and intricacies in order to establish extraordinary selectivity in the ubiquitin proteasome pathway; hence demonstrating the importance of protein degradation.

Deubiquitinating Enzyme (DUB)

Similar to phosphorylation, ubiquitination is reversible due to the action of deubiquitinating enzymes (DUBs). The DUBs belong to the family of cysteine proteases with the exception of metalloproteases. DUBs can be categorized into five classes based on their ubiquitin protease domains: ubiquitin C-terminal hydrolases (UCHs), ubiquitin-specific proteases (USPs), ovarian tumor proteases (OTUs), Machado-Joseph disease proteases (MJDs), and JAMM motif proteases. In addition to structural differences, each of these classes of DUBs is unique in that they exhibit substrate specificity and consequently functional differences [48]. They are responsible for processing ubiquitin precursors, proofreading and editing ubiquitin conjugates. Furthermore, the 26S proteasome itself also contains several intrinsic DUBs for removing polyubiquitin chains from protein substrates. This is to prevent the polyubiquitin chain from interfering with the entering of substrate into the catalytic core for degradation as well as inappropriate degradation of polyubiquitin chains [48]. These unanchored polyubiquitin chains will also be disassembled by DUB because its accumulation will competitively inhibit the binding of ubiquitin conjugates to the proteasome; hence, inhibiting proteasomal degradation [49]. Consequently, the recycling of ubiquitins also helps maintain ubiquitin homeostasis in cells. Like poly-ubiquitination, deubiquitination is equally as important in the ubiquitin proteasome pathway.

3. Proteasomes

The proteasome is a large multi-subunit multi-catalytic protein complex in cells that is responsible for ATP-dependent protein degradation, which is the final destination of poly-ubiquitinated protein substrates. The protein complex is structurally and functionally very well conserved in virtually all organisms from archaeobacteria to eukaryotes. They share a similar structural framework of a hollow barrel-like shape within which the proteolytic activities are carried out. Specifically in eukaryotes, the proteasome is composed of a 20S catalytic core and a cap-shaped 19S regulatory complex, which can occupy both ends that can be assembled into 26S proteasome in an ATP-dependent manner [50]. Intriguingly, in higher eukaryotes, an alternative form of the proteasome, referred to as immunoproteasome, can also be found. It shares substantial structural and sequential homology with the 26S proteasome. Nevertheless, the immunoproteasome and 26S proteasome incorporate different catalytic subunits into their structure and therefore are distinct in the spectrum of peptides generated from proteolysis. As a result, they have been implicated in different biological processes as well as pathological diseases.

a. 26S Proteasome

The 20S catalytic core of 26S proteasome is made up of four stacked heptameric rings each of which is composed of distinct subunits. Specifically, the two inner rings are made up of β subunits, some of which harbor proteolytic activities, and the two outer rings are made up of α subunits that are catalytically inactive. These rings adopt a two-fold symmetry with a $\alpha_{1-7}\beta_{1-7}\beta_{1-7}\alpha_{1-7}$ arrangement which allows for the sequestration of the catalytic active sites. The β subunits that possess protease activity are X (β_5), Y (β_1), and Z (β_2); they have been shown to exhibit chymotrypsin-like (CT-L), caspase-like (C-L) and trypsin-like (T-L) activities respectively. The two outer α rings that sandwich the β rings play a vital role in regulating substrate entry into the 20S core for proteolysis by reinforcing an auto-inhibition mechanism. Specifically, the N-terminal tails of these α subunits impose a topological closure on the 20S channel during its latent state [51]. In parallel with the sequestration of active sites, it represents the defense mechanism against uncontrolled protein degradation which would cause havoc in cells. The activation of the

20S core can only be achieved by binding to a 19S regulatory complex which will then displace the N-terminal tails and therefore opening up the channel for substrate entry [51].

The 19S regulatory complex is also a multi-subunit complex protein comprised of a lid and a base that binds to the α subunits of the 20S core. Two subunits of the lid with poly-ubiquitin chain binding domain that are capable of recognizing and binding to poly-ubiquitinated substrates have been identified thus far [52, 53]. The lid also contains subunits that display intrinsic deubiquitinating activity [54, 55]. The base of the 19S is composed of several subunits including six ATPases that are responsible for an array of ATP-dependent tasks. For example, one of the ATPases, Rpt2, was shown to promote the opening of the gated 20S channel [56]. The mechanism by which the 19S facilitates the conformational changes in the outer α rings was only reported very recently. Specifically, the ATPases were shown to dock its C-terminal into the pockets between neighboring α subunits [57]. This specific interaction induces α subunit rotation and subsequent opening of the gate for substrate entry by displacing the N-terminal tails of these subunits [58]. Furthermore, some of these ATPases exhibit chaperone-like activity which facilitates substrate unfolding and entry into the 20S catalytic core for proteolysis [59]. Alternative 19S regulatory complexes such as 11S/PA28 and Blm10/PA200 have also been identified [60]. While these alternative regulatory complexes are able to bind to the 20S to form functional holoenzymes, they do not contain ATPases, suggesting the possibility of ATP and ubiquitin independent proteolytic functions. For example, the PA28 has been shown to be involved in major histocompatibility complex (MHC) class I antigen processing [61] and possibly plays a role in the regulation of apoptosis [62]. Since each 20S has two identical outer α rings, they are able to accept two different regulatory complexes on opposite ends. This allows for the possibility of generating a repertoire of hybrid proteasomes with diverse proteolytic properties that meets a variety of physiological demands [63].

b. Catalytic Mechanism

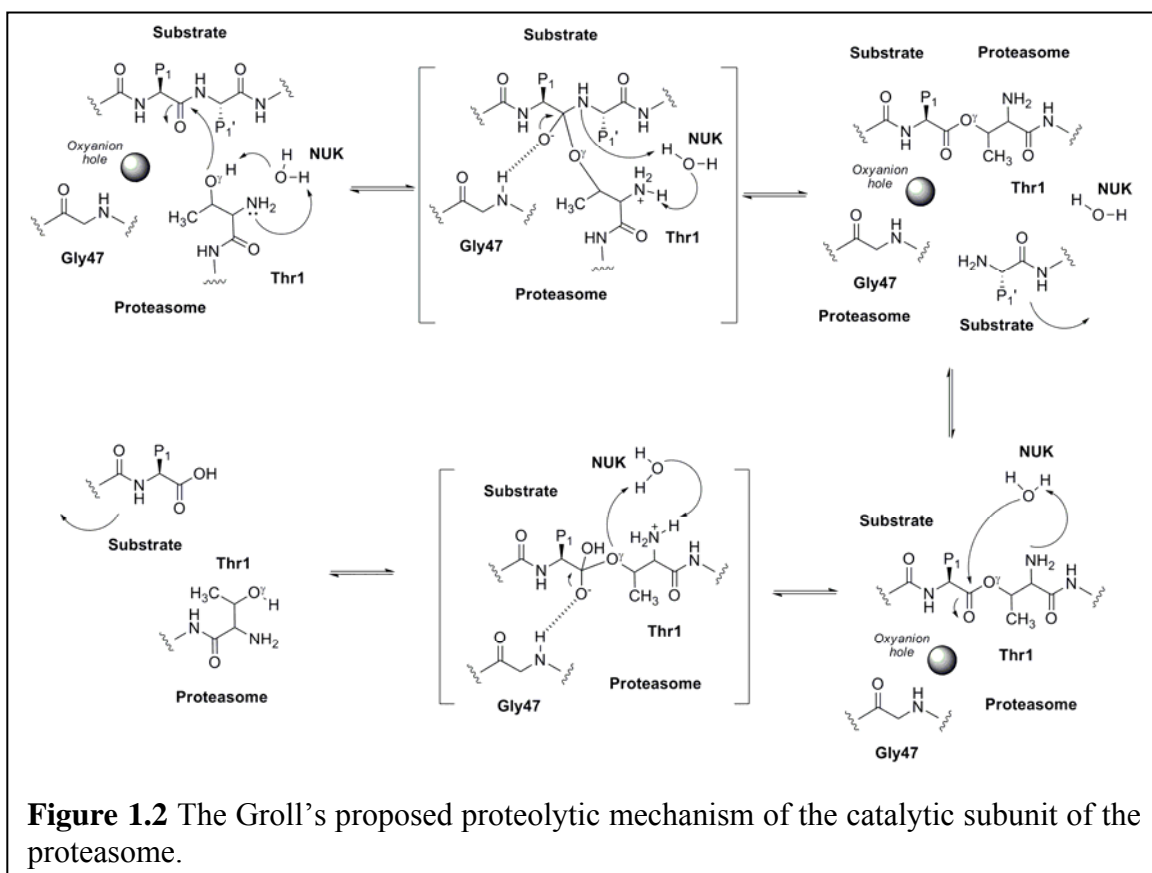
Unlike typical proteases, the 26S proteasome consists of multiple catalytic activities that are able to cleave after all amino acid residues, ensuring the complete degradation of its substrates. As mentioned earlier, the catalytic β subunits X ($\beta 5$), Y ($\beta 1$) and Z ($\beta 2$) contain chymotrypsin-like, caspase-like and trypsin-like activities respectively. Briefly, the chymotrypsin-like activity cleaves peptide bonds after bulky hydrophobic residues, the caspase-like activity cleaves peptide bonds after acidic residues, and the trypsin-like activity cleaves peptide bonds after basic residues. These three major catalytic sites were shown to exhibit a hierarchy in terms of importance in which chymotrypsin-like activity seemed to be the rate determining step of proteolysis [64]. However, the exact mechanism by which each of these individual catalytic subunits come together to regulate proteolysis is still not known. In addition to these well characterized proteolytic activities, the 20S proteasome has also been reported to possess two other minor activities. They have been identified as branched-chain amino acid preferring (BrAAP) and small neutral amino acid preferring (SNAAP) activities [65]. Recent structural studies of the mammalian 20S proteasome were able to assign the active site of SNAAP activity to the $\beta 7$ subunit [66]. However, the active site of BrAAP activity remains to be identified.

The proteasome has been classified as a N-terminal nucleophilic (Ntn) hydrolase, which is a class of enzymes that uses their N-terminal residue as the nucleophile [67]. Further mechanistic insights into proteasome proteolysis were derived from structural and mutational studies of the 20S proteasome [68, 69]. These studies revealed that, in addition to Thr1, Asp/Glu12 and Lys33 are also key players in the catalytic mechanism of proteolysis. Other nearby residues such as Ser129, Asp166, and Ser169 have also been implicated in facilitating catalysis by providing structural integrity to the proteolytic center [70]. A series of well defined water molecules termed nucleophilic water molecules (NUKs) were also found in close proximity to Thr1, Ser129, and Gly47; NUKs may have an important role in proteolysis by serving as proton shuttles during substrate binding and cleavage [70, 71]. Consequently, Groll *et al.* proposed the following mechanism by which substrate hydrolysis is executed (Figure 1.2). Briefly, the nucleophilic attack on the peptide bonds of substrates is carried out by the hydroxyl

group of Thr1, while the amine group of the same Thr1 serves as a proton acceptor. This reaction is facilitated by the oxyanion hole created by the nearby amine group of Gly47 which stabilizes the tetrahedral transition-state intermediate. It is then followed by the formation of an acyl-enzyme ester with the concomitant release of the N-terminal peptide fragment. The ester bond is eventually hydrolyzed, releasing the C-terminal peptide fragment [71, 72].

Protein substrates are degraded by the proteasome in a highly processive manner, which is distinct from the conventional proteases. The 20S proteasome hydrolyzes a single substrate into smaller peptide fragments before attacking the next available substrate [73]. This inherent property of the proteasome prevents the accumulation of partially digested substrates that may have detrimental effects. Nevertheless, the final products of proteolysis have an average length of 3-22 amino acid residues [74]. The majority of these short peptides are further degraded by various downstream aminopeptidases into free amino acids, which are recycled via the cellular metabolism [74]. However, a very small percentage of the short peptides managed to escape further degradation. These peptides, usually 8-10 amino acids long, are transported through the endoplasmic reticulum (ER) to be presented by MHC class I molecules to the immune system [75]. Interestingly, it was demonstrated that the 26S proteasome and the 20S catalytic core exhibit overlapping but yet substantially different cleavage patterns, which suggested the possible involvement of the 19S regulatory complex in influencing the specificity of proteolysis [76].

Despite numerous detailed structural and mutational studies, there is still much to be learned about the exact mechanisms by which the 26S proteasome executes its proteolysis. Some of the questions that remained unanswered are how do the catalytic subunits communicate with one another and how does the 26S proteasome determine its cleavage pattern and specificity.



c. Biological Processes and Substrates Mediated by Proteasome

The substrates of the 26S proteasome are virtually limitless. They range from short-lived to abnormal to long-lived proteins. One of the first protein families discovered to be degraded via the ATP dependent ubiquitin proteasome pathway were the cell cycle regulators. Specifically, the expression levels of cyclins were found to oscillate in parallel with the cell cycle, which were found later to be mediated by the ubiquitin proteasome pathway. To date, some of the best characterized mammalian cell cycle regulators mediated by the proteasome include cyclins A, B, D, E, Cdk inhibitors, p21, p27, tumor suppressor p53, and transcription factors E2F and Rb [33]. Consequently, this degradation pathway has emerged as a major regulatory mechanism for cell division. Similarly, the ubiquitin proteasome pathway is also involved in the regulation of many other non-cell cycle related transcription factors. These proteins can become lethal if their expression levels are left unchecked. Some of the well-studied examples are β -catenin, *c-myc*, HIF-1 α , and nuclear hormone receptors [77]. Furthermore, proteins that induce apoptosis or inhibit apoptosis are all strictly controlled by the ubiquitin proteasome pathway as well. These include mdm2, I κ B α , Bax, Bad, all caspases, and the IAP family of proteins [78]. Due to the depth with which the ubiquitin proteasome pathway is involved in cellular processes, its dysfunction has been implicated in a variety of diseases. As a result, the inhibition of the proteasome has become a very attractive strategy for developing new therapeutics.

One of the most fascinating aspects of proteasomal degradation is the limited proteolysis involved in the processing of NF κ B. NF κ B is a dimeric protein that consists of members of the Rel family of transcription factors. They have been shown to be responsible for a variety of cellular processes such as immune responses, inflammation, apoptosis, and cell proliferation [79]. One of these proteins, namely p105, is synthesized as an inactive precursor in which its C-terminus contains a PEST sequence that acts as a degradation signal [80]. Unlike conventional proteolysis by which a protein is completely degraded by the proteasomes, p105 is partially processed activation to produce the active form p50 [81]. During processing, the C-terminus of p105 is degraded by the proteasome while the N-terminus of NF κ B (p50) is left intact. The inactive precursor of NF κ B appears to have a processing signal identified as the glycine rich region (GRR) hidden

within its sequence that enables the proteasome to recognize the region as a termination factor [82]. Moreover, the proteasome was also shown to possess endoproteolytic activity, which offers an alternative molecular mechanism by which inactive precursors are released after processing by the proteasome [83]. In addition to NF κ B processing, the ubiquitin proteasome pathway is also responsible for the regulation of I κ B α degradation upon NF κ B activation.

In contrast to the orthodox ubiquitin proteasome pathway, there are substrates that are degraded by the proteasome in an ubiquitin independent manner. Primitive organisms such as archaea and certain bacteria have simpler proteasomes that degrade proteins in a ubiquitin independent manner, which indicate that proteasomes are capable of degrading substrates without ubiquitination [84]. In addition, it was reported that the localization of substrates to the proteasome alone is sufficient for proteasomal degradation [85]. Nevertheless, protein best characterized as undergoing such non-canonical proteasomal degradation is ornithine decarboxylase (ODC). It is a key enzyme that is involved in polyamine biosynthesis and it uses antizyme instead of ubiquitin as a recognition signal for the 26S proteasome [86].

Besides degrading unwanted proteins, the ubiquitin proteasome pathway is also involved in the regulation of the immune system. Specifically, the proteasome is required for antigen processing and presentation. This is an important aspect of our immune system because not only is it a means for immune cells to distinguish self from non-self, it also enables the immune system to identify cells that have been invaded by foreign pathogens and thus mark these cells for destruction. Surprisingly, the 20S and 26S proteasomes were found to be responsible for the generation of antigenic peptides for presentation on MHC class I molecules. Inhibition of the proteasome was also shown to effectively reduce antigen presentation [87]. However, only a very small fraction of the peptides generated by the proteasome are transported through the ER to be loaded onto MHC class I molecules. Interestingly, cytokines such as interferon gamma (IFN- γ) were found to stimulate antigen processing and presentation due to an altered proteolytic activity that is favorable to the generation of antigenic peptides. This variation can be attributed to the induction of alternative catalytic subunits, which are LMP2 (low-molecular mass polypeptide 2), LMP7 (low-molecular mass polypeptide 7) and MECL-1

(multicatalytic endopeptidase complex 1) [88]. Hence, this alternative proteasome has been referred to as the immunoproteasome.

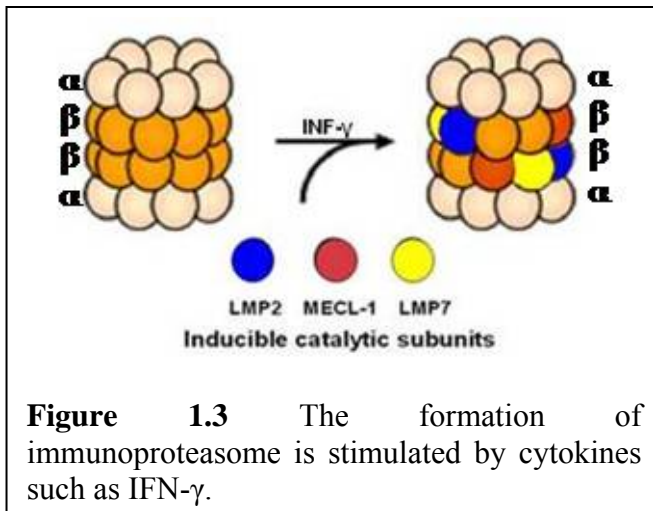
d. Immunoproteasome

While the 26S proteasome is constitutively expressed in the majority of the cells in our body, the expression of the immunoproteasome is limited. Immune tissues such as the spleen constitutively express high levels of immunoproteasome. Even though immunoproteasomes are also expressed at much lower levels in other cell types, they can be induced when cells are stimulated by cytokines such as interferon- γ (IFN- γ) and tumor necrosis factor- α (TNF- α). After exposure to these cytokines during the stress response or infection, the synthesis of the alternative catalytic subunits LMP2 (β 1i), LMP7 (β 5i), and MECL1 (β 2i) are induced and subsequently incorporated into the immunoproteasome (Figure 1.3). These alternative catalytic subunits were found to possess a biased cleavage pattern that enhances the generation of peptides bearing hydrophobic and basic side chains, but not acidic side chains at their C-termini. This altered repertoire of peptides generated has an increased affinity for most MHC class I molecules [89]. Similarly, an alternative regulatory complex known as 11S regulatory complex (PA28) is also induced upon stimulation with IFN- γ , suggesting its involvement in antigen processing. However, like the constitutive proteasome, the immunoproteasome is capable of binding to either 19S or 11S regulatory complexes [90]. In addition, contradicting results have been reported regarding the vital role of 11S in the processing of antigens [91, 92]. These results simply indicate that the 11S is not an obligatory prerequisite for antigen process in general but may subtly affect substrate degradation to enhance the production of MHC class I antigens.

Due to its biased cleavage pattern, the primary function of the immunoproteasome was initially thought to be the generation of MHC class I antigens. It was later demonstrated that even though LMP2 and LMP7 knockout mice have a diminished or altered presentation of certain MHC class I antigens, the processing and presentation of the majority of the antigenic peptides was unaffected [93, 94]. While MECL1 knockout mice did not display any significant changes in their antigen processing and presentation, an altered T cell repertoire was observed after viral infection [95]. In addition, all three

strains of knockout mice were viable, showed no visible abnormalities, and lived to at least one year of age, indicating that these genes are dispensable [93-95]. These results strongly suggest that the 26S proteasome alone is capable of generating most of the necessary antigenic peptides. Therefore, there is a significant probability that the immunoproteasome might have functional purposes other than the optimization of antigenic peptides. Indeed, the immunoproteasome has been implicated in biological functions such as positive and negative selection of T cells in the thymus [96], T cells proliferation [97], and processing of NF κ B [98]. However, it is still unclear why evolution dictated the development of immunoproteasomes but investigation in this area is currently ongoing.

Even though the immunoproteasome and 26S proteasome share high structural homology, the detailed structure of the immunoproteasome still remains to be determined. Sequence alignment studies of the immunoproteasome and 26S proteasome catalytic subunits have determined that the immunoproteasome is also a member of the Ntn hydrolase family as all its catalytic subunits were found to have N-terminal threonine residues [99]. Nevertheless, the structure of the immunoproteasome was predicted via computational modeling from the crystal structural studies of the 20S mammalian proteasome. Specifically, the S1 pockets created by the immunoproteasome's catalytic subunits were observed to be more apolar than that of 26S proteasome, suggesting that



there is an increase in the chymotrypsin-like activity but a decreased in the caspase-like activity [66]. This observation is in support of the previously reported results by which the immunoproteasome have a biased cleavage pattern that favors the generation of MHC class I antigens.

e. *Proteasome Assembly*

The biogenesis of the proteasome is a highly orchestrated multi-step assembly process that requires the assistance of several regulatory proteins. Given that the proteasome catalytic subunits have such broad proteolytic activities, extreme caution is needed for the assembly of the proteasome to prevent premature proteolysis. Specifically, the catalytic β subunits are synthesized as inactive precursors containing propeptides at their N-termini, which are only removed at the end of the proteasome assembly process via an autocatalysis mechanism [100, 101]. Nevertheless, the assembly of the eukaryote proteasome is believed to begin with the formation of the α ring. The β subunits containing inactive precursors are then recruited onto the α ring forming a half proteasome intermediate (16S). Finally, the dimerization of the half proteasomes along with the cleavage of the β propeptides produces the final active 20S proteasome (Figure 1.4) [102].

The earliest stage of the 20S proteasome formation is facilitated by multiple proteasome assembly chaperone proteins termed PAC1, PAC2, PAC3 [103, 104] and a recently identified but uncharacterized PAC4 [105], which is the mammalian counterpart of the yeast Pba1-4 [106] or Poc1-4 [105]. PAC1 and PAC2 form a heterodimer that has been demonstrated to interact directly with $\alpha 5$ and $\alpha 7$ subunits, and subsequently functions as a scaffold to promote the complete assembly of the α ring. Furthermore, the PAC1/2 complex is crucial in ensuring the formation of a productive and competent α ring for the subsequent formation of the half proteasome. It was also demonstrated that the PAC1/2 complex remains associated with the proteasome precursor until assembly is complete and eventually it is degraded by the newly formed 20S proteasome [103]. PAC3 also directly interacts with α subunits to facilitate the assembly of the α ring but has been shown to carry out its function via a separate mechanism. Unlike the PAC1/2 complex, it is released before the formation of the half proteasome is completed. The release of PAC3 also occurs in tandem with the recruitment of POMP (proteasembilin or hUmp1, homolog of yeast Ump1), which is a proteasome maturation factor [104]. Nevertheless, the mode of action of PAC3 is still not well understood.

The next step in the assembly process is the recruitment of the β subunits. POMP is known to be responsible for facilitating the recruitment of the β subunits onto the α

ring [107]. The identification of two distinct 13S and 16S proteasome assembly intermediates [108] suggests that the β subunits are incorporated stepwise into the nascent proteasome. Specifically, pro β 2, pro β 6, β 3 and β 4 are believed to be the first subunits recruited onto the α ring by POMP, composing the mammalian 13S complex. Shortly thereafter, the 13S becomes the 16S upon the addition of pro β 1, pro β 5 and pro β 7 subunits, hence completing the assembly of the β ring [109]. POMP was shown to physically interact with both X (β 5) and LMP7 (β 5i) subunits [110]. However, the immunoproteasome subunit LMP7 (β 5i) seemed to be preferentially incorporated by POMP into the 16S complex in place of the regular subunit X (β 5) [110]. Indeed, it has been demonstrated by Griffin and colleagues that proteasome assembly favors the formation of immunoproteasomes when both types of catalytic subunits are present, which are attributed to the propeptides located at the N-terminus of these β subunits [110-113]. In other words, the cooperative proteasome assembly is strongly influenced by the catalytic β subunit propeptides of both the immunoproteasome and regular proteasome. It was elegantly demonstrated by Griffin and colleagues that the replacement of LMP7 (β 5i) and MECL1 (β 2i) propeptides with that of X (β 5) and Z (β 2) respectively enabled the immuno subunits to be incorporated into the otherwise regular proteasome and vice versa [112, 113]. Furthermore, the propeptides of these catalytic subunits were shown to play an important role in determining the order in which they are incorporated. Specifically, MECL1 (β 2i) requires LMP2 (β 1i) to be incorporated into the β ring efficiently but when the propeptide of MECL1 is replaced by that of Z (β 2), it enables MECL1 to be incorporated without LMP2 [112]. De *at al.* was also able to demonstrate that proteasomes with mixed catalytic subunits from both the regular proteasome and immunoproteasome is a possible occurrence [112].

The final step of 20S proteasome biogenesis involves the dimerization of the half proteasomes and the activation of the catalytic β subunits. In addition to recruiting β subunits, POMP is also believed to be involved in facilitating the dimerization of half proteasome, since a significant reduction in 20S proteasome but normal α rings and half proteasomes were observed in POMP knockdown cells [103]. The propeptides of the catalytic β subunits are removed via an autocatalysis mechanism and the cleavage of the propeptides of the other non-catalytic β subunits are then carried out by their active

neighbors [64]. Similar to PAC1/2, POMP is eventually degraded by the newly formed 20S proteasome as well [110]. Interestingly, Heink *et al.* showed that IFN- γ treatment not only induces the synthesis of immunoproteasome catalytic subunits but also increases POMP mRNA [110]. On the other hand, a rapid decrease in POMP protein levels was observed. In addition, the immunoproteasomes were also found to assemble four times faster than regular proteasomes as well as possess a shorter half life than that of regular proteasomes when treated with IFN- γ . These results suggest that the immunoproteasome is intrinsically less stable and its induction by IFN- γ is an accelerated and transient response [110].

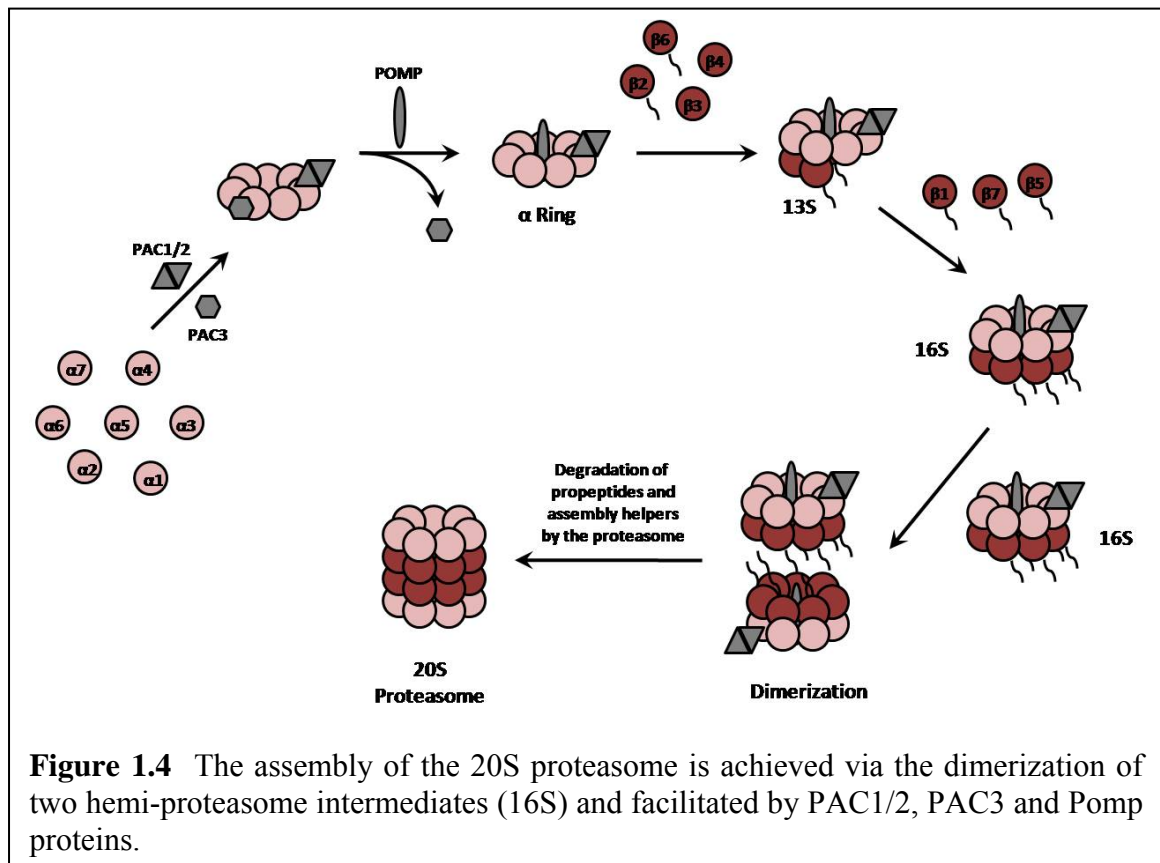


Figure 1.4 The assembly of the 20S proteasome is achieved via the dimerization of two hemi-proteasome intermediates (16S) and facilitated by PAC1/2, PAC3 and Pomp proteins.

4. Physiological Disorders Implicated in the Ubiquitin Proteasome Pathway

As the ubiquitin proteasome pathway is involved in the regulation of a multitude of cellular processes, it is not unexpected to find that defects in the components of the ubiquitin proteasome pathway were found to result in a range of physiological disorders. In order to decipher the molecular mechanisms of pathogenesis, these components were studied extensively, which has significantly benefited the biological understanding of the ubiquitin proteasome pathway. Consequently, the pathway has emerged as a very attractive therapeutic target. A few examples of genetic disorders and acquired diseases caused by the aberrations in the ubiquitin proteasome pathway are described below.

a. Genetic Disorders

A well known genetic disorder associated with the ubiquitin proteasome pathway is the Angelman's Syndrome, which is a neurological disorder [114]. Genetic studies have revealed that the mutations in UBE3A genes to be the primary underlying cause of this disorder. The UBE3A gene encodes an ubiquitin HECT E3 ligase termed E6-AP, which has been shown to promote the ubiquitination of p53 for proteasomal degradation in the presence of the E6 oncoprotein produced by human papillomavirus [35]. However, the target protein(s) of E6-AP in Angelman's Syndrome has not yet been identified. Recent studies have shown that, in addition to functioning as an E3 ligase, E6-AP acts as a transcriptional coactivator as well. As a result, the deficiency of E6-AP resulted in abnormal dendritic spine morphology, which may be due to its regulation of synaptic plasticity [115]. Nevertheless, it is still unclear how the loss of E6-AP resulted in Angelman's Syndrome.

Von Hippel-Lindau (VHL) Syndrome is a rare genetic disorder that is caused by mutations of the gene that encodes the VHL tumor suppressor. The VHL protein is a component of the ubiquitin RING E3 ligase complex that targets members of the hypoxia-inducible transcription factor family (HIF) for degradation under normoxic condition. The α and β subunits of the heterodimeric HIF regulate physiological responses to hypoxia by stimulating cellular processes such as angiogenesis. In the presence of oxygen, a conserved proline residue in the HIF- α is hydroxylated, which serves as a proteasomal degradation signal specifically recognized by the VHL ubiquitin

ligase complex [116]. Therefore, mutations in the VHL gene result in the constitutive stabilization and activation of the HIF protein, which causes the overproduction of its gene products such as vascular endothelial growth factor (VEGF) [117]. Subsequently, the mutation is translated into an inherited susceptibility to various forms of cancer including pancreatic and renal cell carcinomas [118].

b. *Acquired Disorders*

In addition to the inherited predisposition to cancer, the ubiquitin proteasome pathway is also implicated in the etiology of many other malignant cancers. In general, cancers can result from either constitutive activation of oncogenes or deactivation of tumor suppressor genes [119]. The aberration in the regulation of both oncoproteins and tumor suppressor proteins can often be attributed to the exploitation of the ubiquitin proteasome pathway by the disease state as a means to manipulate the expression levels of these proteins to their liking.

Cancer is essentially an abnormal growth of cells caused by uncontrolled cell division; hence, it is not unexpected to frequently find disrupted cell cycle regulation in cancer. Some of the well known cell cycle regulators frequently found mutated in cancer includes tumor suppressors p27 and p53 as well as oncoprotein cyclin E. Both p27 and p53 are capable of inducing cell cycle arrest following anti-mitogenic signals or DNA damage to ensure everything is in order before the cell cycle is proceed to completion. In addition, cellular levels of these proteins are tightly regulated by the ubiquitin proteasome pathway. However, in addition to mutations within the p27 and p53 genes, aberrant downregulation of p27 and p53 proteins, observed in some cases of cancer, result from overactivation of the ubiquitin proteasome pathway [120, 121]. Specifically, low levels of p53 and p27 can be caused by overexpression of their cognate E3 ligases, Mdm2 and SCF^{Skp2}, respectively [120, 122]. Furthermore, low levels of these proteins have been associated with tumor progression and poor prognosis in various cancers such as sarcomas, colon, breast, prostate, ovarian and brain cancer [120, 123].

On the other hand, oncoproteins such as cyclin E were found to be aberrantly upregulated in several types of human cancer, which is often used as a prognosis indicator [124]. Proper cell cycle progression is highly dependent on the timely

accumulation of the four well known cyclins A, B, D, E and their interaction with their cyclin-dependent kinases (Cdks). Specifically, the accumulation of the cyclin E-Cdk2 complex initiates the transition of the cell cycle from G1 phase to S phase. Cyclin E is then phosphorylated and subsequently recognized by the SCF^{Fbw7} E3 ligase for proteasomal degradation [125]. However, defective SCF^{Fbw7} has been observed in some cancers in which the failure of the ubiquitin proteasome pathway to degrade cyclin E resulted in the overexpression of cyclin E [4]. On a different note, recent studies by Ho *et al.* reported that some cancers have differential expression levels of immunoproteasome catalytic subunits which can be correlated with the malignancy of cancer [126]. This sheds an interestingly new light on the possible role of immunoproteasomes in the malignancy mechanism of cancer.

Some well studied cancers that are known to have defective ubiquitin proteasome pathways include cervical and colorectal cancers. The cervical carcinoma tumors that were caused by a high risk HPV strain have very low expression levels of tumor suppressor gene p53. The E6 protein encoded by the HPV was found to bind to E6-AP ubiquitin ligase and subsequently p53. This ternary complex was shown to eventually promote ubiquitination and proteasomal degradation of p53 [35]. Similarly, mutations in another tumor suppressor gene, adenomatous polyposis coli (APC), were found in a significant fraction of non-hereditary colorectal cancers [127]. The APC gene product is known to associate with the oncogene β -catenin [128]. This interaction enables the APC gene product to regulate the cellular levels of β -catenin via the ubiquitin proteasome pathway [129, 130]. Therefore, mutations in the APC gene disrupt this complex formation preventing the proteasomal degradation of β -catenin, which results in the constitutive activation of its downstream effectors.

In addition to cancers, the ubiquitin proteasome pathway has also been implicated in the pathogenesis of various progressive neurodegenerative diseases such as Alzheimer's disease (AD) and Huntington's disease (HD). These diseases are characterized by the accumulation of abnormal protein aggregates or inclusion bodies in the brain. The aggregates were also found to contain ubiquitins and interestingly, they were shown to directly inhibit the proteolytic activity of the ubiquitin proteasome pathway [131]. Recent studies have demonstrated that the ubiquitin proteasome pathway

helps regulate proteolysis in synaptic plasticity, which is thought to be responsible for learning and memory [132]. Interestingly, it was recently shown that the brains of AD patients express higher levels of immunoproteasome catalytic subunits than those of the non-demented elderly whereas it is negligible in younger brains [133]. A similar increase in immunoproteasome catalytic subunits was also observed in brains affected by HD [134]. These intriguing results have drawn considerable attention because the brain is historically thought to be an immunologically privileged organ with almost no expression of the immunoproteasome. In spite of numerous speculations, the functional relevance of the upregulation of immunoproteasomes in these diseases remains to be determined.

Last but not least, autoimmune diseases are also one of the many physiological disorders believed to arise from defective ubiquitin proteasome pathway. This class of diseases is characterized by the inability of the immune system to recognize self proteins, which results in an immune response against the body itself. In addition to MHC class I antigen processing, the ubiquitin proteasome pathway was also found to play a significant role in regulating T cell receptors (TCR) and CD28 costimulatory receptors, which are required for optimal T cell activation [135]. Consequently, any defect within the ubiquitin proteasome pathway that would result in a faulty immune response would trigger the development of autoimmune diseases such as rheumatoid arthritis, type I diabetes, and Sjögren's Syndrome. Even though these diseases have some abnormalities in their ubiquitin proteasome pathway or exhibit elevated levels of the immunoproteasome [136-138], the exact mechanism by which the ubiquitin proteasome pathway is involved in their pathogenesis is still unclear. The immune system is an extremely complex network about which there is still much to be learned; hence, in order to decipher the pathological mechanism of the ubiquitin proteasome pathway in disease, we need to first better understand how the immune system works.

B. Proteasome Inhibitors

Given that the dysregulation of proteasome-mediated protein degradation is observed in such a wide array of disease states, it is not unexpected that proteasome inhibitors have been pursued as therapeutic agents. Initially, inhibitors of other members of the protease family, such as cysteine or serine proteases, were used as proteasome inhibitors. Alternatively, nature has provided potent proteasome inhibitors with unique pharmacophores. Thus far, many synthetic proteasome inhibitors with different pharmacophores have been developed for therapeutic purposes. Specifically, a boronic acid pharmacophore-based synthetic inhibitor (bortezomib) was the first FDA approved proteasome inhibitor, indicated for the treatment of relapsed multiple myeloma [139]. This has not only validated the ubiquitin proteasome pathway as a target for therapeutic intervention, but it has also set a precedent for the approval of other proteasome inhibitors for clinical applications.

Proteasome inhibitors can be broadly divided into two categories: active site-directed and non-active site directed inhibitors. In addition, more specialized proteasome inhibitors, such as subunit-specific or immunoproteasome-specific inhibitors, have been pursued to improve efficacy. In particular, the observation that the levels of the immunoproteasome catalytic subunits are elevated in a number of disease states has prompted the initiation of an immunoproteasome-specific inhibitor development program.

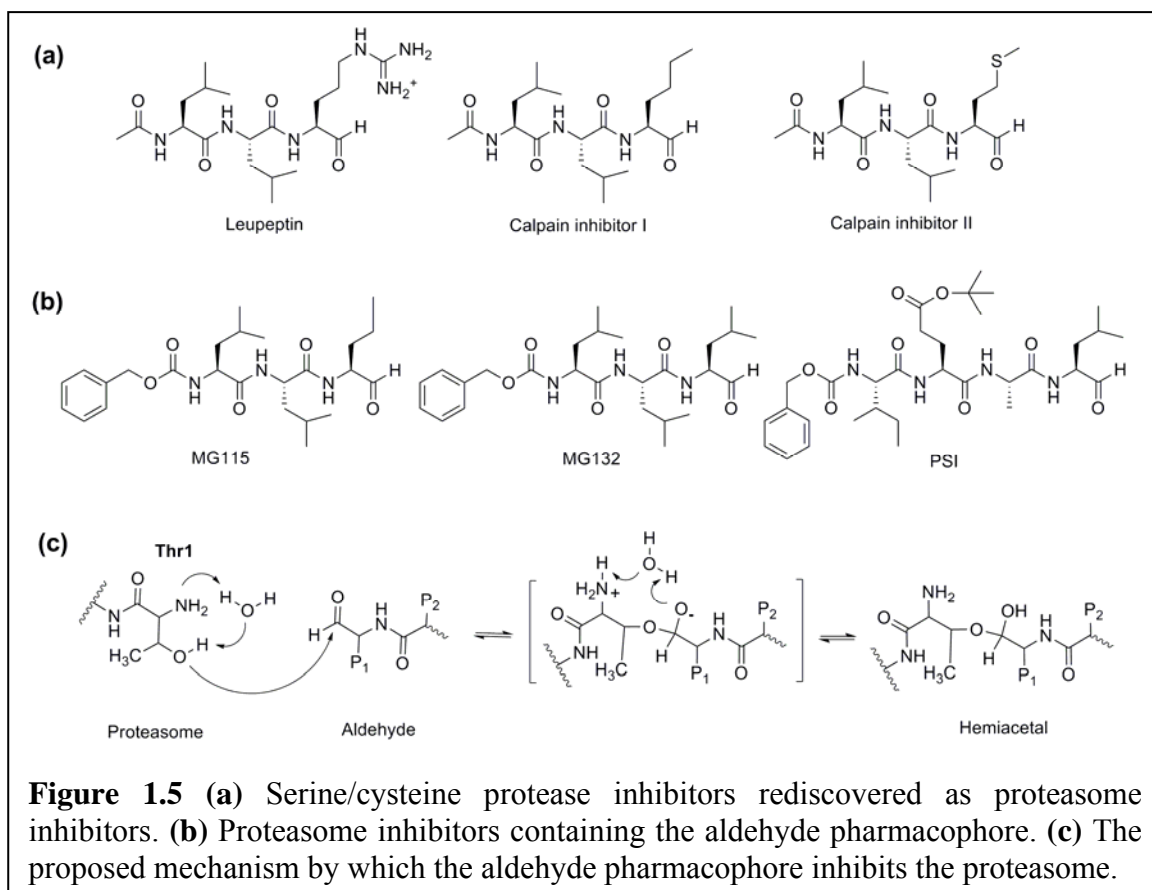
1. Active Site Directed Proteasome Inhibitors

The proteasome is an Ntn hydrolase, which uses its N-terminus threonine as a nucleophile to catalyze hydrolysis reactions. Consequently, these catalytic threonines within active sites have become the primary targets for the development of proteasome inhibitors. Because the catalytic activities of the 20S proteasome closely resemble that of cellular proteases, it is not surprising to find one of the first proteasome inhibitors originated from a protease inhibitor [140]. For instance, leupeptin (Figure 1.5a), a conventional serine and cysteine protease inhibitor, was shown to inhibit the proteasome with a selectivity towards T-L activity [141]. In addition, calpain inhibitors I and II (Figure 1.5a) were shown to selectively target CT-L activity of the 20S proteasome [142]. Similar to these peptide aldehyde inhibitors, the majority of active site-directed

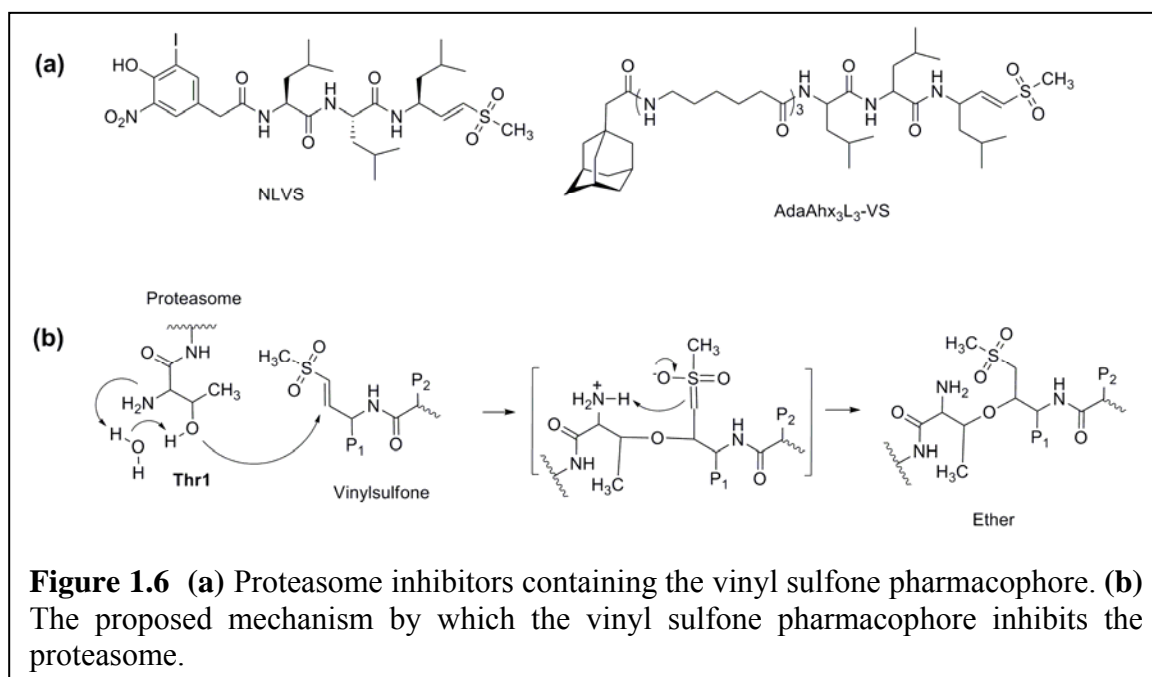
proteasome inhibitors developed to date are composed of a peptide or peptide-like backbone. Despite the fact that these inhibitors commonly target the catalytic threonines, they are composed of a wide variety of pharmacophores [140]. While many of these inhibitors are relatively more selective towards the proteasomes than proteases, they are not particularly specific to the constitutive or immunoproteasomes. Furthermore, several inhibitors developed thus far have also been shown to display specificity towards the individual catalytic activities of both constitutive and immunoproteasomes. Accordingly, these inhibitors can be classified as either broad spectrum or catalytic subunit specific proteasome inhibitors.

a. *Broad Spectrum Proteasome Inhibitors*

The rediscovery of protease inhibitors as proteasome inhibitors has prompted the development of more potent and selective proteasome inhibitors. For example, Rock *et al.* developed potent tripeptide aldehyde inhibitors, MG132 and MG115 (Figure 1.5b), which have been two of the most widely used molecular probe of proteasome biology [87]. Wilk *et al.* have also developed another peptide aldehyde inhibitor known as PSI (Figure 1.5b), which displayed a particularly high potency and selectivity towards CT-L activity [143]. Proteasomal inhibition by these peptide aldehyde inhibitors was subsequently shown to occur via the formation of a reversible hemiacetal linkage between the aldehyde pharmacophore and the hydroxyl side chain of the N-terminus threonine (Thr1O^γ) of the catalytic β subunits (Figure 1.5c) [69, 70]. Nevertheless, the peptide aldehyde inhibitors have cross-reactivity with other cellular proteases, which has limited their potential as therapeutic agents.

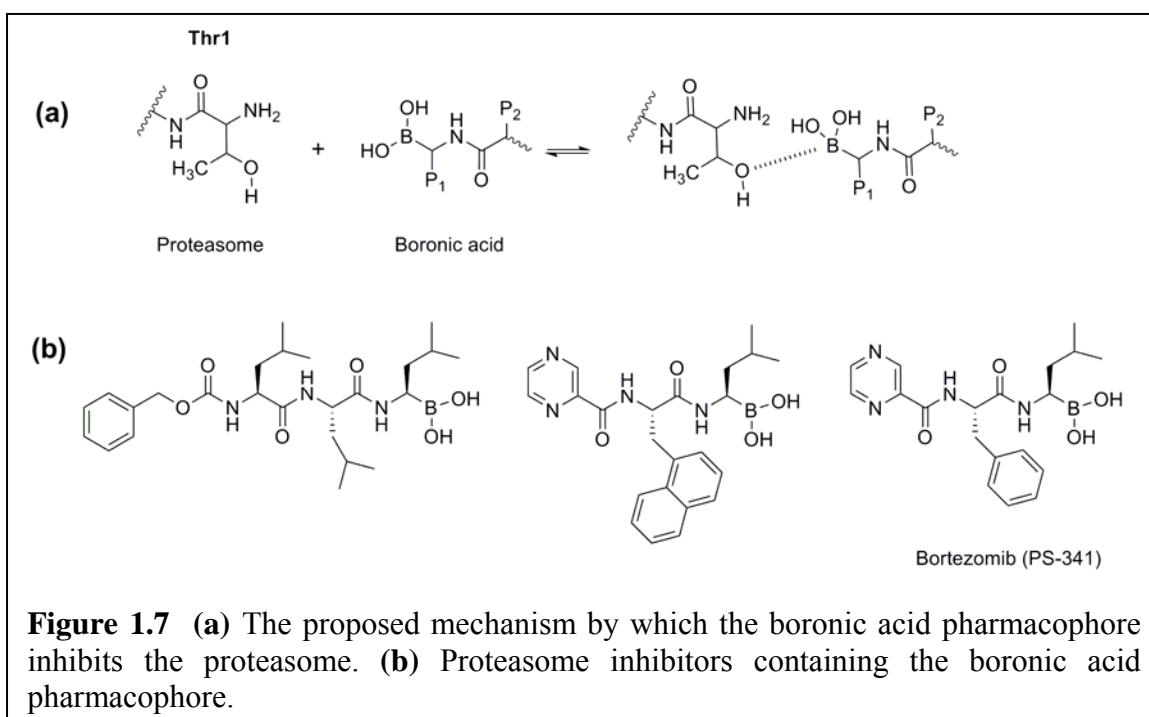


The vinyl sulfone is another unique pharmacophore that was first utilized by Bogyo *et al.* for the development of a novel class of proteasome inhibitors (Figure 1.6a) [144]. The vinyl sulfones were first introduced by Palmer and colleagues as a mechanism-based cysteine protease inhibitor that acts as a Michael acceptor solely at its active site [145, 146]. Similarly, the peptide vinyl sulfone proteasome inhibitor also serves as a Michael acceptor by forming a covalent bond with the hydroxyl group at the proteasome's catalytic sites (Figure 1.6b). Shortly thereafter, Kessler *et al.* developed a more potent peptide vinyl sulfone with an extended hydrocarbon chain that does not appear to discriminate against any of the catalytic activities [147]. Nevertheless, like the peptide aldehyde inhibitors, this class of proteasome inhibitors also lacks specificity due to off-targets issues.



The first FDA approved proteasome inhibitor contains a distinct pharmacophore known as boronic acid. The peptide boronates was first developed to target serine proteases such as thrombin [148]. The inhibitory mechanism was thought to occur via the formation of a stable pseudo-tetrahedral complex between the boron and the hydroxyl group of threonine, conferring it a high selectivity towards serine proteases. Specifically, the empty *p*-orbital of the boron atom is positioned to accept the oxygen lone pair from the serine residue located in the catalytic site (Figure 1.7a) [148]. Using this unique pharmacophore, Adams *et al.* developed a library of potent and selective di- and tripeptidyl inhibitors (Figure 1.7b) [149]. Among this library was bortezomib, a highly selective dipeptidyl boronic acid proteasome inhibitor (Figure 1.7b), which eventually became the first in its class to be approved by the FDA for clinical application [150]. Bortezomib was initially approved for the treatment of relapsed multiple myeloma but due to its remarkable potency, multiple clinical trials in other haematological cancers as well as solid tumors are currently ongoing [151]. Nevertheless, severe drug associated side effects [152, 153] as well as drug resistance [154] have also been reported, which could restrict the widespread application of bortezomib. Just like wild fire, the effort in

proteasome inhibitor development for therapeutic purposes has increased significantly since the approval of bortezomib for clinical application. For examples, another boronic acid proteasome inhibitor, CEP-18770 was recently discovered to be as a potential therapeutic agent for cancer [155, 156]. However, additional preclinical studies will be required to determine its potency and selectivity.



In addition to synthetic approaches, nature has also provided us with some of the most selective and potent proteasome inhibitors to date. One such natural product is lactacystin, a proteasome inhibitor with a β -lactone pharmacophore (Figure 1.8a) [157]. Lactacystin was initially discovered as a *Streptomyces lactacystinaeus* metabolite shown to induce neutrite outgrowth in the murine neuroblastoma cell line. It was later revealed that lactacystin requires aqueous condition for activation by which structural rearrangement will yield its active form *clasto*-lactacystin- β -lactone (Figure 1.8a) [158, 159]. Subsequently, Fenteany *et al.* demonstrated that lactacystin targets the proteasome via the covalent modification of the Thr1O^γ of catalytic β subunits (Figure 1.8b) [160]. Despite initial assumptions, lactacystin was later found to target other cellular proteases

as well [161, 162]. Another elegant example of β -lactone containing proteasome inhibitor created by nature is Salinosporamide A (NPI-0052) (Figure 1.8c) [163]. It is a novel marine-derived proteasome inhibitor that is distinct from bortezomib in terms of its irreversibility and inhibitory potency of the catalytic sites [164]. Recent structural studies revealed that NPI-0052 is covalently bound to all six catalytic sites via an ester linkage between the Thr1O γ of the catalytic β subunits and the β -lactone carbonyl of the inhibitor [71]. Due to its high potency, NPI-0052 has also been shown to be effective against bortezomib-resistant multiple myeloma [154]. Interestingly, recent studies have shown that combinatorial treatment with bortezomib and NPI-0052 induces a synergistic cytotoxicity in multiple myeloma [165]. With such promising preclinical trial results, NPI-0052 has entered Phase I clinical trial for relapsed multiple myeloma.

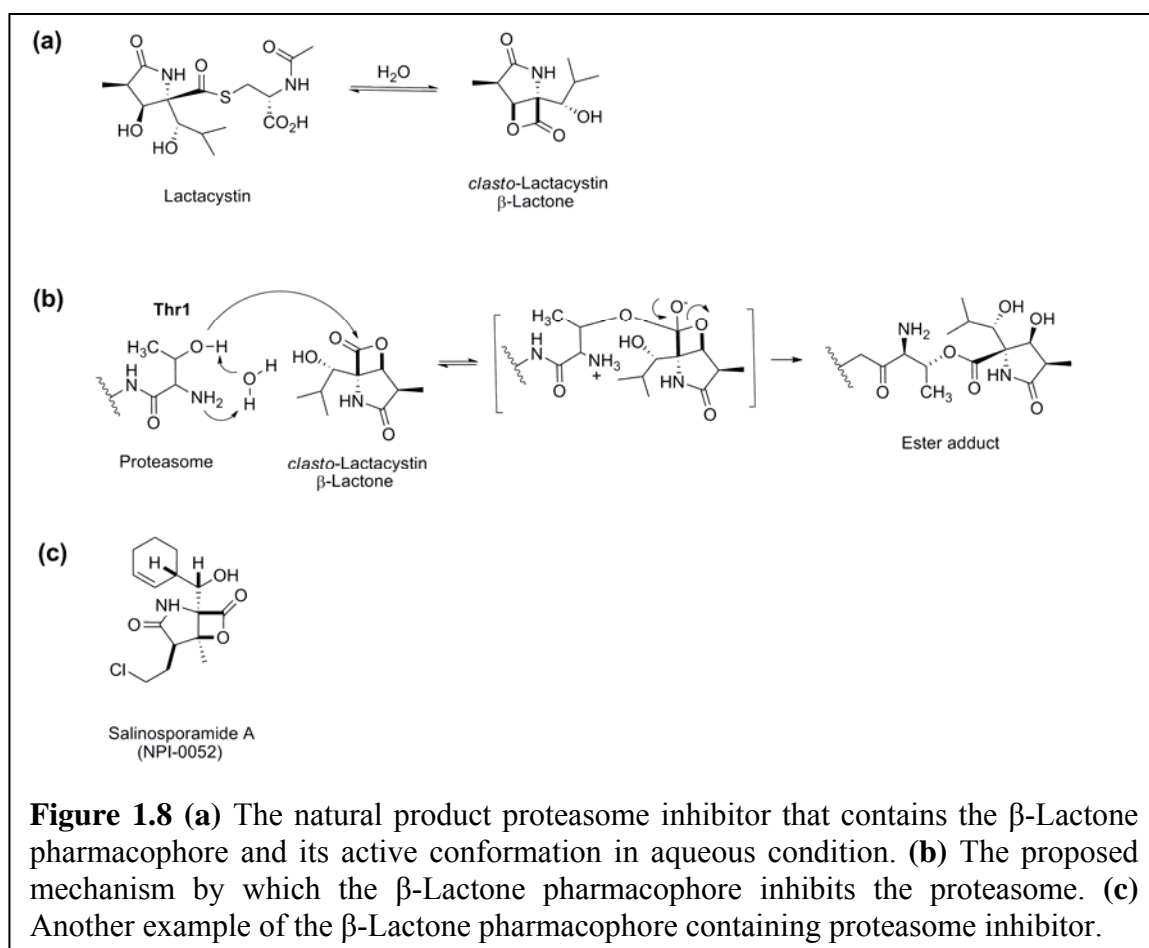
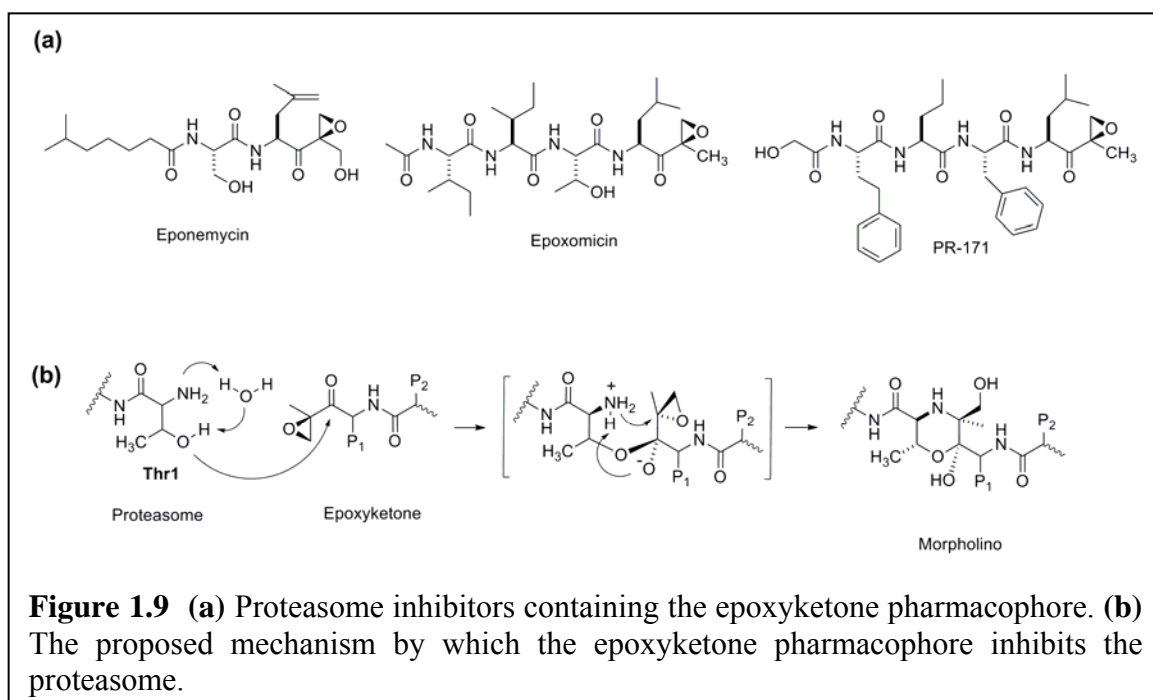
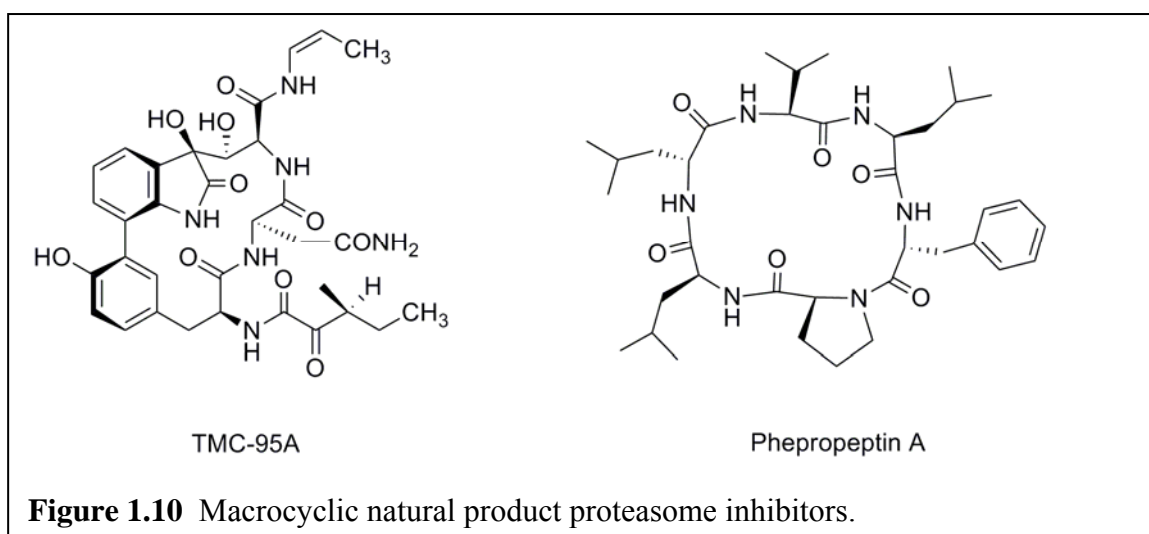


Figure 1.8 (a) The natural product proteasome inhibitor that contains the β -Lactone pharmacophore and its active conformation in aqueous condition. (b) The proposed mechanism by which the β -Lactone pharmacophore inhibits the proteasome. (c) Another example of the β -Lactone pharmacophore containing proteasome inhibitor.

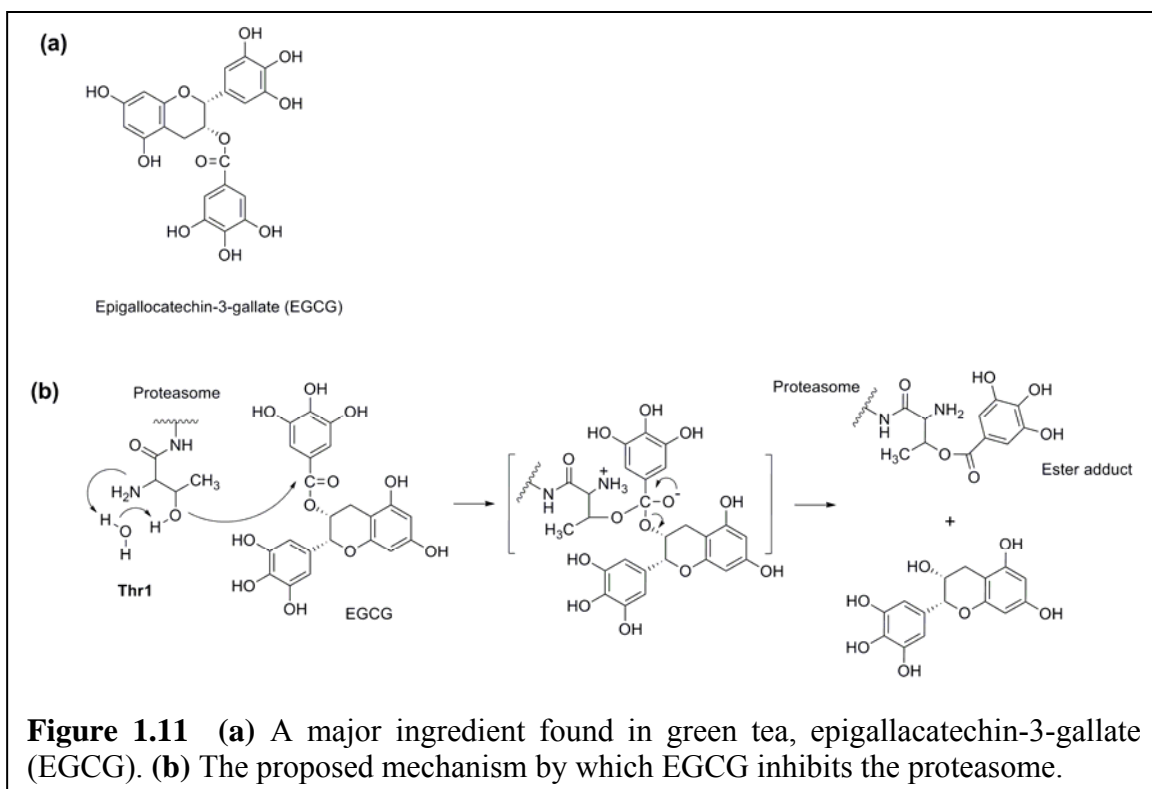
Another class of broad spectrum natural product proteasome inhibitor is the family of linear peptide epoxyketones. The first peptide epoxyketones discovered were epoxomicin and eponomycin (Figure 1.9a), isolated from an unidentified strain of *Actinomycete* (Q996-17) and *Streptomyces hygroscopicus* (P247-271) respectively. They were initially shown to be anti-angiogenic and cytotoxic against B16 melanoma [166, 167]. Subsequently, Crews and colleagues revealed that these peptide epoxyketones exhibit exceptionally high selectivity towards the 20S proteasome [168, 169]. Their selectivity was later demonstrated by structural studies, to be attributed to the unusual formation of a six-membered morpholino ring between with the Thr10^y of the catalytic β subunits and the α' β' -epoxyketone pharmacophore of epoxomicin (Figure 1.9b) [170]. In addition to epoxomicin, eponemycin and other peptide epoxyketone proteasome inhibitors that have been isolated from natural resources [171], synthetic approaches based on the epoxyketone peptide skeleton have also yielded several valuable proteasome inhibitors. One of the most recent developments is carfilzomib, also known as PR171, an epoxomicin derivative (Figure 1.9a) [172]. Needless to say, carfilzomib is also a potent proteasome inhibitor but with a greater selectivity for CT-L activity, which will be discussed further in the sections below.



Given the success of lactacystin and epoxomicin as highly selective proteasome inhibitors, systematic screening approaches of natural products were carried out to identify proteasome inhibitors with greater efficacy. Some of the novel natural product proteasome inhibitors identified include a series of unusual macrocyclic molecules isolated from the fermentation broth of *Apiospora montagnei* Sacc. (TC1093) such as TMC-95 (Figure 1.10) [173, 174]. Despite their unusual structural features, these compounds are potent and highly selective proteasome inhibitors with a preference for CT-L activity. Even so, no evidence of off-target activities has been published. Structural studies showed that the cyclic peptides bind to proteasome non-covalently with high affinity via the formation of multiple hydrogen-bond networks [175]. The discovery of these cyclic peptides as potent proteasome inhibitors has subsequently sparked the synthetic effort to optimize the catalytic site specificity of TMC-95 analogs [176]. In addition to TMC-95, cyclic hexapeptide phepropeptins were identified by Sekizawa *et al.* as proteasome inhibitors but with a weaker inhibition activity (Figure 1.10) [177]. One noteworthy advantage to utilizing such peculiar peptide skeletons as proteasome inhibitors is their high resistance to cellular proteases. Nevertheless, it remains to be determined whether this class of natural products will be developed into therapeutic agents.



Traditional remedies have long been used to treat illnesses in many parts of the world. While many of these medicines have been proven to be effective, their modes of action are often not clearly understood. In recent years, some traditional medicines have been shown to inhibit proteasomal activity. For example, green tea is known to be a potent cancer preventive dietary agent and one of its main constituents, epigallocatechin-3-gallate (EGCG) (Figure 1.11a) was shown to inhibit the CT-L activity of the 20S proteasome [178, 179]. It was suggested by Nam *et al.* that the ester linkage located between the two aromatic residues of EGCG is a vital element to the inhibition of 20S proteasome (Figure 1.11b) [179]. Furthermore, a number of other plants- and fruits-derived chemopreventive dietary agents have also been shown to inhibit proteasomal activities [180-183]. Specifically, flavonoids and triterpenoids are two of the most commonly found classes of chemopreventive dietary agents. While some of these natural products have been suggested by computational studies to directly interact with the catalytic β subunits [180], the detailed mechanisms by which these molecules achieve their chemopreventive effects remains to be determined.



b. Subunit-Specific Proteasome Inhibitors

While most proteasome inhibitors were shown to primarily target the CT-L activity of the 20S proteasome, they still partially inhibit other catalytic activities. Therefore, these proteasome inhibitors were referred to as broad spectrum proteasome inhibitors. However, the ability of these inhibitors to target all three catalytic activities simultaneously has complicated efforts to study the functions of the individual catalytic subunits. It is known that the CT-L activity of the proteasome is the rate determining step of proteolysis [64]; hence, most synthetic efforts have been focused on the development of CT-L activity specific proteasome inhibitors with the assumption that such molecule will enhance efficacy. As a result, the lack of T-L-specific or C-L-specific inhibitors has resulted in poor understanding of the cellular functions of the T-L and C-L activities. Therefore, there have been considerable recent efforts to develop more refined proteasome inhibitors, such as T-L or C-L activity specific proteasome inhibitors.

In an effort to aid the functional studies of the other two catalytic activities, a number of T-L or C-L activity specific proteasome inhibitors have been developed thus far. Examples include the bi-functional and bi-valent peptide aldehyde inhibitors (Figure 1.12a), which selectively target T-L activity [184, 185]. The rationale behind the design of these T-L activity specific molecules was based on the unique topography of the T-L responsible catalytic subunits in the 20S proteasome. The incorporation of a basic amino acid residue such as arginine into these inhibitors was found to be crucial in directing their selectivity towards T-L activity. Meanwhile, Bogyo and colleagues have also successfully developed T-L activity specific proteasome inhibitors using the vinyl sulfone pharmacophore (Figure 1.12b) [186]. Other T-L specific proteasome inhibitors are the peptide based vinyl esters (Figure 1.12c) [187, 188]. These T-L specific inhibitors were shown to be non-toxic and do not affect cell proliferation but they were found to modify the processing of MHC class I antigens [188], which could be the first indication of the functional role of the catalytic subunit bearing T-L activity.

Crews and colleagues developed C-L activity specific proteasome inhibitors by the derivatization of epoxomicin (Figure 1.12d) [189]. The inhibition of C-L activity by these peptide epoxyketone inhibitors was shown to be insufficient to render total inhibition of protein degradation in cells. Recently, Kisselev and colleagues have

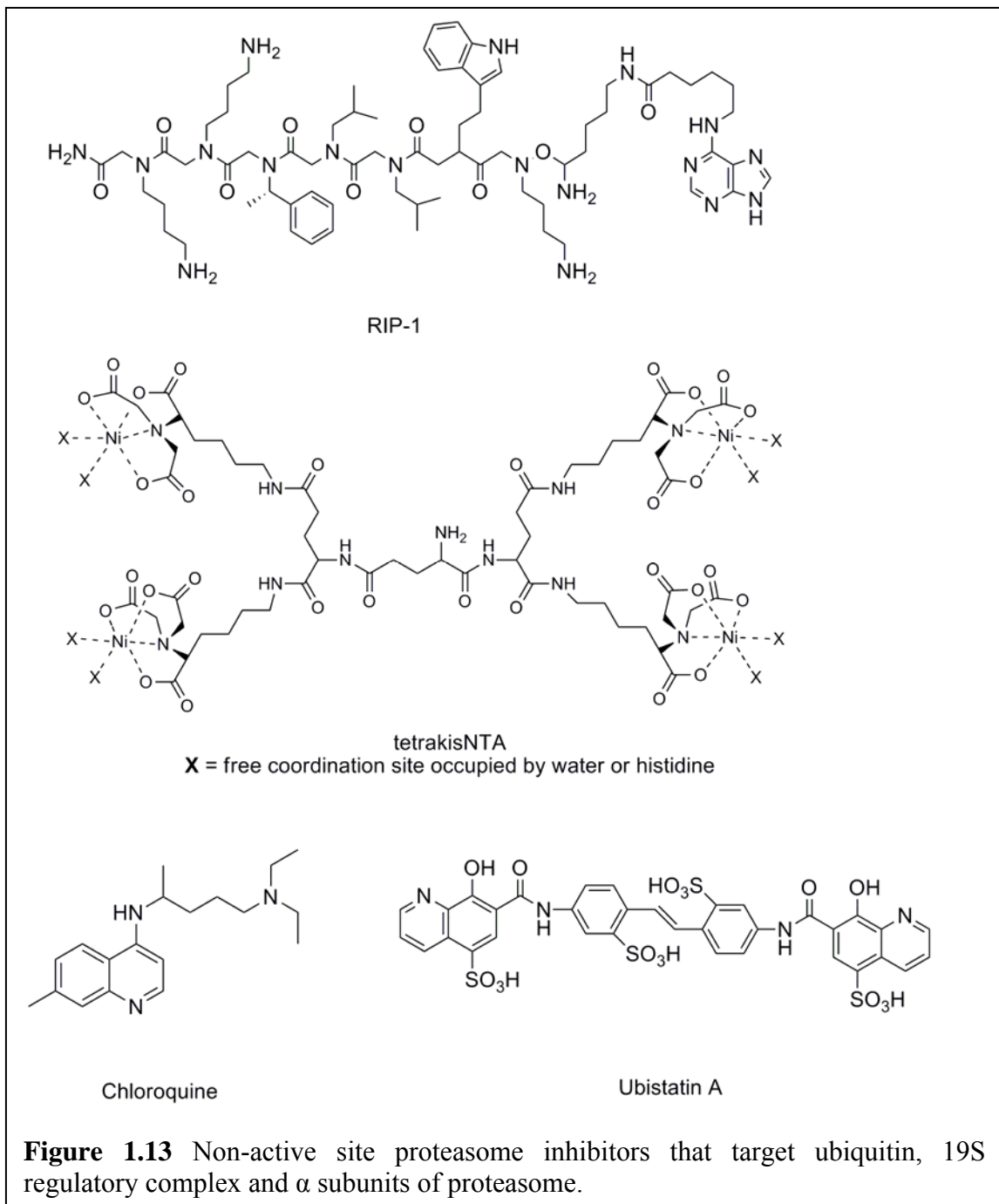
2. Non-Active Sites Directed Proteasome Inhibitors

Due to the cross activity of the majority of the active site-directed proteasome inhibitors with other proteases, alternative approaches to indirectly inhibit proteolytic activity are beginning to emerge. Specifically, the new generation of proteasome inhibitors is focused on the non-catalytic components of the ubiquitin proteasome pathway, which includes the regulatory complex, ubiquitin and its enzymatic cascade. One noteworthy advantage to this approach is that the possibility of these proteasome inhibitors cross-reacting with other cellular proteases is significantly reduced.

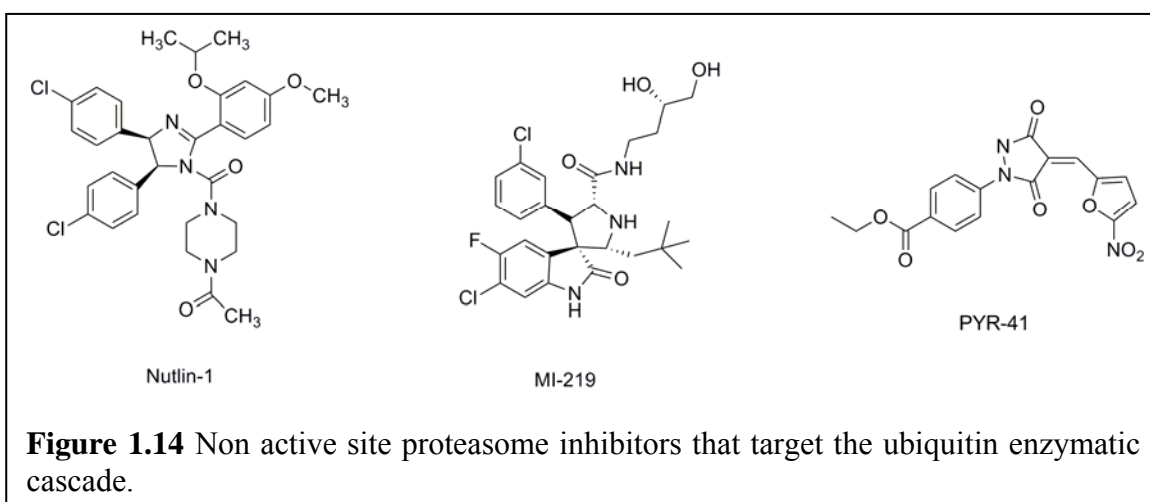
Recently, the first regulatory complex inhibitor has been identified from a “one bead one compound” peptoid library screening, which was called RIP-1 (Regulatory Particle Inhibitor Peptoid-1) (Figure 1.13) [191]. The peptoid inhibitor was shown to block proteasomal activity in living cells by interfering with the protein unfolding activity of the Rpt proteins [191]. It was later demonstrated that RIP-1 specifically target one of the six ATPases in the 19S complex, Rpt4 [192]. The inhibitor was then optimized, which generated an analog with a smaller mass that exhibited better cellular activity [193]. This RIP-1 analog is currently undergoing further optimization to produce a derivative with an increased potency. Another synthetic gatekeeper molecule that inhibits substrate entry into the 20S catalytic core was recently reported [194]. The molecule, TetrakisNTA (Figure 1.13), was shown to selectively bind to the His-tagged N-termini of α subunits in the 20S proteasome, which blocked the unfolded proteins from accessing the catalytic β subunits in a gatekeeper manner [194]. This inhibitor provides an unprecedented investigative tool that would allow the precise control and manipulation of the proteasome. Chloroquine, an anti-malaria drug, was very recently shown to inhibit proteasome by targeting the α - β subunit interface of the 20S proteasome [195]. This unique interaction was suggested to either interfere with substrate translocation or induce allosteric changes that render the neighboring proteolytic sites inactive. The discovery of a new targeting site on the proteasome is important for further drug development [195].

Another class of proteasome inhibitors that targets the non-catalytic component of the ubiquitin proteasome pathway is ubistatins (Figure 1.13), which is a synthetic proteasome inhibitor obtained from a chemical genetic screen in *Xenopus* extracts [196]. This class of inhibitors was found to block the proteolysis of cyclin B and Sic1, which

resulted in cell cycle arrest. Verma *et al.* have also elegantly demonstrated that ubistatins target an ubiquitin-ubiquitin interface that is essential for the recognition of polyubiquitinated substrates [196], disrupting a vital step in the early stages of the ubiquitin proteasome pathway, which results in the inhibition of proteasomal proteolysis.



Not surprisingly, the enzymatic cascade that dictates substrate specificity was also targeted. Particularly, the E3 ligase Mdm2, which is specific to the tumor suppressor p53 and is commonly mutated in cancers. Therefore, an increasing effort was put into developing Mdm2 inhibitors as a potential therapeutic strategy for the treatment of malignant cancers. Two Mdm2 inhibitors have been reported thus far and they are known as nutlin [197, 198] and MI-219 (Figure 1.14) [199]. Both of these inhibitors were shown to bind to Mdm2, which disrupts the Mdm2-p53 interaction resulting in the activation of the p53 pathway in cancer cell lines. Inhibition of Mdm2 and subsequent p53 activation was shown to result in cell cycle arrest and eventually apoptosis in cancer cell lines [198, 199]. These results further validate the targeting of Mdm2 as a potential drug candidate for cancer therapy. The first ubiquitin activating enzyme E1 inhibitor was recently reported and it was referred to as PYR-41 (Figure 1.14) [200]. Theoretically, such an inhibitor should block all ubiquitinations, but it was shown to preferentially induce apoptosis in transformed cells with wild type p53. Specifically, PYR-41 was shown to inhibit NFκB activation as well as increase levels of p53 and its downstream effectors [200]. This suggests that this new class of inhibitor may be useful as a potential cancer therapeutic agent as well as a valuable research tool for the biological studies of ubiquitination. Even though these non-proteasome targeting inhibitors cannot yet replace the proteasome active site-directed inhibitors, preliminary studies have been promising.

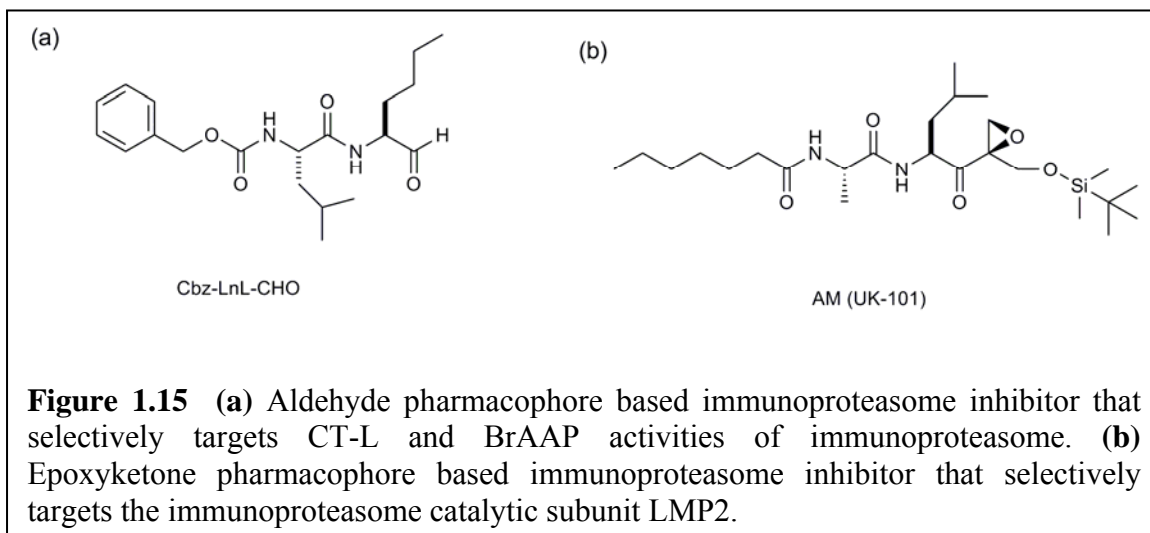


3. Immunoproteasome Inhibitors

The immunoproteasome is an alternative form of the proteasome that has a biased proteolytic cleavage pattern towards the generation of MHC class I antigens. Furthermore, its elevated expression level has been implicated in the pathogenesis of numerous physiological disorders. However, the advancement of immunoproteasome biology has been greatly hindered, due in large part to the lack of appropriate molecular probes such as immunoproteasome specific inhibitors. Consequently, much interest has been aroused due to the need for an immunoproteasome specific inhibitor, which would benefit immunoproteasome biology while also providing potential therapeutic interventions. Despite all the available proteasome inhibitors, there are still no known inhibitors that are selective for the immunoproteasome. Most inhibitors were demonstrated to target both the regular proteasome and immunoproteasome. This is due in large part to the high structural homology between the regular proteasome and immunoproteasome catalytic subunits, which has made the rational design of immunoproteasome inhibitors very challenging.

Nevertheless, recent effort has been focused on the optimization of available proteasome inhibitors that also target immunoproteasomes. For example, Orlowski *et al.* developed an aldehyde based immunoproteasome inhibitor that was shown to display greater than 100-fold preference for the CT-L and BrAAP activities of immunoproteasomes (Figure 1.15a). Even though it was shown to induce apoptosis in hematological cancers that constitutively express the immunoproteasome, its modes of actions are still unclear [201]. In addition, a novel class of inhibitor that was shown to specifically target the immunoproteasome catalytic subunit LMP2 was very recently developed by Ho *et al.* (Figure 1.15b) [126]. It was observed that the aggressive and metastatic prostate cancer cell line PC3 expresses higher levels of LMP2 compared to the benign prostate cancer cell line LNCaP. This differential expression level of LMP2 was also demonstrated to correlate with an increased susceptibility of these cancer cells to the LMP2 specific inhibitor UK-101 [126]. Preliminary data revealed that UK-101 does not inhibit the usual NF κ B activation pathway even though it was shown to induce apoptosis and cell cycle arrest in PC3 cells (unpublished data by Ho *et al.*). Nonetheless, these results suggest that cancer therapy using immunoproteasome inhibitors may be applied

not only to hematological cancers but also to solid tumors. One noteworthy advantage of this immunoproteasome targeting approach is that the immunoproteasome inhibitor will not target the essential regular proteasome that is present in all eukaryotic cells giving it lower toxicity. Finally, this type of therapeutic agent will help usher medicine into the era of personalized chemotherapeutics.



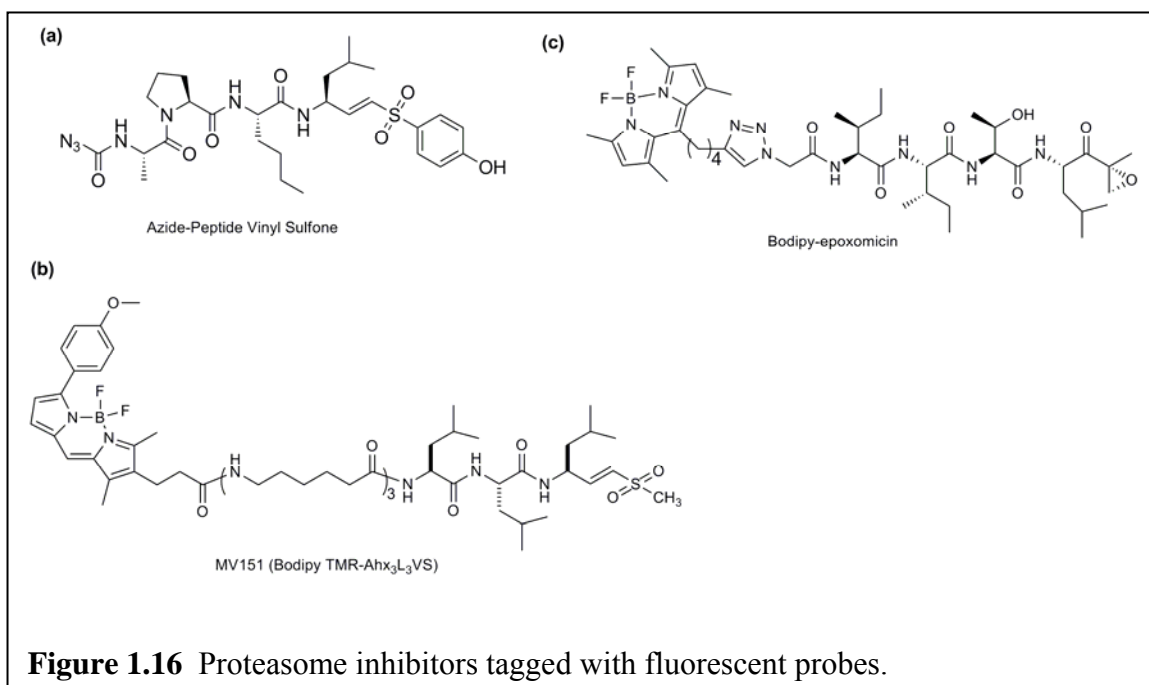
4. Activity-based Proteasome Probes

While the development of proteasome inhibitors for therapeutic purposes is a recent phenomenon, proteasome inhibitors have traditionally been used as molecular probes for the functional studies of the proteasome itself. Even though we have gained a great deal of understanding in the last two decades since the discovery of the proteasome, there are still many questions that remained to be answered. In the past, fluorogenic substrates were used to measure proteasomal activity. However, a new generation of activity-based proteasome probes is beginning to emerge, which will be of tremendous help in the functional dissection of the proteasome. Specifically, these activity-based proteasome probes would allow for the real-time measurement of proteasomal activity in living cells while retaining the integrity of the 26S proteasome, which may provide crucial information on protein homeostasis and possibly disease progression.

In general, this field of activity-based proteomics utilizes small-molecule inhibitors as activity-based probes that specifically interact with the catalytic sites of an enzyme by forming a stable covalent modification. Subsequently, the activity-based probes require a tag to provide a means to measure enzymatic activity. There are, however, many different tagging methods such as isotope, fluorescent, tandem, and affinity tags [202]. One of the first active site directed molecular probes that targets the proteasome is the tritiated lactacystin that was developed by Fenteany *et al* [160]. Using this tritium labeled lactacystin, Fenteany *et al.* was able to show that lactacystin selectively targets the proteasome via the covalent modification of the N-terminus threonine of the catalytic $\beta 5$ subunits. On the other hand, Kisselev and colleague developed an activity-based probe for the proteasomal C-L activity that is labeled with an azide moiety at its N-terminal (Figure 1.16a) [190]. This labeling enables the direct visualization of C-L activity, which may be very useful during the further investigation of the biological functions of C-L activity and its associated catalytic subunits. Another class of activity-based proteasome probes is the fluorescent- tagged proteasome inhibitors [203-206]. For example, MV151 (Bodipy TMR-Ahx₃L₃VS) (Figure 1.16b) developed by Verdoes *et al.* was shown to label all catalytic subunits of the proteasome both in vitro and in vivo [204]. The applications of this broad spectrum probe include clinical profiling of proteasome activity, biochemical analysis of subunit specificity of inhibitors, and

biological analysis of the proteasome function and dynamics in living cells [204]. Also, epoxomicin was modified into an activity-based probe by Verdoes *et al.* using the Bodipy dye (Figure 1.16c), which can be employed for the direct assessment of the catalytic activity of the proteasome in living cells [205].

The recently reported LMP2 specific inhibitor by Ho *et al.* is also an excellent candidate for the development of an activity-based probe for the immunoproteasome. Further research will be needed to determine a tagging method that would not affect its inhibitory activity. Importantly, the success of an activity-based immunoproteasome probe will provide an additional tool to elucidate the biological functions of the immunoproteasome.



5. Conclusions

Based on this preponderance of evidence, it is now widely accepted that the proteasome is a validated target for the development of therapeutic agents, particularly in cancer therapy. This is bolstered especially by the first FDA approved proteasome inhibitor bortezomib. Even though bortezomib has shown significant therapeutic success both as a single agent and as a combinatorial agent, drug-associated side effects still remain a major concern because it indiscriminately targets all proteasomes in the body. Consequently, considerable efforts have been put forth to develop low toxicity proteasome inhibitors. One such attempt is evidenced by the recent developments of proteasome inhibitors that target the non-catalytic sites such as the upstream components of the ubiquitin proteasome pathway and the non-catalytic subunits of the 26S proteasome. These indirect strategies have proven to be successful *in vitro* but they have yet to be tested for therapeutic intervention.

Another approach to circumvent the drug-associated side effects of broad spectrum proteasome inhibitors is the selective inhibition of proteasome in disease states. Despite the initial assumption that the primary function of immunoproteasome is the generation of MHC class I antigens, recent evidence suggests otherwise. The immunoproteasome has been implicated in the pathogenesis of some diseases as well as the maintenance of normal immune system function. Specifically, overexpression of immunoproteasome catalytic subunits has been observed in diseases such as neurodegenerative diseases, autoimmune diseases, and cancer. Therefore, the immunoproteasome has drawn considerable attention as a potential therapeutic target. Currently, the lack of an immunoproteasome specific inhibitor is hindering not only the advancement of immunoproteasome biology but also the validation of immunoproteasome as a drug discovery target. Hence, it is at this point that I began my research work in the development of immunoproteasome specific inhibitors and its potential application in cancer.

C. Hypothesis and Specific Aims

HYPOTHESIS

The hypothesis set forth in this work is that a selective immunoproteasome inhibitor will target cancers that predominantly express the immunoproteasome, while sparing normal cells, alleviating toxicity. This research project will focus on the development of an immunoproteasome catalytic subunit (LMP2) inhibitor using dihydroeponemycin as a reference molecule. The selected lead compound will then be tested in commercially available prostate cancer cell lines for its therapeutic potential.

SPECIFIC AIMS

Specific Aim 1. Synthesize a small library of novel analogs of dihydroeponemycin with selectivity for the immunoproteasome catalytic subunit LMP2. This study will require the synthesis of a small library of novel dihydroeponemycin analogs, with the goal of achieving significant selectivity for the immunoproteasome catalytic subunit LMP2. Earlier work has shown that dihydroeponemycin targets both regular and immunoproteasome catalytic subunits. Furthermore, the linear hydrocarbon chain of dihydroeponemycin was shown to direct its subunit binding preference towards that of the immunoproteasome. These synthetic experiments will produce a small library of dihydroeponemycin analogs with amino acid residue substitutions at the P2 region and modification of the P1' region with various commercially available protective groups.

Specific Aim 2. Evaluate the synthesized library for its ability to selectively target the immunoproteasome catalytic subunit LMP2. In this study, the synthesized analogs of dihydroeponemycin will be screened for their ability to selectively target LMP2 using a previously established competition assay. The murine lymphoma (EL4) cells will be treated concurrently with dihydroeponemycin analog and a competing agent to determine the immunoproteasome catalytic subunit LMP2 binding specificity of the analogs. Biotin-

tagged dihydroeponemycin and epoxomicin will be used in these experiments as competing agents as well as labeling probes for visualization.

Specific Aim 3. Investigate and characterize the immunoproteasome subunit binding specificity of the selected lead compound in human cancer cell lines. As a novel compound, the immunoproteasome catalytic subunit binding specificity of the selected lead compound will be determined and characterized in commercially available human cancer cell lines. A similar competition assay will be performed to reconfirm the LMP2 specificity of the selected lead compound in prostate cancer cell lines. The binding of the lead compound to LMP2 will also be further characterized in prostate cancer cells for its dose and time dependent properties as well as binding activity.

Specific Aim 4. Determine whether the selected lead compound is cytotoxic to normal endothelial cells that do not express immunoproteasomes. A 3D endothelial cell sprouting assay will be used to determine the cytotoxicity of the selected lead compound in normal endothelial cells. These cells do not express immunoproteasomes, which will enable the investigation of whether the selected compound will target the constitutive proteasomes. The results obtained could be translated into potential systemic cytotoxicity of the selected lead compound.

Specific Aim 5. Investigate the modes of action of the selected lead compound in commercially available prostate cancer cell lines. Using commercially available prostate cancer cell lines, the correlation between LMP2 inhibition and cell survival will be investigated using the MTT cell proliferation assay. Subsequently, the biological effects of the selected lead compound in apoptosis, cell cycle, proteolysis, and inflammation will be analyzed in the effort to help determine the mode of action of the selected lead compound. The results obtained will facilitate better understanding of not only the mode of action of the lead compound but also the biological functions of LMP2.

CHAPTER TWO: SYNTHESIS AND EVALUATION OF DIHYDROEPONEMYCIN ANALOGS

A. Introduction

The primary goal of this study is to synthesize and evaluate dihydroeponemycin analogs in order to discover a selective immunoproteasome catalytic subunit LMP2 inhibitor. Among the broad spectrum proteasome inhibitors that target both the regular proteasome and immunoproteasome, the epoxyketone dihydroeponemycin was selected for derivatization purposes, as it was previously reported to target only the LMP2, LMP7 and X catalytic subunits [207]. Dihydroeponemycin is composed of four different moieties, labeled as P3, P2, P1 and P1' (Figure 2.1a). The P3 moiety is an isooctanoic acid whose linear hydrocarbon skeleton was demonstrated to be responsible for targeting the immunoproteasome catalytic subunits [208]. While the P2 moiety is a serine amino acid residue, the P1 moiety contains the vital α',β' -epoxyketone pharmacophore that was shown to selectively target the catalytic subunits of proteasome via covalent modification [170]. Finally, the P1' moiety is a free hydroxyl group believed to be involved in determining immunoproteasome subunit binding specificity [209].

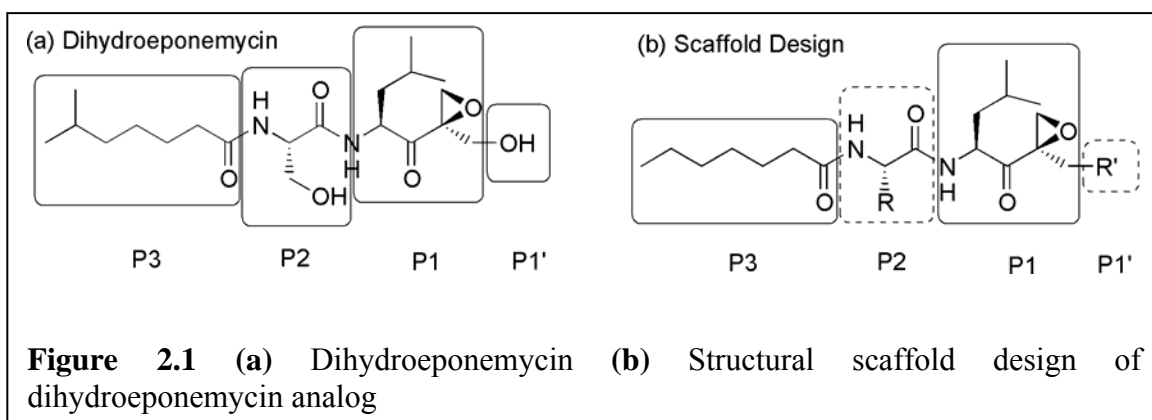
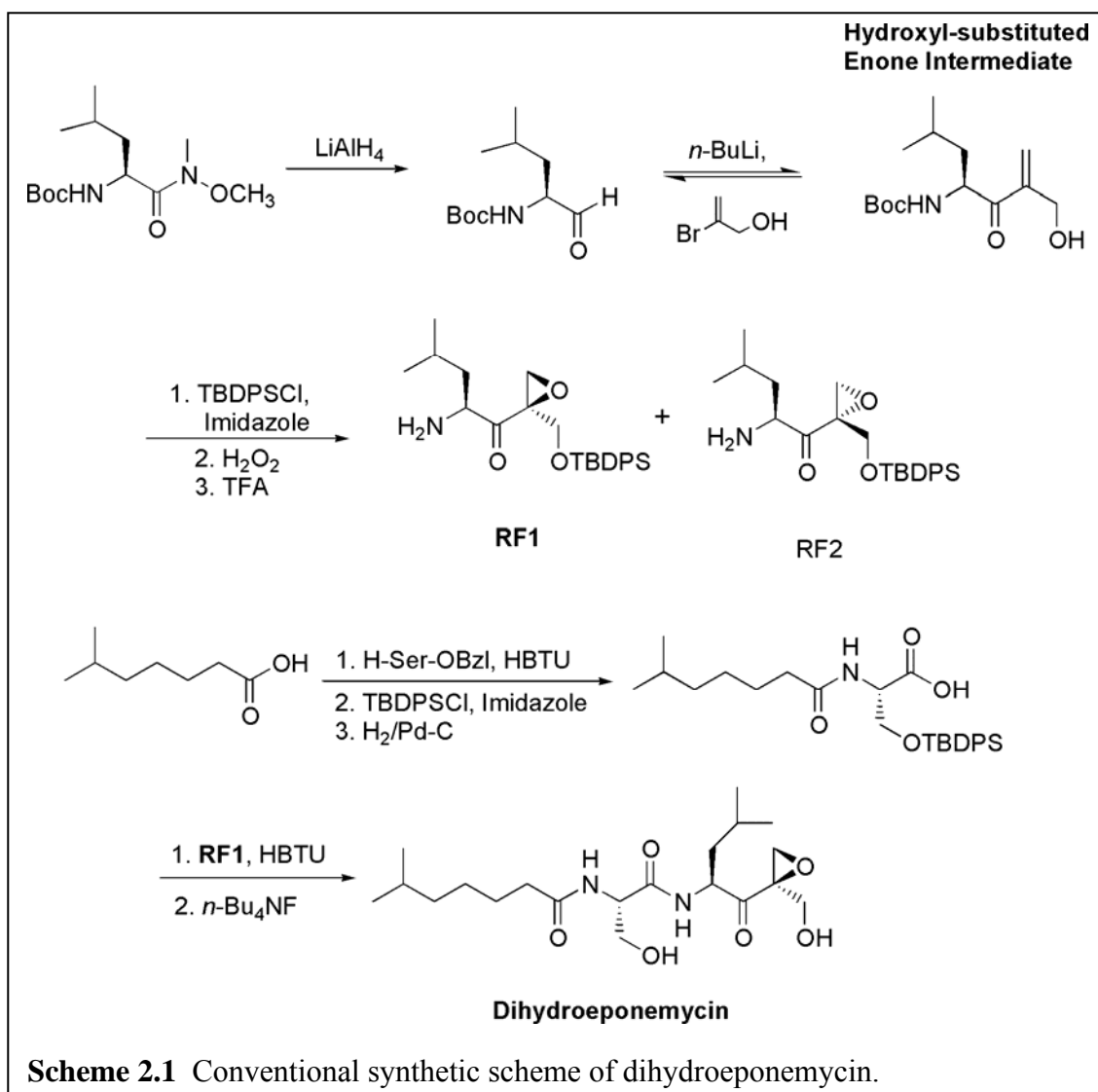


Figure 2.1 (a) Dihydroeponemycin (b) Structural scaffold design of dihydroeponemycin analog

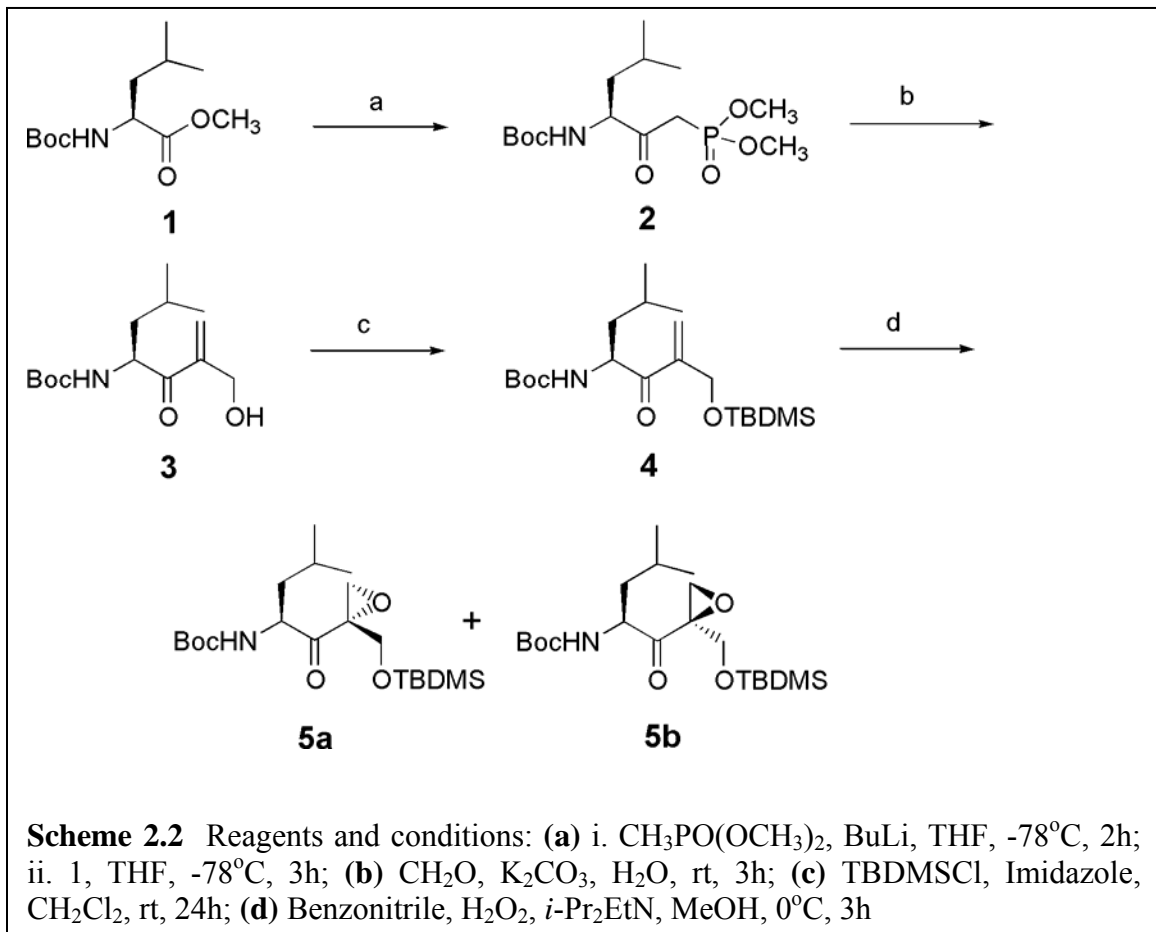
Based on this structural information, an isooctanoic-based dihydroeponemycin analog may provide an opportunity for the development of immunoproteasome specific inhibitors. As shown in Figure 2.1b, a dihydroeponemycin-based scaffold design will be used as a reference for the synthesis of the first generation of dihydroeponemycin analogs. Specifically, the P3 and P1 moieties will be fixed while the P2 and P1' moieties will be replaced with a variety of amino acid residue and a plethora of commercially available hydroxyl protective groups, respectively. Nevertheless, synthetic challenges presented themselves and were resolved by the development of an alternative and improved synthetic strategy for dihydroeponemycin. This strategy allowed for the modification of the two moieties and combinations of the individual modification to generate numerous dihydroeponemycin analogs. The small library was then screened for its immunoproteasome catalytic subunit specificity using a competition assay. In order to successfully carry out the competition assay, biotin-tagged dihydroeponemycin and epoxomicin were synthesized to serve as competing agents as well as labeling probes.

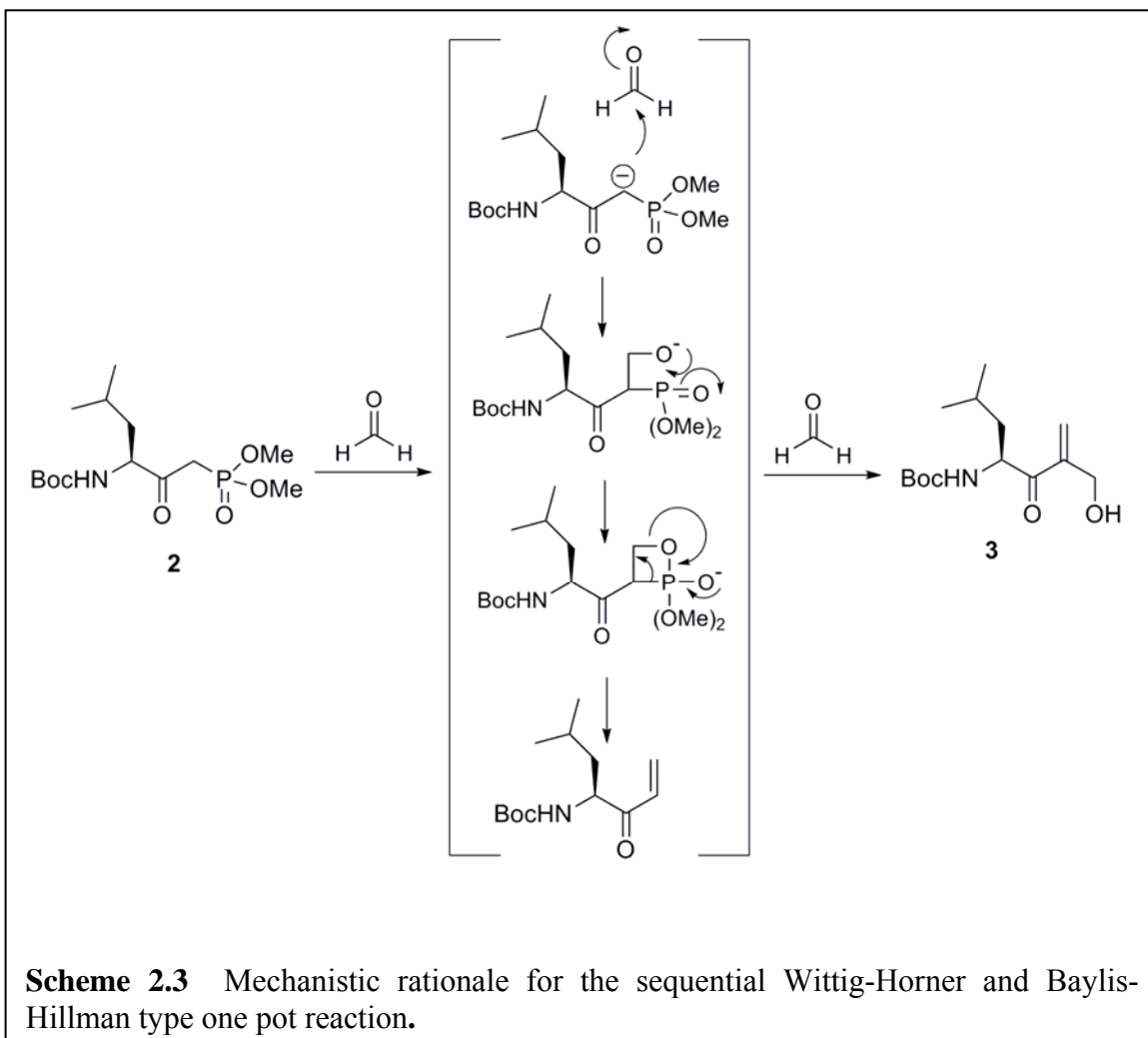
B. Development of an Improved Synthetic Strategy

Even though several synthetic routes have been reported over the years, the efficient synthesis of dihydroeponemycin has remained a challenge due in large part to the lack of an efficient synthetic approach for the hydroxymethyl-substituted enone intermediate (Scheme 2.1). This particular intermediate is the precursor to the right hand fragment of dihydroeponemycin, which contains the P1 and P1' moieties. Such a bottleneck has undoubtedly hindered the large scale preparation of P1' dihydroeponemycin derivatives. Therefore, an improved synthetic strategy for the hydroxymethyl-substituted enone intermediate was developed to overcome this particular obstacle [210].



Briefly, the starting material Boc-Leu-OMe (**1**) was prepared from the reaction of Boc-Leu-OH with iodomethane in dimethylformamide (DMF). The following reaction of Boc-Leu-OMe (**1**) with dimethyl methylphosphonate treated with *n*-butyllithium (BuLi) yielded compound **2**. Finally, the combination of Wittig-Horner and Baylis-Hillman type one-pot reactions produced the hydroxymethyl-substituted enone **3** in high yield (Scheme 2.2). This reaction may be mechanistically rationalized as shown in Scheme 2.3. In the following steps of Scheme 2.2, the derivatization of the P1' moiety occurs. The resulting enone **3** could be modified with a variety of commercially available hydroxyl protective group. For example, enone **3** was treated with *tert*-butyl dimethylchlorosilane (TBDMSCl) to yield compound **4**. Next, the epoxidation of **4** with hydrogen peroxide afforded two epoxyketone isomers **5a** and **5b** in a 1:1.5 mixture that were readily separated by flash column chromatography using an elution system (hexanes-ethyl acetate = 10:1, v/v). The isomer 2-(R)-epoxide **5b**, which migrated faster than 2-(S)-epoxide **5a** isomer in thin-layer chromatography (TLC), was found to have the same configuration as that of eponemycin. Although epoxidation could occur at a higher stereo-selectivity, it is of great interest to employ both isomers for biological study purposes [210]. While the *S* configuration of the epoxide in the **5a** isomer has been shown to be inactive in epoxomicin and dihydroeponemycin, it is essential to utilize the dihydroeponemycin analog containing the inactive epoxide as negative control (For more details, please refer to [210]). This novel synthetic strategy has an improved yield as well as a simpler methodology, which has greatly facilitated the synthesis and derivatization of dihydroeponemycin analogs.



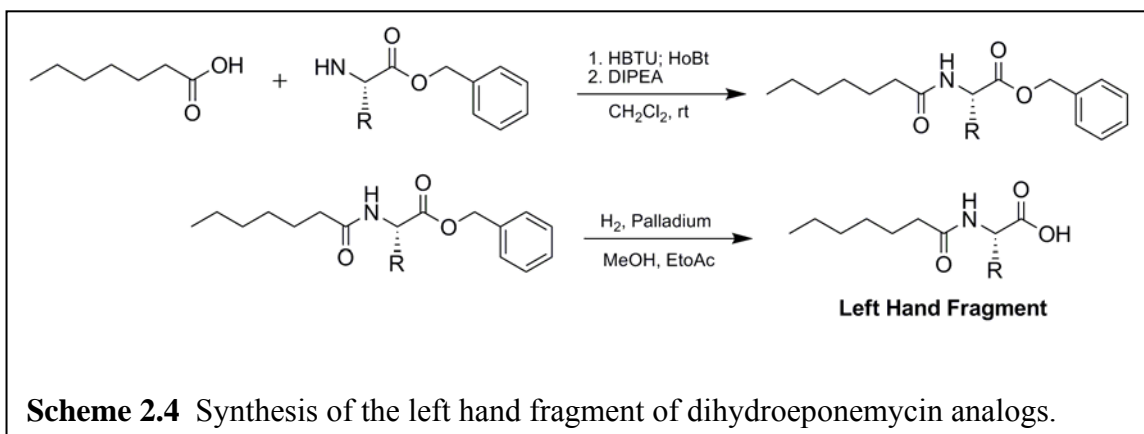


C. Synthesis of Dihydroeponemycin Analogs

In the course of this study, three major synthetic routes were carried out in order to obtain a small library of dihydroeponemycin analogs. Generally, the P2 moiety is replaced with an alternative amino acid residue and the P1' moiety is modified using a variety of commercially available hydroxyl protective groups. The three general procedures utilized in this study are referred to as General Reactions 1-3. General Reaction 1 involves an amide linkage formation between heptanoic acid and an amino acid residue, which gives the left hand fragment containing the P3 and P2 moieties. General Reaction 2 involves the derivatization of the free hydroxyl group in the hydroxymethyl-substituted enone (**3**), which was described in the previous section. Finally, General Reaction 3 is the final coupling reaction between the right hand and left hand fragments. These reactions are further illustrated below:

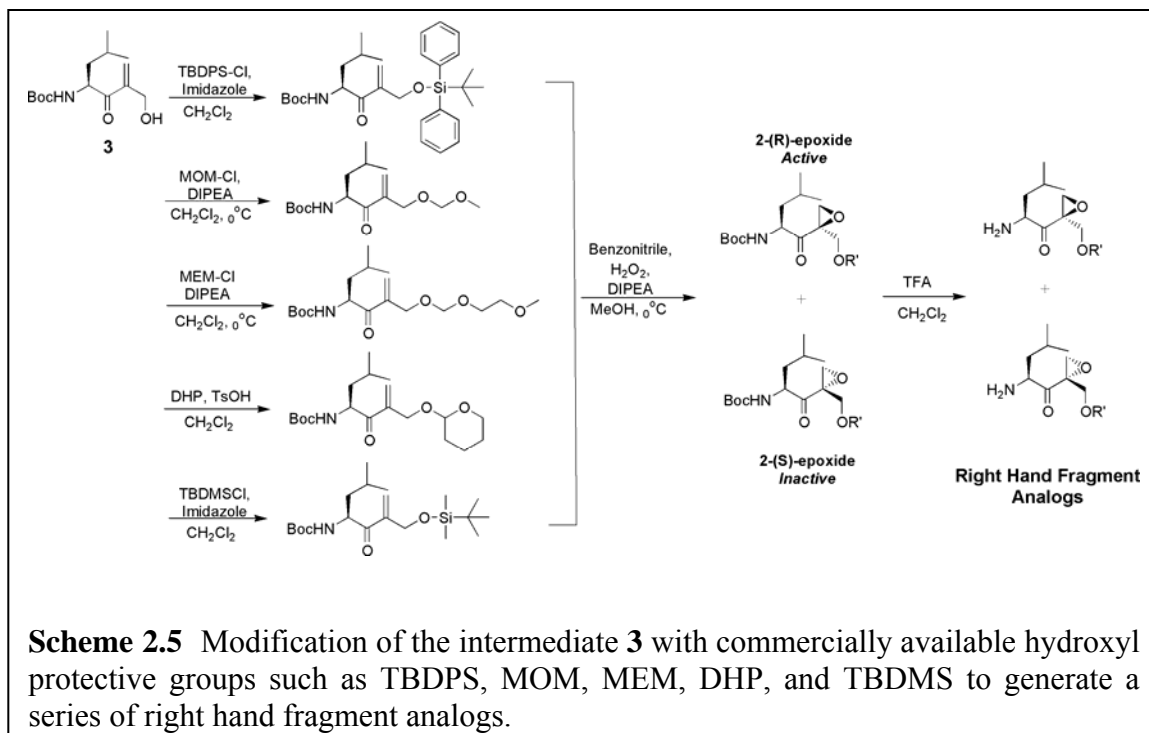
General Reaction 1:

In order to determine whether the serine residue in the P2 moiety plays a role in proteasomal inhibition, alternative amino acid residues such as alanine was used in place of serine. Equimolar amounts of heptanoic acid and amino acid residue with protected carboxyl group were added to the peptide coupling reagents O-Benzotriazole-N,N,N',N'-tetramethyluronium hexafluorophosphate (HBTU) and 1-hydroxybenzotriazole (HoBt) hydrate in methylene chloride (CH₂Cl₂). The coupling reagent HoBt was used particularly to help reduce the formation of stereoisomers at the **R** position. Finally, N,N-diisopropylethylamine (DIPEA) was added last to the reaction solution as a base to accelerate the reaction. The resulting product mixture is easily purified via silica gel column chromatography. Finally, the benzyl protective group is cleaved via hydrogenation in methanol (MeOH) and ethyl acetate (EtOAc) giving a free hydroxyl group for the next coupling reaction (See Scheme 2.4).



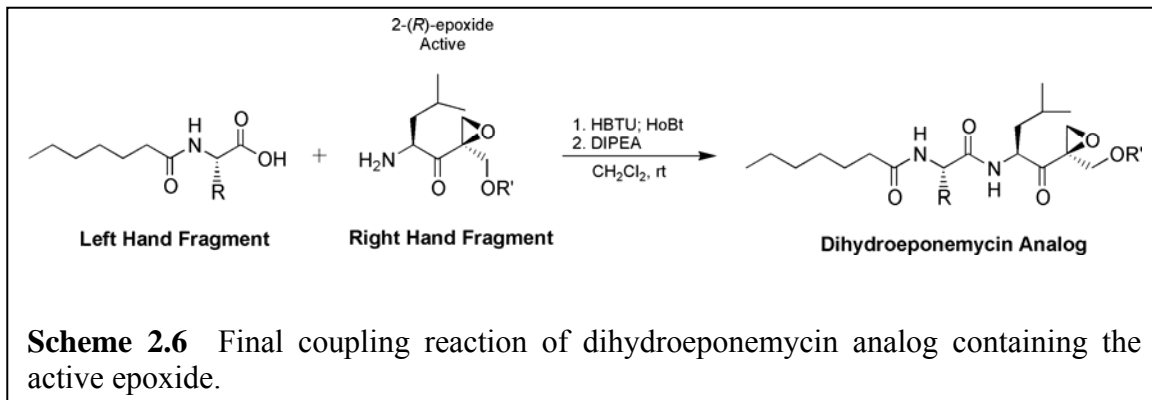
General Reaction 2:

Derivatization of the P1' moiety is achieved via modifying the free hydroxyl group of the hydroxymethyl-substituted enone (**3**) with commercially available hydroxyl protective groups such as *tert*-butyldiphenylsilyl (TBDPS), TBDMS, methoxy methyl (MOM), methoxyethoxy methyl (MEM), and tetrahydropyran (THP). Briefly, hydroxymethyl-substituted enone (**3**) obtained from the reactions described in the previous section was subjected to numerous derivatizations before epoxidation. This particular succession of reactions has been determined experimentally to give a higher yield compared to when epoxidation occurs before derivatization. The discrepancy may be explained by the steric hindrance of the epoxide, which could prevent the coupling of the protective groups to the hydroxyl group. The epoxidation reaction also yielded two diastereomers at the C-2 stereocenter, which gave a mixture of epoxide epimers. The mixtures were readily separated by column chromatography and the stereochemistry of these epoxide rings has been previously determined [169]. Specifically, Sin *et al.* reported that the epoxide ring with an *R* configuration is the active form of epoxide found in epoxomicin [169]. Finally, the Boc protecting group is cleaved with excess trifluoroacetic acid (TFA) in CH₂Cl₂ (See Scheme 2.5). Upon completion of the reaction, TFA is thoroughly removed by drying under vacuum overnight.

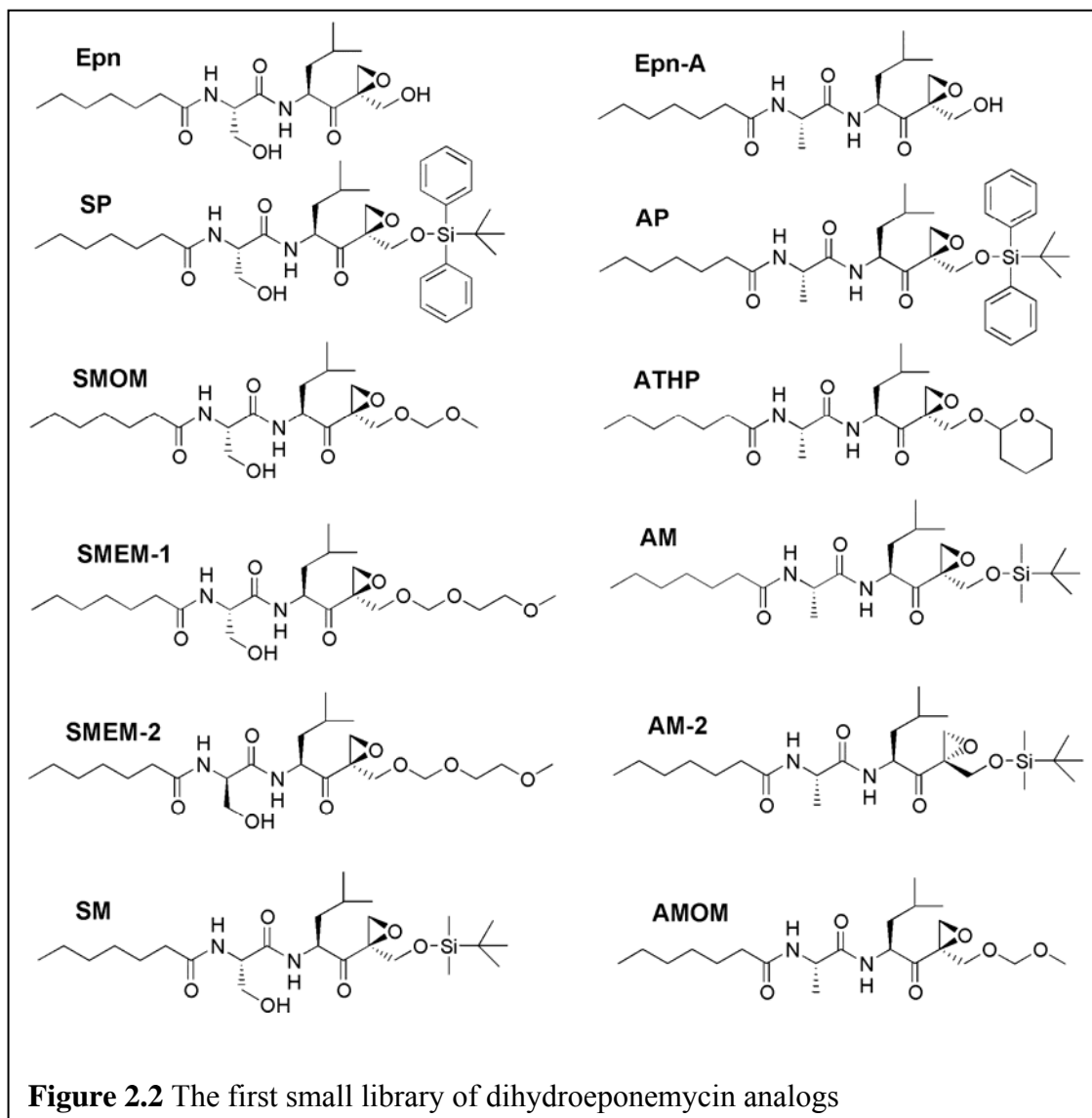


General Reaction 3:

The final coupling reaction to obtain the dihydroeponemycin analogs containing the active epoxide was achieved by adding equimolar amounts of active right hand and left hand fragments to a solution of HBTU and HoBt hydrate in methylene chloride. Similarly, DIPEA was added last to the reaction mixture (See Scheme 2.6). The resulting product mixture was purified via silica gel column chromatography. The dihydroeponemycin analogs were then structurally confirmed using nuclear magnetic resonance (NMR).

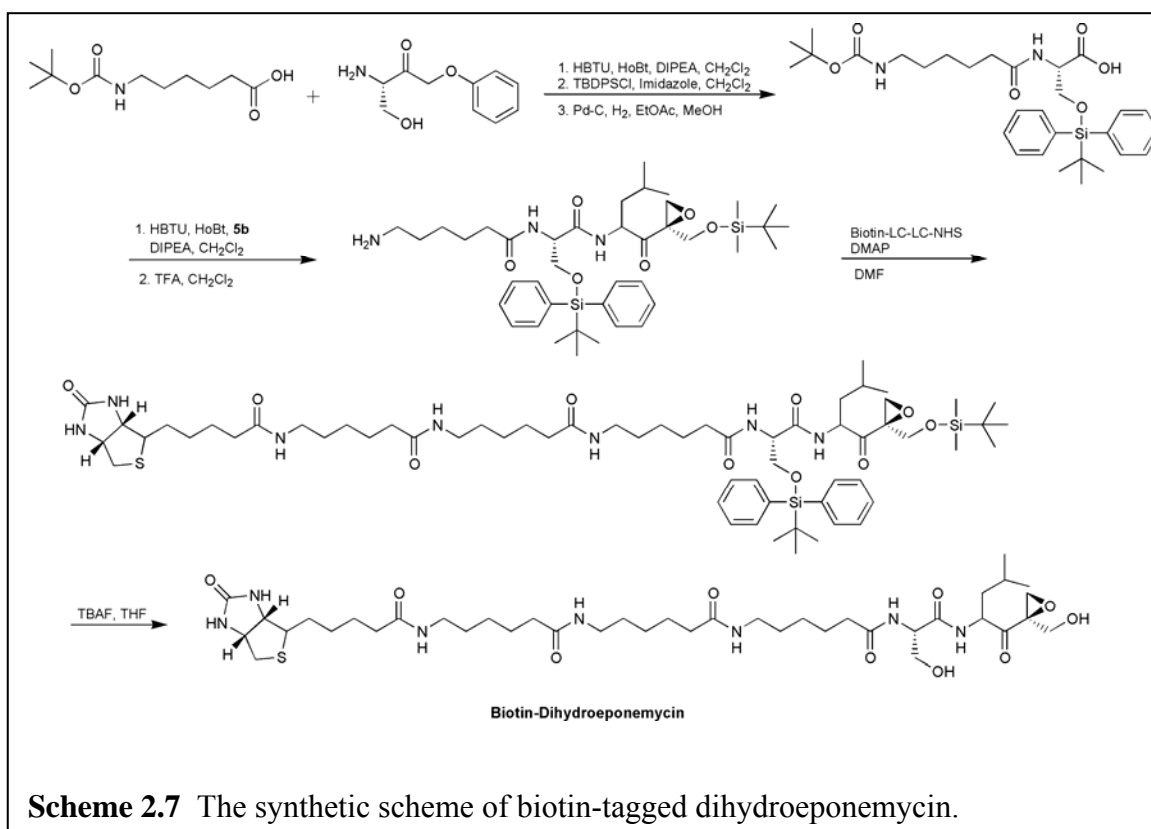


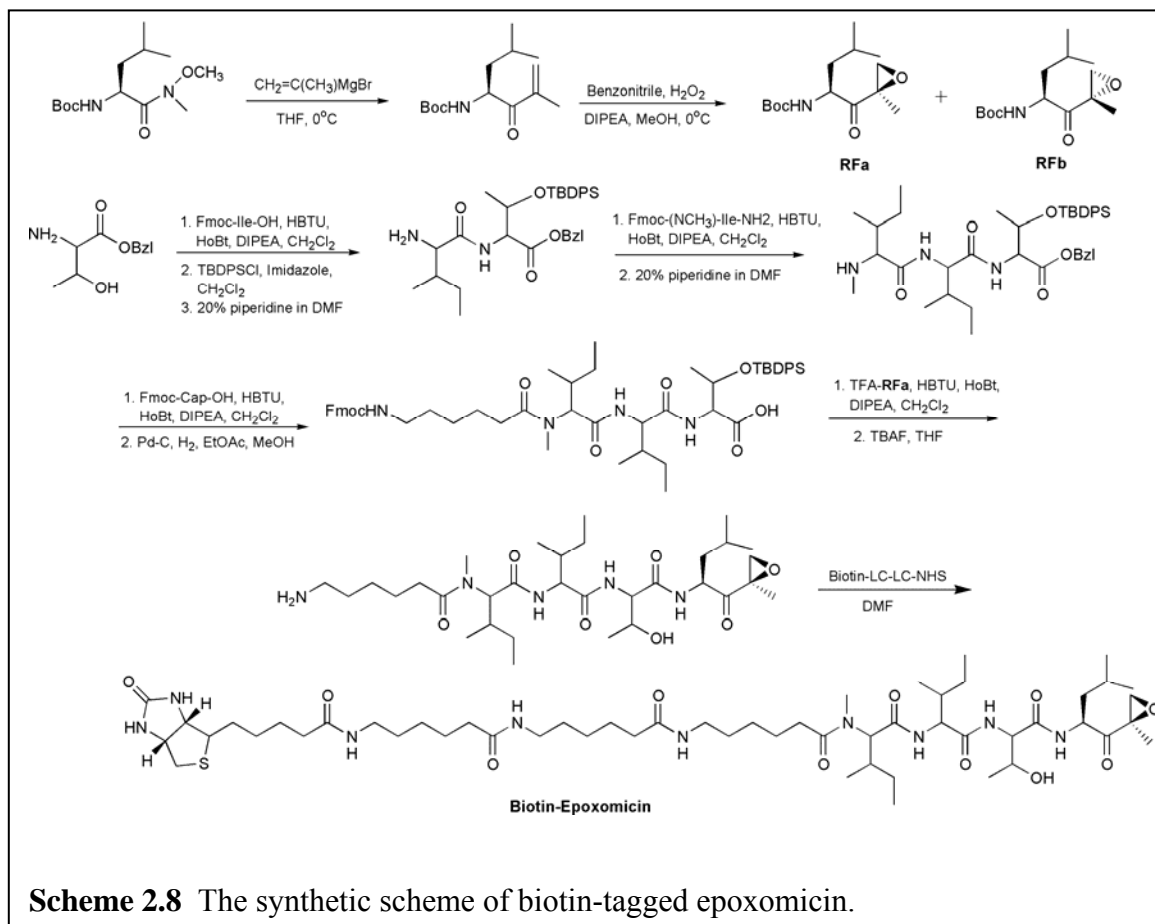
Based on these general reactions, a total of 12 compounds were successfully synthesized as the first small library of dihydroeponemycin analogs (Figure 2.2). Among these derivatives is **Epn** (Figure 2.2). Even though its P3 moiety is a heptanoic acid instead of an isooctanoic acid, it has been shown to exhibit very similar binding pattern and biological activity as dihydroeponemycin (data not shown). Therefore, **Epn** would be used in the following experiments in place of dihydroeponemycin. Furthermore, these analogs can also be divided into two categories: those with a serine residue and those with an alanine residue at the P2 site. As mentioned earlier, dihydroeponemycin contains two stereocenters, which are at the C-2 and C'-2 positions. While the active configurations at these stereocenters have been previously determined [169, 207], the library of dihydroeponemycin analogs has included two compounds containing the inactive configurations for confirmation purposes. As shown in figure 2.2, **SMEM-2** contains the inactive *R* configuration at C'-2 position and **AM-2** contains the inactive *S* configuration at C-2 position. The alternative configurations of **SMEM-2** and **AM-2** were determined by comparison of NMR data between the inactive and active configurations found in the other analogs. Subsequently, these analogs underwent a screening process using a competition assay in order to select a lead compound that specifically targets the immunoproteasome catalytic subunits.



D. Synthesis of Biotin Probes

In order to successfully carry out the competition assay, biotin-tagged dihydroeponemycin and epoxomicin were needed to serve as competing agents as well as labeling probes for visualization purposes. The syntheses of biotin-tagged dihydroeponemycin and epoxomicin have been previously reported by Sin *et al.* [169, 207]. However, the previously described synthetic strategy of hydroxymethyl-substituted enone (**3**) was incorporated along with some minor changes, resulting in the improved synthetic schemes of biotin-tagged dihydroeponemycin and epoxomicin which are shown in Schemes 2.7 and 2.8. These molecules were structurally verified using NMR and mass spectrometry.

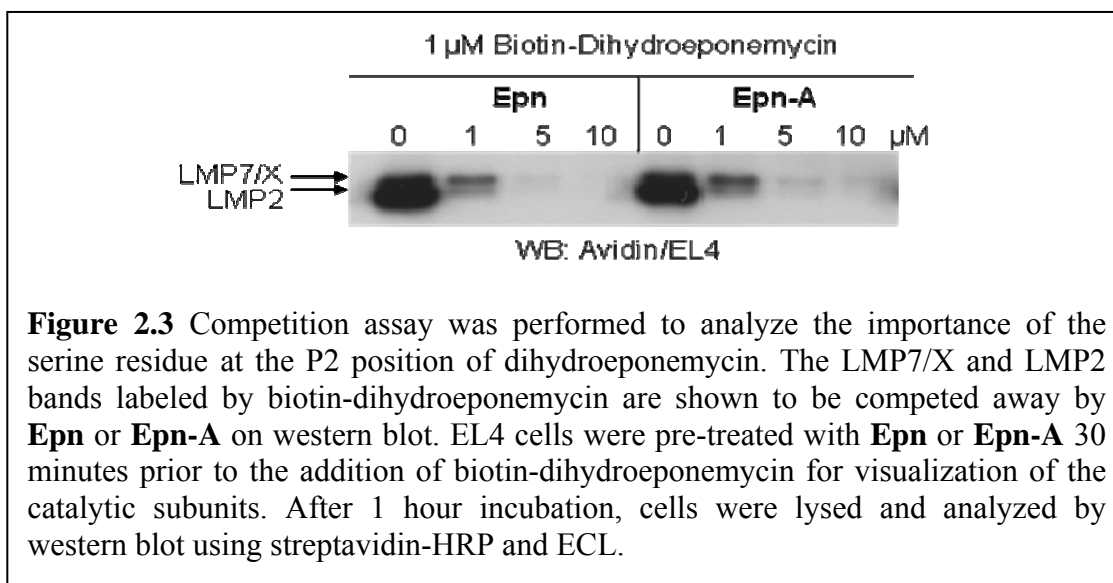




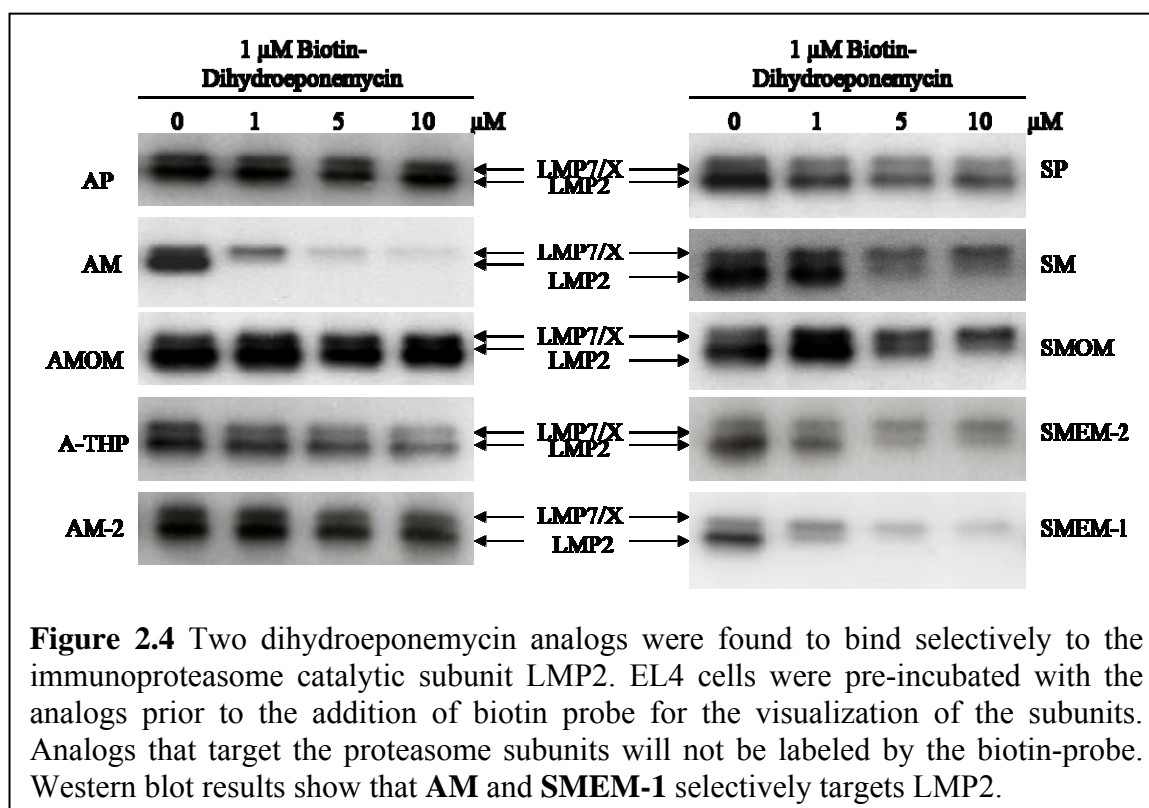
E. Screening of Dihydroeponemycin Analogs

In order to screen for an immunoproteasome catalytic subunit specific compound, the competition assay by which a dihydroeponemycin analog competes with biotin-tagged dihydroeponemycin for the immunoproteasome catalytic subunit LMP2 was developed. Briefly, the murine lymphoma EL4 cells were treated with increasing concentrations of the dihydroeponemycin analog 30 minutes prior to the addition of biotin-tagged dihydroeponemycin or epoxomicin and then incubated for an additional hour. Western blotting was subsequently carried out using a streptavidin-horseradish peroxidase (HRP) antibody that specifically labels biotin. The visualization of biotinylated proteins indicates the presence covalent protein adduct formation [169]. The EL4 cell system was used in this screening assay because these cells express high levels of both the constitutive and immunoproteasome catalytic subunits. It was expected that pre-incubation of a LMP2-specific inhibitor in EL4 cells will result in the covalent modification of the threonine catalytic residue of the LMP2 subunit. The occupied LMP2 subunit will then prevent further modification by the biotin-tagged assay probes. Without the probes, the LMP2 catalytic subunit will not be visualized on western blot. On the other hand, catalytic subunits that are not targeted by the LMP2 inhibitor will be covalently labeled by the assay probe and visualized on western blot.

Analogs **Epn** and **Epn-A** were first tested to determine whether the hydroxyl group on the serine residue that is commonly present in both epoxomicin and dihydroeponemycin plays an important role in the preferential targeting of immunoproteasome catalytic subunits. As shown in Figure 2.3, a major 23 kDa and a minor 25 kDa proteins were observed in cells that were treated with only biotin-tagged dihydroeponemycin. These two bands have been previously identified as LMP7/X and LMP2 [168, 208]. As expected, these protein bands were efficiently competed away by excess **Epn**, which is structurally and biologically very similar to dihydroeponemycin. In addition, the bands were also efficiently competed away by **Epn-A** (Figure 2.3). Both analogs were observed to compete with biotin-dihydroeponemycin at a comparable rate. This result suggested that the serine residue of dihydroeponemycin is not crucial for its immunoproteasome catalytic subunit binding [210].

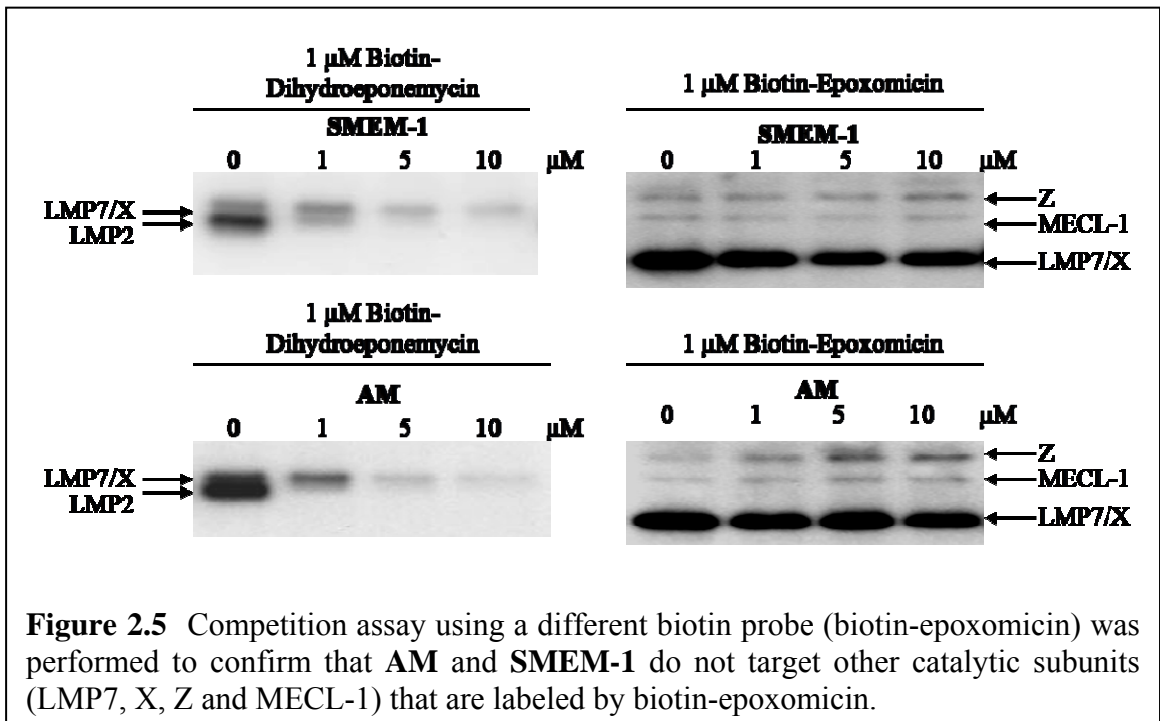


Next, we tested the remaining dihydroeponemycin analogs in a similar competition assay. As shown in Figure 2.2, the heptanoic acid moiety was retained while the P2 and P1' sites were modified. First, the commonly available short linear MOM hydroxyl protective group was used to prepare analogs **AMOM** and **SMOM**. These substitutions induced a significant loss in the potency and specificity compared to **Epn** (Figure 2.4). Similarly, analogs with a bulky TBDPS protective group (**AP** and **SP**) or THP protective group (**ATHP**) also resulted in the loss of subunit-binding activity against immunoproteasomes.



Surprisingly, when the MOM protective group was replaced with a longer linear MEM protective group (**SMEM-1**), a relatively higher specificity towards LMP2 was observed (Figure 2.4). However, analog **SMEM-2**, with alternative chirality at its P2 site, lost its LMP2 selectivity shown in analog **SMEM-1**. This discrepancy confirms that the *S* configuration of P2 moieties is the active configuration. Furthermore, when a TBDMS protective group was attached at the C-terminal hydroxyl group with an alanine residue at its P2 site (**AM**), an even higher specificity towards the LMP2 subunit was observed (Figure 2.4). Pre-incubation of EL4 cells with 1 μM of the analog **AM** was sufficient to covalently modify all of the LMP2 subunit in EL4 cells, therefore preventing further modification of the LMP2 subunit by biotin-tagged dihydroeponemycin. This resulted in the selective attenuation of the LMP2 protein band as shown on the western blot (Figure 2.4). However, when the alanine residue of **AM** was substituted with a serine residue, which produced analog **SM**, the LMP2 specificity was dramatically reduced (Figure 2.4). In addition, when the inactive configuration of the epoxide moiety was used (**AM-2**), the LMP2 selectivity of **AM** was completely abolished, as expected (Figure 2.4).

On the other hand, a similar competition experiment was carried out using an alternative assay probe (biotin-epoxomicin), which was previously shown to covalently label proteasome subunits LMP7, X, MECL-1, and Z [169]. Western blot results clearly showed that analogs **AM** and **SMEM-1** do not compete with biotin-epoxomicin (Figure 2.5). This negative result further supported the conclusion that both analogs **AM** and **SMEM-1** selectively target the LMP2 subunit but not other proteasome subunits [126].



F. Conclusions

This study was undertaken to develop and evaluate dihydroeponemycin analogs as inhibitors for the immunoproteasome catalytic subunit LMP2. The development of the first immunoproteasome inhibitor would contribute tremendously to the advancement of immunoproteasome biology as well as the investigation into the pathogenesis of many diseases. The design and synthesis of the first generation of dihydroeponemycin analogs yielded a small library of 12 molecules, which was focused on the modification of the P1' site utilizing a variety of hydroxyl protective groups. These analogs were then screened for LMP2 selectivity via competition assay. The results obtained from the screening assay produced a promising lead compound **AM**, which was shown to exhibit the highest selectivity for the LMP2 subunit (Figure 2.4 and 2.5). These results also revealed that when the P1' site of dihydroeponemycin analogs were modified with a linear, cyclic, or large bulky protective group, not only did they not show selectivity towards any of the immunoproteasome catalytic subunits, their ability to bind to the proteasome was completely abolished as well (Figure 2.4). In addition, the P2 moiety might play a role in determining subunit specificity because a noticeable difference in the LMP2 selectivity between the analogs **SM** and **AM** were observed on western blot (Figure 2.4). Therefore, the lead compound will undergo further optimization by modifying the P2 site with various amino acid residues while the rest of the molecular structure is retained.

G. Methods and Materials

The following includes the experimental protocols and structural characterization of the dihydroeponemycin analogs and biotin-tagged probes. In addition, the experimental procedure of the competition assay is further elaborated.

General Remarks: Unless otherwise stated, all reactions were carried out under Nitrogen with dry freshly distilled solvents, over-dried glassware, and magnetic stirring. All solvents were reagent grade. Tetrahydrofuran (THF) was distilled from sodium/benzophenone. CH₂Cl₂ was distilled from calcium hydride. Diethyl ether anhydrous was purchased from EMD Chemicals and used without further purification. All other reagents were purchased from Sigma-Aldrich and used without further purification. All reactions were monitored by TLC using E. Merk 60^{F254} pre-coated silica gel plates. Flash column chromatography was performed using E. Merk silica gel 60 (particle size 0.040-0.063mm) and with the indicated solvents. ¹H and ¹³C NMR spectra were recorded in deuterated chloroform (CDCl₃) using a Varian 300MHz spectrometer at ambient temperature using an internal deuterium lock unless stated otherwise. Chemical shift are referenced to residual chloroform ($\delta = 7.27$ ppm for ¹H and $\delta = 77.0$ ppm for ¹³C). High and low resolution mass spectra were carried out by the University of Kentucky Mass Spectrometry Facility.

(4S)-3-(tert-butoxycarbonyl)amino-5-methylhexa-2-one-1-dimethylphosphonate (2).

To a solution of dimethyl methylphosphonate (9mL, 82.3mmol) in THF (50mL) at -78°C , *t*-BuLi (2.5M in hexane, 33mL, 82.3mmol) was added drop wise. The solution was stirred at -78°C for 2h. A solution of Boc-Leu-OCH₃ (12) (5.05g, 20.6mmol) in THF (30mL), was then added to the mixture at -78°C . After stirring for 3h, the resulting mixture was poured into water (100mL) and extracted with diethyl ether (3 \times 80mL). The organic layers were combined, washed with brine, dried with Na₂SO₄, filtered and concentrated under reduced pressure. The product was then subjected to flash column chromatography (hexane:EtOAc, 1:1) to give a soft white solid **2** (11.5g, 93%): ¹H NMR: $\delta = 5.22$ (d, 1 H, NH), 4.34 (m, 1 H, 3-H), 3.81 (d, 3 H, ³J_{H-P} = 3.3Hz, CH₃O(PO)OCH₃), 3.77 (d, 3 H, ³J_{H-P} = 3.3Hz, CH₃O(PO)OCH₃), 3.22 (dd, 1 H, ²J_{H-P} =

94.8Hz, $^2J_{\text{H-H}} = 13.8\text{Hz}$, 1-H^a), 3.22 (dd, 1 H, $^2J_{\text{H-P}} = 50.1\text{Hz}$, 1-H^b), 1.67 (m, 2 H, 6-H, 5-H^a), 1.45 (s, 9 H, H_{Boc}), 1.38 (m, 1 H, 5-H^b), 0.96 (d, $^3J = 3.6\text{Hz}$, 3 H, CH₃CHCH₃), 0.94 (d, 3 H, $^3J = 3.6\text{Hz}$, 3 H, CH₃CHCH₃) ppm. ¹³C NMR: $\delta = 202.41$ (C-2), 155.62 (CO_{Boc}), 76.80 (Boc), 59.09 (C-1), 53.40 (C-3), 40.14 (C-4), 39.15 (CH₃O(PO)OCH₃), 37.43 (CH₃O(PO)OCH₃), 28.62 (Boc), 25.14 (C-5), 23.59 (C-5)CH₃, 21.85 (C-6) ppm. HRMS (EI): $m/z = 338.1709$, calcd. for C₁₄H₂₇DNO₆P: $m/z = 338.1712$. Synthetic procedures were performed as previously described [210].

(4S)-4-(tert-butoxycarbonyl)amino-2-hydroxy-methyl-6-methylhept-1-en-3-one (3).

K₂CO₃ solution (1.51g, 10.2mmol, in 33.3mL H₂O) was added drop wise using a dropping funnel over a period of 15 min to a vigorously stirring solution of **2** in formaldehyde (10mL, 360mmol). The solution was then stirred vigorously at room temperature for 4h. The resulting mixture was poured into water (80mL) and the crude product was extracted with diethyl ether (3 × 50mL). The combined organic layers were washed with brine, dried with Na₂SO₄, filtered and concentrated under reduced pressure. Flash column chromatography (hexane:EtOAc, 3:1) afforded **3** as a yellowish oil (5.15g, 55.6%). ¹H NMR: $\delta = 6.24$ (s, 1 H, 1-H^a), 6.12 (s, 1 H, 1-H^b), 5.13 (br, 1 H, NH), 5.03 (m, 1 H, 4-H), 4.34 (dd, 2 H, $^2J = 15.3\text{Hz}$, $^2J = 15.6\text{Hz}$, (C-2)CH₂), 2.38 (br, 1 H, OH), 1.74 (m, 1 H, 6-H), 1.50 (m, 1 H, 5-H^a), 1.43 (s, 9 H, H_{Boc}), 1.38 (m, 1 H, 5-H^b), 1.01 (d, $^3J = 6.6\text{Hz}$, 3 H, CH₃CHCH₃), 0.92 (d, 3 H, $^3J = 6.6\text{Hz}$, 3 H, CH₃CHCH₃) ppm. ¹³C NMR: $\delta = 201.86$ (C-3), 155.69 (CO_{Boc}), 145.01 (C-2), 126.44 (C-1), 76.84 (Boc), 62.66 (C-2)CH₂, 53.31 (C-4), 43.06 (C-5), 28.70 (Boc), 25.37 (C-6), 23.74 (C-7), 22.08 (C-6)CH₃ ppm. HRMS (EI): $m/z = 272.1844$, calcd. for C₁₄H₂₄DNO₄: $m/z = 272.1846$. Synthetic procedures were performed as previously described [210].

(4S)-4-(tert-butoxycarbonyl)amino-2-tert-butyltrimethylsilyloxymethyl-6-methylhept-1-en-3-one (4).

To a solution of **3** (137mg, 0.50mmol) in CH₂Cl₂ (5mL), imidazole (100mg, 1.46mmol) and *tert*-butyltrimethylsilyl chloride (228mg, 1.51mmol) was added. After stirring at room temperature for 24h, the resulting mixture was concentrated under reduced pressure and was subjected to flash column chromatography (hexane:EtOAc, 10:1) giving **4** (158mg, 81%) as a yellowish oil. ¹H NMR: $\delta = 6.20$ (d, $^2J = 10.2\text{Hz}$, 2 H,

1-H), 5.07 (m, 2 H, NH, 4-H), 4.36 (dd, $^2J = 30.90\text{Hz}$, $^2J = 14.70\text{Hz}$, 2 H, (C-2)CH₂), 1.72 (m, 1 H, 6-H), 1.48 (m, 1 H, 5-H^a), 1.42 (s, 9 H, H_{Boc}), 1.31 (m, 1 H, 5-H^b), 1.01 (d, $^3J = 6.6\text{Hz}$, 3 H, CH₃CHCH₃), 0.91 (s, 9 H, (C-2)*t*Bu-H), 0.90 (d, 3 H, $^3J = 6.4\text{Hz}$, 3 H, CH₃CHCH₃), 0.07 (d, $^4J = 5.6\text{Hz}$, 6 H, (C-2)CH₃SiCH₃) ppm. Synthetic procedures were performed as previously described [210].

(2*RS*,4*S*)-4-(tert-butoxycarbonyl)amino-2-tert-butyltrimethylsilyloxymethyl-6-methyl-1,2-oxiranyl-heptane (5a, 5b). To a solution of **4** (158mg, 0.40mmol) in MeOH (5mL) at 0°C was added benzonitrile (0.3mL, 3.0mmol), H₂O₂ (0.45mL, 50% solution in H₂O, 7.8mmol), and diisopropylethylamine (0.5mL, 3.0mmol). The reaction was stirred at 0°C for 3h. The resulting mixture was concentrated under reduced pressure and subjected to flash column chromatography to yield **5a** and **5b** with a ratio of 1:1.5 (107mg, 65%). **5b** ¹H NMR: δ = 4.80 (br, 1 H, NH), 4.43 (d, $^2J = 11.7\text{Hz}$, 1 H, (C-2)CH^a₂), 4.34 (m, 1 H, 4-H), 3.57 (d, $^2J = 11.4\text{Hz}$, 1 H, (C-2)CH^b₂), 3.18 (d, $^2J = 4.3\text{Hz}$, 1 H, 1-H^a), 3.01 (d, $^2J = 4.3\text{Hz}$, 1 H, 1-H^b), 1.74 (m, 1 H, 6-H), 1.62 (m, 1 H, 5-H^a), 1.41 (s, 9 H, H_{Boc}), 1.07 (m, 1 H, 5-H^b), 0.99 (d, $^3J = 6.3\text{Hz}$, 3 H, CH₃CHCH₃), 0.94 (d, 3 H, $^3J = 6.3\text{Hz}$, 3 H, CH₃CHCH₃), 0.87 (s, 9 H, (C-2)*t*Bu-H), 0.06 (d, $^4J = 5.2\text{Hz}$, 6 H, (C-2)CH₃SiCH₃) ppm. MS (ESI): *m/z* = 526, calcd. for C₃₀H₄₂DNO₅Si: *m/z* = 526. Synthetic procedures were performed as previously described [210].

(2*R*,4*S*)-2-Hydroxymethyl-4-[(*S*)-*N*-heptanoyl-serylamino]-6-methyl-1,2-oxiranylheptane (Epn). HBTU (142mg, 0.374mmol), HoBt (57mg, 0.372mmol), and lastly, DIPEA (0.22mL, 1.26mmol) were added to a solution of (2*R*,4*S*)-4-amino-2-tert-butyltrimethylsilyloxymethyl-6-methyl-1,2-oxiranylheptane (75mg, 0.248mmol) and (*S*)-*O*-tert-butyl-diphenylsilyloxymethyl-*N*-heptanoyl-serine (108mg, 0.237mmol) in CH₂Cl₂ (5mL). The reaction solution was stirred at room temperature overnight. The resulting mixture was concentrated under reduced pressure and subject to flash column chromatography (Hex:EtOAc, 5:1) which yielded the TBDMS-TBDPS-protected **Epn** as a white solid (40mg, 23%). ¹H NMR: δ = 7.71 (d, *J* = 7.8Hz, 2 H, Ar-H), 7.63 (dd, *J* = 16.9Hz, *J* = 6.7Hz, 2 H, Ar-H), 7.41 (m, 6 H, Ar-H), 7.02 [d, *J* = 8.4Hz, 1 H, NH(C-4)], 6.18 [d, *J* = 6.6 Hz, 1 H, NH(C-4)], 4.63 (m, 2 H, 2',4-H), 4.45 [dd, *J* = 19 Hz, *J* = 11.6

Hz, 1 H, (C-2)CH^a₂], 4.02 (m, 1 H, 3'-H^a), 3.71 (m, 1 H, 3'-H^b), 3.55 [dd, *J* = 11.4 Hz, *J* = 8.8 Hz, 1 H, (C-2)CH^b₂], 3.17 (d, *J* = 5.1 Hz, 1 H, 1-H^a), 3.01 (d, *J* = 4.8 Hz, 1 H, 1-H^b), 2.13 (t, *J* = 7.5 Hz, 2 H, 2''-H), 1.63 (m, 4 H, 3''-H^a, 5-H^a, 6-H and 6''-H), 1.27 (m, 4 H, 4''-H, 5-H^b, 3''-H^b), 1.16 (m, 2 H, 5''-H), 1.06 [s, 9 H, (C-3'')*t*Bu-H], 0.96 (d, *J* = 6.2 Hz, 3 H, CH₃CHCH₃), 0.93 (d, 3 H, *J* = 6.1 Hz, 3 H, CH₃CHCH₃), 0.87 [s, 9 H, (C-2)*t*Bu-H], 0.06 [d, ⁴*J* = 5.6 Hz, 6 H, (C-2)CH₃SiCH₃] ppm.

To a solution of TBDMS-TBDPS-protected **Epn** (40mg, 0.0541mmol) in tetrahydrofuran (THF) (0.5mL), tetrabutylammonium fluoride (TBAF) (1.0M in THF, 20μL, 0.069mmol) was added. The reaction solution was stirred at room temperature for 10 minutes. The resulting mixture was then concentrated under reduced pressure and subjected to flash column chromatography (Hex:EtOAc, 1:4) to give the final product **Epn** as a yellowish oil (3.5mg, 16.7%). ¹H NMR: δ = 7.13 [d, *J* = 7.1 Hz, 1 H, NH(C-4)], 6.50 [d, *J* = 7.1 Hz, 1 H, NH(C-2')], 4.49 (m, 2 H, 2', 4-H), 4.19 [d, *J* = 12.6 Hz, 1 H, (C-2)CH^a₂], 4.00 (dd, *J* = 11.4 Hz, *J* = 3.4 Hz, 1 H, 3'-H^a), 3.70 [d, *J* = 12.6 Hz, 1 H, (C-2)CH^b₂], 3.55 (dd, *J* = 11.4 Hz, *J* = 5.8 Hz, 1 H, 3'-H^b), 3.29 (d, *J* = 4.9 Hz, 1 H, 1-H^a), 3.07 (d, *J* = 4.9 Hz, 1 H, 1-H^b), 2.20 (s and t, *J* = 7.6 Hz, 3 H, 2''-H and OH), 1.62 (s, 1H, OH), 1.57 (m, 4 H, 3''-H^a, 5-H^a, 6-H and 6''-H), 1.27 (m, 4 H, 4''-H, 5-H^b, 3''-H^b), 1.16 (m, 2 H, 5''-H), 0.92 (d, *J* = 6.2 Hz, 3 H, CH₃CHCH₃), 0.91 (d, 3 H, *J* = 6.1 Hz, 3 H, CH₃CHCH₃) ppm. ¹³C NMR: δ = 208.64 (C-3), 174.65 (C-1''), 172.12 (C-1'), 63.43 (C-3'), 62.99 (C-2), 62.23 (C-9), 54.13 (C-2'), 25.22 (C-4), 50.08 (C-1), 39.25 (C-5 and C-5''), 37.19 (C-2''), 28.46 (C-6''), 27.68 (C-4''), 26.53 (C-3''), 25.96 (C-6), 23.97 (C-8), 23.24 (C-7'' and C-8''), 21.74 (C-7) ppm.

(2*R*,4*S*)-2-Hydroxymethyl-4-[(*S*)-*N*-heptanoyl-alanyl-amino]-6-methyl-1,2-

oxiranylheptane (Epn-A). To a solution of **AP** (48mg, 0.0788mmol) in THF (0.5mL), TBAF (1.0M in THF, 0.20mL, 0.69mmol) was added. The reaction solution was stirred at room temperature for 30 minutes. The resulting mixture was then concentrated under reduced pressure and subjected to flash column chromatography (Hex:EtOAc, 1:1) to give the final product **Epn-A** as a yellowish oil (20mg, 68%). ¹H NMR: δ = 6.80 (d, *J* = 7.8 Hz, 1H, 4-NH), 6.96 (d, *J* = 6.6 Hz, 1H, 2'-NH), 4.53 (m, 2H, 4-H, 2'-H), 4.18 (d, *J* =

12 Hz, 1H, 2- CH^a_2), 3.74 (d, $J = 12$ Hz, 1H, 2- CH^b_2), 3.34 (d, $J = 5.4$ Hz, 1H, 1- H^a), 3.08 (d, $J = 4.2$ Hz, 1H, 1- H^b), 2.17 (t, $J = 7.5$ Hz, 2H, 2''-H), 1.62 (m, 4H, 6-H, 5- H^a , H_{Hep}), 1.34 (d, $J = 6.6$ Hz, 3H, 3'- CH_3), 1.25 (m, 6H, H_{Hep}), 0.94 (t, $J = 5.7$ Hz, 6H, CH_3CHCH_3), 0.85 (m, 3H, 7''- CH_3) ppm.

(2R,4S)-2-tert-Butyldiphenylsiloxymethyl-4-[(S)-N-heptanoyl-serylamino]-6-methyl-1,2-oxiranylheptane (SP). HBTU (32mg, 0.0843mmol), HoBt (13mg, 0.0848mmol) and lastly DIPEA (50 μ L, 0.287mmol) were added to a solution of (2R,4S)-4-amino-2-tert-butylidiphenylsiloxymethyl-6-methyl-1,2-oxiranylheptane (77mg, 0.18mmol) and (S)-N-heptanoyl-serine (12mg, 0.0552mmol) in CH_2Cl_2 (3mL). The reaction solution was stirred at room temperature for 3h. The resulting mixture was concentrated under reduced pressure and subject to flash column chromatography (Hex:EtOAc, 3:1) which yielded the **SP** as a colorless oil (8mg, 23%). 1H NMR: $\delta = 7.67$ (m, 4H, Ar-H), 7.40 (m, 6H, Ar-H), 7.01 (d, $J = 7.2$ Hz, 1H, 4-NH), 6.53 (d, $J = 6.9$ Hz, 1H, 2'-NH), 4.54 (m, 3H, 4-H, 2'-H, 2- CH^a_2), 4.09 (d, 1H, 3'- H^a), 3.60 (m, 1H, 3'- H^b), 3.47 (m, 1H, 2- CH^b_2), 3.2 (d, $J = 4.8$ Hz, 1H, 1- H^a), 2.99 (d, $J = 4.5$ Hz, 1H, 1- H^b), 2.25 (m, 2H, 2''-H), 1.69 (m, 4H, 6-H, 5- H^a , H_{Hep}), 1.27 (m, 6H, H_{Hep}), 1.01 [s, 12H, (C-2)*t*Bu-H, 7''- CH_3], 0.97 (m, 6H, CH_3CHCH_3), 0.87 (m, 3H, 7''- CH_3) ppm.

(2R,4S)-2-methoxymethoxymethyl-4-[(S)-N-heptanoyl-serylamino]-6-methyl-1,2-oxiranylheptane (SMOM). HBTU (66mg, 0.174mmol), HoBt (27mg, 0.176mmol) and lastly DIPEA (0.10mL, 0.574mmol) were added to a solution of (2R,4S)-4-amino-2-methoxymethoxymethyl-6-methyl-1,2-oxiranylheptane (27mg, 0.116mmol) and (S)-*O*-tert-butylidiphenylsiloxymethyl-N-heptanoyl-serine (53mg, 0.116mmol) in CH_2Cl_2 (3mL). The reaction solution was stirred at room temperature overnight. The resulting mixture was concentrated under reduced pressure and subject to flash column chromatography (Hex:EtOAc, 3:1) which yielded the TBDPS-protected **SMOM** as a colorless oil (14.8mg, 19%). 1H NMR: $\delta = 7.71$ (m, 4H, Ar-H), 7.42 (m, 6H, Ar-H), 7.00 (d, $J = 8.1$ Hz, 1H, 4-NH), 6.16 (d, $J = 6.6$ Hz, 1H, 2'-NH), 4.62 (s, 2H, 2-O CH_2 O), 4.59 (m, 2H, 4-H, 2'-H), 4.38 (d, $J = 11.4$ Hz, 1H, 2- CH^a_2), 4.02 (m, 1H, 3'- H^a), 3.70 (m, 3H, 3'- CH^b_2), 3.47 (d, $J = 11.4$ Hz, 1H, 2- CH^b_2), 3.34 (s, 3H, 2-O CH_3), 3.28 (d, $J = 5.1$ Hz, 1H, 1- H^a), 3.04 (d, $J =$

5.1 Hz, 1H, 1-H^b), 2.12 (m, 2H, 2''-H), 1.60 (m, 4H, 6-H, 5-H^a, H_{Hep}), 1.25 (m, 6H, H_{Hep}), 1.06 (s, 9H, 3'-*t*Bu), 0.96 (d, $J = 6.0$ Hz, 3H, CH₃CHCH₃), 0.90 (d, $J = 6.3$ Hz, 3H, CH₃CHCH₃), 0.85 (m, 3H, 7''-CH₃) ppm.

To a solution of TBDPS-protected **SMOM** (14.8mg, 0.0221mmol) in THF (0.5mL), TBAF (1.0M in THF, 20 μ L, 0.069mmol) was added. The reaction solution was stirred at room temperature for 15 minutes. The resulting mixture was then concentrated under reduced pressure and subjected to flash column chromatography (Hex:EtOAc, 1:2) to give the final product **SMOM** as a colorless oil (3.5mg, 16.7%). ¹H NMR: $\delta = 6.95$ (d, $J = 6.9$ Hz, 1H, 4-NH), 6.46 (d, $J = 7.2$ Hz, 1H, 2'-NH), 4.61 (s, 2H, 2-OCH₂O), 4.50 (m, 2H, 4-H, 2'-H), 4.37 (d, $J = 11.4$ Hz, 1H, 2-CH^a₂), 4.02 (m, 1H, 3'-H^a), 3.70 (m, 3H, 3'-CH^b₂), 3.44 (d, $J = 11.4$ Hz, 1H, 2-CH^b₂), 3.34 (s, 3H, 2-OCH₃), 3.27 (d, $J = 4.8$ Hz, 1H, 1-H^a), 3.05 (d, $J = 4.8$ Hz, 1H, 1-H^b), 2.21 (m, 2H, 2''-H), 1.64 (m, 4H, 6-H, 5-H^a, H_{Hep}), 1.28 (m, 6H, H_{Hep}), 0.95 (m, 6H, CH₃CHCH₃), 0.87 (m, 3H, 7''-CH₃) ppm.

(2R,4S)-2-methoxyethoxymethoxymethyl-4-[(SR)-N-heptanoyl-serylamino]-6-

methyl-1,2-oxiranylheptane (SMEM-1, SMEM-2). HBTU (68mg, 0.179mmol), HoBt (27mg, 0.176mmol), and lastly, DIPEA (0.10mL, 0.574mmol) were added to a solution of (2R,4S)-4-amino-2-methoxyethoxymethoxymethyl-6-methyl-1,2-oxiranylheptane (33mg, 0.119mmol) and (*S*)-*O*-*tert*-butyldiphenylsiloxymethyl-*N*-heptanoyl-serine (65mg, 0.142mmol) in CH₂Cl₂ (5mL). The reaction solution was stirred at room temperature for 3h. The resulting mixture was concentrated under reduced pressure and subject to flash column chromatography (Hex:EtOAc, 3:1) which yielded the TBDPS-protected **SMEM-1** and **SMEM-2** as colorless oils (59mg, 67%). TBDPS-protected **SMEM-1**: ¹H NMR: $\delta = 7.71$ (m, 4H, Ar-H), 7.44 (m, 6H, Ar-H), 7.02 (d, $J = 8.4$ Hz, 1H, 4-NH), 6.17 (d, $J = 6.6$ Hz, 1H, 2'-NH), 4.72 (s, 2H, 2-OCH₂O), 4.60 (m, 2H, 4-H, 2'-H), 4.42 (d, $J = 11.4$ Hz, 1H, 2-CH^a₂), 4.03 (m, 1H, 3'-H^a), 3.70 (m, 3H, 3'-CH^b₂, 2-OCH₂CH₂O), 3.55 (m, 2H, 2-OCH₂CH₂O), 3.52 (d, $J = 11.4$ Hz, 1H, 2-CH^b₂), 3.40 (s, 3H, 2-OCH₃), 3.29 (d, $J = 5.4$ Hz, 1H, 1-H^a), 3.04 (d, $J = 4.8$ Hz, 1H, 1-H^b), 2.13 (t, $J = 7.6$ Hz, 2H, 2''-H), 1.63 (m, 4H, 6-H, 5-H^a, H_{Hep}), 1.26 (m, 6H, H_{Hep}), 1.07 (s, 9H, 3'-*t*Bu), 0.96 (d, $J = 6.3$ Hz, 3H, CH₃CHCH₃), 0.91 (d, $J = 6.3$ Hz, 3H, CH₃CHCH₃), 0.86 (t, $J = 7.6$ Hz, 3H, 7''-CH₃)

ppm. TBDPS-protected **SMEM-2**: $^1\text{H NMR}$: $\delta = 7.71$ (m, 4H, Ar-H), 7.44 (m, 6H, Ar-H), 7.02 (d, $J = 8.4$ Hz, 1H, 4-NH), 6.17 (d, $J = 6.6$ Hz, 1H, 2'-NH), 4.72 (s, 2H, 2-OCH₂O), 4.66 (m, 1H, 2'-H), 4.55 (m, 1H, 4-H), 2'-H), 4.42 (d, $J = 11.4$ Hz, 1H, 2-CH^a₂), 4.03 (m, 1H, 3'-H^a), 3.70 (m, 3H, 3'-CH^b₂, 2-OCH₂CH₂O), 3.55 (m, 2H, 2-OCH₂CH₂O), 3.52 (d, $J = 11.4$ Hz, 1H, 2-CH^b₂), 3.40 (s, 3H, 2-OCH₃), 3.29 (d, $J = 5.4$ Hz, 1H, 1-H^a), 3.04 (d, $J = 4.8$ Hz, 1H, 1-H^b), 2.13 (t, $J = 7.6$ Hz, 2H, 2''-H), 1.63 (m, 4H, 6-H, 5-H^a, H_{Hep}), 1.26 (m, 6H, H_{Hep}), 1.07 (s, 9H, 3'-*t*Bu), 0.96 (d, $J = 6.3$ Hz, 3H, CH₃CHCH₃), 0.91 (d, $J = 6.3$ Hz, 3H, CH₃CHCH₃), 0.86 (t, $J = 7.6$ Hz, 3H, 7''-CH₃) ppm.

To a solution of TBDPS-protected **SMEM-1** (30mg, 0.0280mmol) in THF (1mL), TBAF (1.0M in THF, 50 μ L, 0.173mmol) was added. The reaction solution was stirred at room temperature for 30 minutes. The resulting mixture was then concentrated under reduced pressure and subjected to flash column chromatography (Hex:EtOAc, 1:2) to give the final product **SMEM-1** as a yellowish oil (16mg, 80%). $^1\text{H NMR}$: $\delta = 6.83$ (d, $J = 7.5$ Hz, 1H, 4-NH), 6.44 (d, $J = 7.5$ Hz, 1H, 2'-NH), 4.71 (s, 2H, 2-OCH₂O), 4.50 (m, 2H, 4-H, 2'-H), 4.41 (d, $J = 11.7$ Hz, 1H, 2-CH^a₂), 4.08 (m, 1H, 3'-H^a₂), 3.68 (m, 2H, 2-OCH₂CH₂O), 3.55 (m, 3H, 2-OCH₂CH₂O, 3'-H^b₂), 3.46 (d, $J = 11.7$ Hz, 1H, 2-CH^b₂), 3.40 (s, 3H, 2-OCH₃), 3.27 (d, $J = 5.1$ Hz, 1H, 1-H^a), 3.05 (d, $J = 4.8$ Hz, 1H, 1-H^b), 2.22 (m, 2H, 2''-H), 1.60 (m, 4H, 6-H, 5-H^a, H_{Hep}), 1.28 (m, 6H, H_{Hep}), 0.96 (d, $J = 3.9$ Hz, 3H, CH₃CHCH₃), 0.94 (d, $J = 3.9$ Hz, 3H, CH₃CHCH₃), 0.88 (t, $J = 6.7$ Hz, 3H, 7''-CH₃) ppm. MS (ESI): $m/z = 475$, calcd. for C₂₃H₄₂N₂O₈: $m/z = 474.59$.

To a solution of TBDPS-protected **SMEM-2** (23mg, 0.0322mmol) in THF (1mL), TBAF (1.0M in THF, 33 μ L, 0.114mmol) was added. The reaction solution was stirred at room temperature for 30 minutes. The resulting mixture was then concentrated under reduced pressure and subjected to flash column chromatography (Hex:EtOAc, 1:2) to give the final product **SMEM-2** as a yellowish oil (9mg, 58%). $^1\text{H NMR}$: $\delta = 6.83$ (d, $J = 7.5$ Hz, 1H, 4-NH), 6.44 (d, $J = 7.5$ Hz, 1H, 2'-NH), 4.71 (s, 2H, 2-OCH₂O), 4.50 (m, 2H, 4-H, 2'-H), 4.41 (d, $J = 11.4$ Hz, 1H, 2-CH^a₂), 4.08 (m, 1H, 3'-H^a₂), 3.68 (m, 2H, 2-OCH₂CH₂O), 3.62 (m, 1H, 3'-H^b₂), 3.55 (m, 2H, 2-OCH₂CH₂O), 3.46 (d, $J = 11.7$ Hz, 1H, 2-CH^b₂), 3.40 (s, 3H, 2-OCH₃), 3.27 (d, $J = 5.1$ Hz, 1H, 1-H^a), 3.05 (d, $J = 4.8$ Hz,

1H, 1-H^b), 2.22 (m, 2H, 2''-H), 1.60 (m, 4H, 6-H, 5-H^a, H_{Hep}), 1.28 (m, 6H, H_{Hep}), 0.96 (d, *J* = 3.9 Hz, 3H, CH₃CHCH₃), 0.94 (d, *J* = 3.9 Hz, 3H, CH₃CHCH₃), 0.88 (t, *J* = 6.7 Hz, 3H, 7''-CH₃) ppm. MS (ESI): *m/z* = 475, calcd. for C₂₃H₄₂N₂O₈: *m/z* = 474.59.

(2R,4S)-2-tert-Butyldimethylsiloxymethyl-4-[(S)-N-heptanoyl-serylamino]-6-methyl-1,2-oxiranylheptane (SM). HBTU (32mg, 0.0843mmol), HoBt (13mg, 0.0848mmol), and lastly, DIPEA (50μL, 0.287mmol) were added to a solution of (2R,4S)-4-amino-2-tert-butyl-dimethylsiloxymethyl-6-methyl-1,2-oxiranylheptane (24mg, 0.0796mmol) and (S)-N-heptanoyl-serine (29mg, 0.0632mmol) in CH₂Cl₂ (3mL). The reaction solution was stirred at room temperature for 3h. The resulting mixture was concentrated under reduced pressure and subject to flash column chromatography (Hex:EtOAc, 3:1) which yielded **SM** as a colorless oil (10mg, 31%). ¹H NMR: δ = 6.87 (d, *J* = 7.2 Hz, 1H, 4-NH), 6.47 (d, *J* = 6.9 Hz, 1H, 2'-NH), 4.52 (m, 2H, 4-H, 2'-H), 4.43 (m, 1H, 2-CH^a₂), 4.08 (m, 1H, 3'-H^a₂), 3.56 (m, 2H, 2-CH^b₂, 3'-H^a₂), 3.18 (d, *J* = 5.1 Hz, 1H, 1-H^a), 3.01 (d, *J* = 5.1 Hz, 1H, 1-H^b), 2.24 (m, 2H, 2''-H), 1.62 (m, 4H, 6-H, 5-H^a, H_{Hep}), 1.27 (m, 6H, H_{Hep}), 0.95 (m, 6H, CH₃CHCH₃), 0.87 [s, 12H, (C-2)*t*Bu-H, 7''-CH₃], 0.05 [d, *J* = 4.5Hz, 6 H, (C-2)CH₃SiCH₃] ppm.

(2R,4S)-2-tert-Butyldiphenylsiloxymethyl-4-[(S)-N-heptanoyl-alanyl-amino]-6-methyl-1,2-oxiranylheptane (AP). HBTU (130mg, 0.342mmol), HoBt (52mg, 0.339mmol), and lastly, DIPEA (0.2mL, 1.148mmol) were added to a solution of (2R,4S)-4-amino-2-tert-butyl-diphenylsiloxymethyl-6-methyl-1,2-oxiranylheptane (97mg, 0.227mmol) and (S)-N-heptanoyl-alanine (46mg, 0.228mmol) in CH₂Cl₂ (3mL). The reaction solution was stirred at room temperature for 3h. The resulting mixture was concentrated under reduced pressure and subject to flash column chromatography (Hex:EtOAc, 3:1) which yielded **AP** as a colorless oil (53.8mg, 38%). ¹H NMR: δ = 7.66 (m, 5H, Ar-H), 7.40 (m, 5H, Ar-H), 6.37 (d, *J* = 6.6 Hz, 1H, 4-NH), 5.90 (d, *J* = 6.6 Hz, 1H, 2'-NH), 4.55 (m, 3H, 4-H, 2'-H, 2-CH^a₂), 3.47 (d, *J* = 10.8 Hz, 1H, 2-CH^b₂), 3.19 (d, *J* = 4.5 Hz, 1H, 1-H^a), 2.98 (d, *J* = 4.5 Hz, 1H, 1-H^b), 2.18 (m, 2H, 2''-H), 1.65 (m, 4H, 6-H, 5-H^a, H_{Hep}), 1.34 (d, *J* = 6.6 Hz, 3H, 3'-CH₃), 1.27 (m, 6H, H_{Hep}), 1.00 [s, 9H, (C-2)*t*Bu-H], 0.95 (m, 6H, CH₃CHCH₃), 0.87 (m, 3H, 7''-CH₃) ppm.

(2R,4S)-2-tert-Butyldimethylsiloxymethyl-4-[(S)-N-heptanoyl-alanyl-amino]-6-methyl-1,2-oxiranylheptane (AM). HBTU (92mg, 0.242mmol), HoBt (37mg, 0.241mmol), and lastly, DIPEA (0.14mL, 0.803mmol) were added to a solution of (2R,4S)-4-amino-2-tert-butyl-dimethylsiloxymethyl-6-methyl-1,2-oxiranylheptane (49mg, 0.16mmol) and (S)-N-heptanoyl-alanine (33mg, 0.163mmol) in CH₂Cl₂ (3mL). The reaction solution was stirred at room temperature for 3h. The resulting mixture was concentrated under reduced pressure and subject to flash column chromatography (Hex:EtOAc, 3:1) which yielded **AM** as a colorless oil (21.5mg, 27%). ¹H NMR: δ = 6.34 (d, *J* = 7.8 Hz, 1H, 4-NH), 5.91 (d, *J* = 7.5 Hz, 1H, 2'-NH), 4.55 (m, 2H, 4-H, 2'-H), 4.43 (d, *J* = 11.1 Hz, 1H, 2-CH^a₂), 3.55 (d, *J* = 11.1 Hz, 1H, 2-CH^b₂), 3.19 (d, *J* = 4.2 Hz, 1H, 1-H^a), 3.01 (d, *J* = 5.4 Hz, 1H, 1-H^b), 2.18 (t, *J* = 7.0 Hz, 2H, 2''-H), 1.63 (m, 4H, 6-H, 5-H^a, H_{Hep}), 1.34 (d, *J* = 6.6 Hz, 3H, 3'-CH₃), 1.26 (m, 6H, H_{Hep}), 0.94 (m, 6H, CH₃CHCH₃), 0.87 [s, 12H, (C-2)*t*Bu-H, 7''-CH₃], 0.06 [d, *J* = 3.0Hz, 6 H, (C-2)CH₃SiCH₃] ppm.

(2S,4S)-2-tert-Butyldimethylsiloxymethyl-4-[(S)-N-heptanoyl-alanyl-amino]-6-methyl-1,2-oxiranylheptane (AM-2). HBTU (31mg, 0.0817mmol), HoBt (12.5mg, 0.0816mmol), and lastly, DIPEA (50μL, 0.287mmol) were added to a solution of (2S,4S)-4-amino-2-tert-butyl-dimethylsiloxymethyl-6-methyl-1,2-oxiranylheptane (16.5mg, 0.0547mmol) and (S)-N-heptanoyl-alanine (11mg, 0.0546mmol) in CH₂Cl₂ (3mL). The reaction solution was stirred at room temperature for 3h. The resulting mixture was concentrated under reduced pressure and subject to flash column chromatography (Hex:EtOAc, 3:1) which yielded **AM-2** as a colorless oil (6.4mg, 24%). ¹H NMR: δ = 6.58 (d, *J* = 8.1 Hz, 1H, 4-NH), 6.07 (d, *J* = 6.9 Hz, 1H, 2'-NH), 4.82 (m, 1H, 2'-H), 4.49 (m, 1H, 4-H), 4.26 (m, 1H, 2-CH^a₂), 3.80 (m, 1H, 2-CH^b₂), 3.02 (m, 1H, 1-H^a), 2.92 (m, 1H, 1-H^b), 2.19 (m, 2H, 2''-H), 1.60 (m, 4H, 6-H, 5-H^a, H_{Hep}), 1.35 (d, *J* = 6.9 Hz, 3H, 3'-CH₃), 1.28 (m, 6H, H_{Hep}), 0.93 (m, 6H, CH₃CHCH₃), 0.87 [s, 12H, (C-2)*t*Bu-H, 7''-CH₃], 0.06 [d, *J* = 3.3Hz, 6 H, (C-2)CH₃SiCH₃] ppm.

(2R,4S)-2-methoxymethoxymethyl-4-[(S)-N-heptanoyl-alanyl-amino]-6-methyl-1,2-oxiranylheptane (AMOM). HBTU (32mg, 0.0843mmol), HoBt (13mg, 0.0848mmol),

and lastly, DIPEA (50 μ L, 0.287mmol) were added to a solution of (2*R*,4*S*)-4-amino-2-methoxymethoxymethyl-6-methyl-1,2-oxiranylheptane (13mg, 0.0562mmol) and (*S*)-*N*-heptanoyl-alanine (13.5mg, 0.067mmol) in CH₂Cl₂ (3mL). The reaction solution was stirred at room temperature for 3h. The resulting mixture was concentrated under reduced pressure and subject to flash column chromatography (Hex:EtOAc, 1:1) which yielded **AMOM** as a colorless oil (10.5mg, 45%). ¹H NMR: δ = 6.67 (d, *J* = 7.5 Hz, 1H, 4-NH), 6.04 (d, *J* = 7.2 Hz, 1H, 2'-NH), 4.61(s, 2H, 2-OCH₂O), 4.54 (m, 2H, 4-H, 2'-H), 4.34 (d, *J* = 11.1 Hz, 1H, 2-CH^a₂), 3.45 (d, *J* = 11.1 Hz, 1H, 2-CH^b₂), 3.34 (s, 3H, 2-OCH₃), 3.30 (d, *J* = 5.1 Hz, 1H, 1-H^a), 3.04 (d, *J* = 4.8 Hz, 1H, 1-H^b), 2.17 (t, *J* = 7.8 Hz, 2H, 2''-H), 1.63 (m, 4H, 6-H, 5-H^a, H_{Hep}), 1.33 (d, *J* = 6.9 Hz, 3H, 3'-CH₃), 1.28 (m, 6H, H_{Hep}), 0.94 (m, 6H, CH₃CHCH₃), 0.87 (m, 3H, 7''-CH₃) ppm.

(2*R*,4*S*)-2-tetrahydropyranoxymethyl-4-[(*S*)-*N*-heptanoyl-alanyl-amino]-6-methyl-1,2-oxiranylheptane (ATHP). HBTU (42mg, 0.11mmol), HoBt (17mg, 0.111mmol), and lastly, DIPEA (70 μ L, 0.401mmol) were added to a solution of (2*R*,4*S*)-4-amino-2-tetrahydropyranoxymethyl-6-methyl-1,2-oxiranylheptane (20mg, 0.073mmol) and (*S*)-*N*-heptanoyl-alanine (15mg, 0.074mmol) in CH₂Cl₂ (3mL). The reaction solution was stirred at room temperature for 3h. The resulting mixture was concentrated under reduced pressure and subject to flash column chromatography (Hex:EtOAc, 1:1) which yielded **ATHP** as a colorless oil (9mg, 26%). ¹H NMR: δ = 6.6 (d, *J* = 7.2 Hz, 1H, 4-NH), 6.04 (d, *J* = 7.5 Hz, 1H, 2'-NH), 4.56 (m, 2H, 4-H, 2'-H), 4.22 (m, 1H, 2-CH^a₂), 3.84 (m, 2H, 2-OTHP), 3.66 (m, 1H, 2-CH^b₂), 3.51 (m, 1H, 2-OTHP), 3.25 (m, 1H, 1-H^a), 3.06 (m, 1H, 1-H^b), 2.19 (m, 2H, 2''-H), 1.63 (m, 4H, 6-H, 5-H^a, H_{Hep}), 1.34 (d, *J* = 7.2 Hz, 3H, 3'-CH₃), 1.28 (m, 6H, H_{Hep}), 0.95 (m, 6H, CH₃CHCH₃), 0.87 (m, 3H, 7''-CH₃) ppm.

Biotin-Dihydroeponemycin. To a solution of TBDMS- and TBDPS-protected biotin-dihydroeponemycin (51mg, 0.043mmol) in THF was added TBAF (1.0M in THF, 20 μ L, 0.069mmol). After stirring at room temperature for 10 minutes, the resulting mixture was then concentrated under reduced pressure. The crude product was subjected to flash column chromatography (CH₂Cl₂:MeOH, 98:2) to give the final product **Ep_n** as a yellowish oil (9mg, 0.01mmol, 23%). ¹H NMR: δ = 7.12 (br, 1H), 4.36 (m, 1H), 4.30 (t,

$J = 5.9$, 1H), 4.20 (t, $J = 5.7$ Hz, 1H), 3.72 (m, 1H), 3.49 (t, $J = 10.9$ Hz, 1H), 3.26 (d, $J = 12.0$ Hz, 1H), 3.09 (m, 2H), 2.95 (d, $J = 4.8$ Hz, 1H), 2.81 (dd, $J = 13.0, 4.8$ Hz, 1H), 2.62 (d, $J = 12.4$ Hz, 1H), 2.16 (m, 1H), 2.06 (t, $J = 6.1$ Hz, 1H), 1.51 (m, 6H), 1.31 (m, 4H), 1.15 (m, 4H), 0.83 (d, $J = 5.9$ Hz, 3H), 0.75 (d, $J = 6.9$ Hz, 3H) ppm. MS (ESI): $m/z = 840$, calcd. for $C_{40}H_{69}N_7O_{10}S$: $m/z = 840.08$. Synthetic procedures were performed as previously described [207].

Biotin-Epoxomicin. Synthetic procedures were performed as previously described [169].

Cell Culture and Competition Assay. Murine lymphoma EL4 cells were purchased from ATCC and grown in RPMI Medium (Gibco), 10% Fetal Bovine Serum, and 1% of penicillin and streptomycin at 37°C in a 5% CO₂ incubator. Cells were pretreated with increasing concentrations of dihydroeponemycin analogs 30 minutes prior to the addition of 1 μM biotin-dihydroeponemycin or biotin-epoxomicin. Cells lysates were analyzed with 12% sodium dodecyl sulfate polyacrylamide gel electrophoresis (SDS-PAGE) and transferred to a polyvinylidene fluoride (PVDF) membrane. Biotinylated proteins were visualized by enhanced chemiluminescence (ECL) using streptavidin-conjugated HRP and Biomax X-ray film (Kodak).

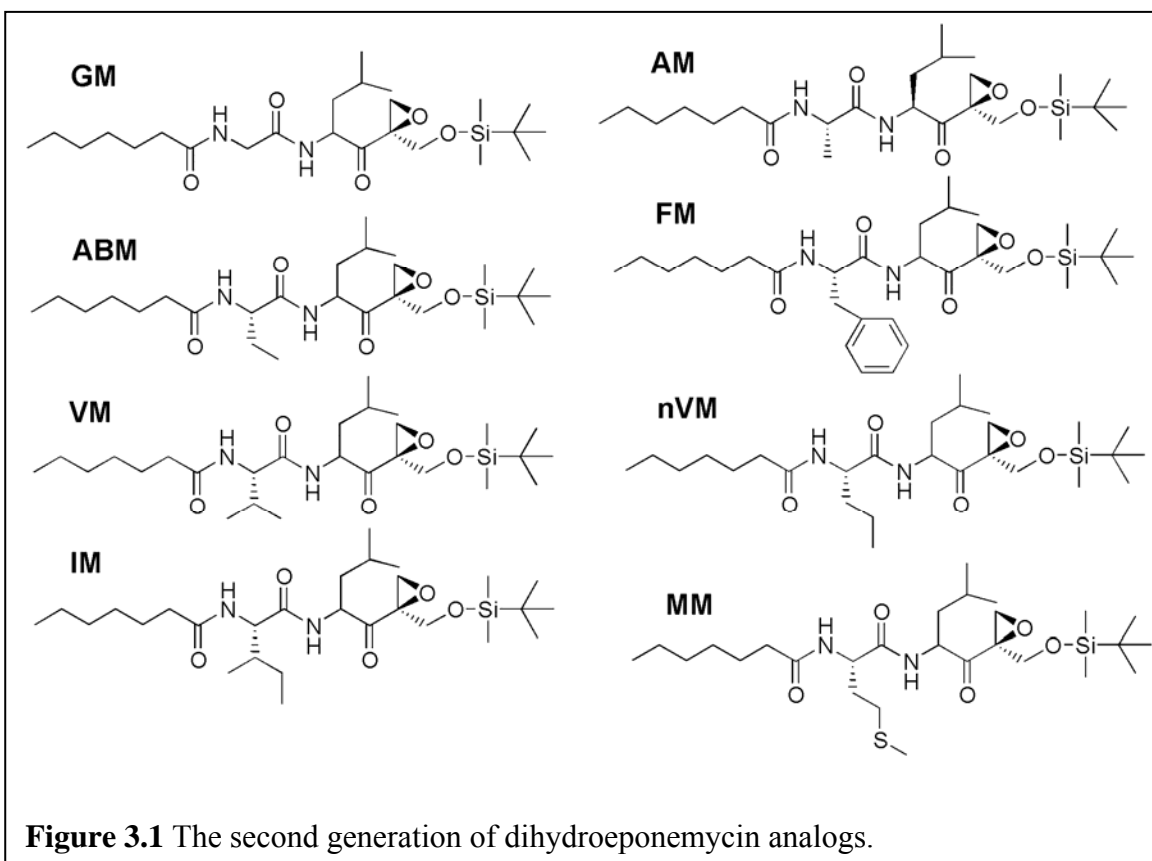
CHAPTER THREE: LEAD OPTIMIZATION AND SCREENING

A. Introduction

The first small library of dihydroeponemycin analogs yielded analog **AM** as the lead compound due to its high specificity towards the LMP2 subunit. While modification of P1' site was previously suggested to play a role in determining proteasome catalytic subunit specificity, the preliminary screening results of the dihydroeponemycin analogs also suggested that the P2 site is involved in conferring the analogs' catalytic subunit selectivity. While the analogs **Epn** and **Epn-A** were first shown to exhibit almost no difference in the binding of immunoproteasome catalytic subunits (Figures 2.2 and 2.3), analogs **AM** and **SM** were found to display a definite difference in their respective LMP2 binding specificity (Figure 2.4). Specifically, the replacement of the serine residue (**SM**) with alanine (**AM**) appeared to direct the specificity of the molecule towards LMP2 catalytic subunit. The discrepancy between the two pairs of analogs piqued an interest in further investigating the structure-activity relationship at the P2 site. Therefore, the lead compound **AM** was further optimized by replacing the alanine residue at the P2 site with a variety of amino acid residues. These optimized dihydroeponemycin analogs will then undergo a similar screening assay to determine the most selective LMP2 inhibitor.

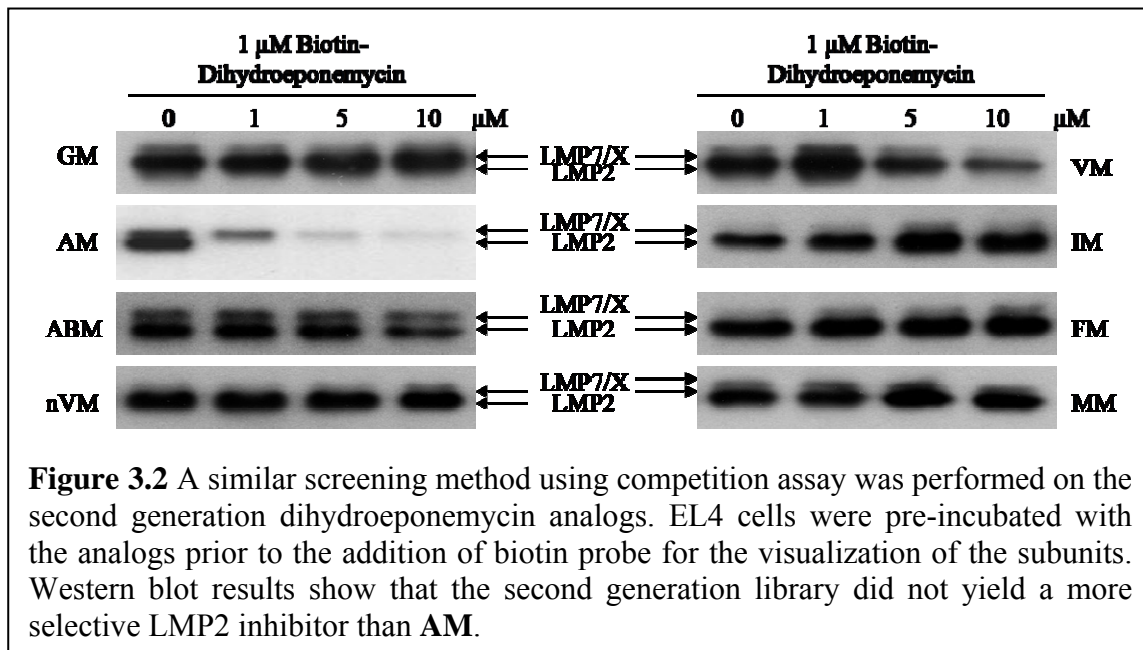
B. Optimization of the Lead Compound

The general synthetic procedures used to prepare the second generation of dihydroeponemycin analogs are as described previously in General Reactions 1-3. Specifically, heptanoic acid and the TBDMS protective group were retained at the P3 and P1' sites, respectively, while the P2 site was substituted with a glycine, aminobutyric acid, valine, isoleucine, phenylalanine, norvaline, or methionine amino acid residue. Consequently, a total of 7 compounds were successfully synthesized as the second generation optimized small library of dihydroeponemycin analogs (Figure 3.1).



C. Screening of the Second Generation of Dihydroeponemycin Analogs

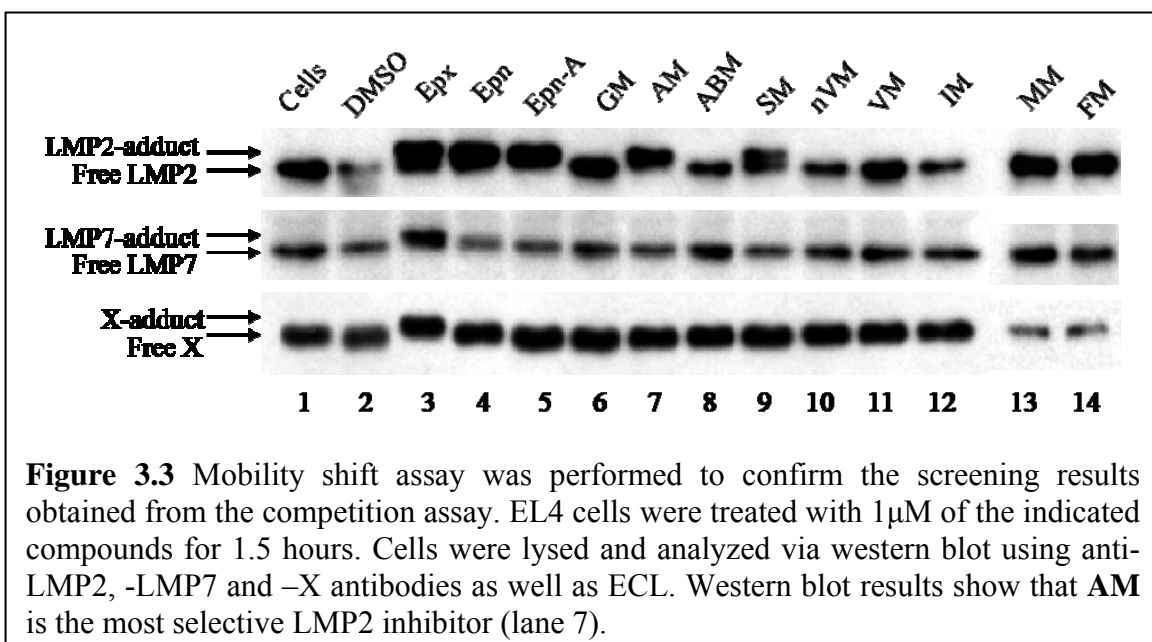
Similarly, each of these analogs was screened for its ability to selectively target the LMP2 catalytic subunit via the competition assay that was previously described in Chapter 2-E. Briefly, EL4 cells were treated with increasing concentrations of the optimized dihydroeponemycin analog 30 minutes prior to the addition of biotin-tagged dihydroeponemycin and incubated for an additional hour. Surprisingly, all of the seven second generation analogs did not display similar LMP2 specificity as that of **AM** (Figure 3.2). The results obtained clearly showed that the alanine residue at the P2 site is vital to determining the catalytic subunit specificity of these analogs. Therefore, analog **AM** remains the most selective LMP2 inhibitor.



In order to confirm the results obtained from the competition assay, the mobility shift of the analog-LMP2 adduct was investigated in EL4 cells. The epoxyketone pharmacophore containing proteasome inhibitors were previously shown to covalently modify proteasome catalytic subunits [170]; hence, analogs that covalently modify the subunits will induce a mobility shift on western blot due to the increase in molecular weight. Specifically, EL4 cells were incubated with dihydroeponemycin analogs and

broad spectrum proteasome inhibitors for 1.5 hours at 37°C. Whole cell lysates were then analyzed by western blot with anti-LMP2, -LMP7 and -X antibodies. Broad spectrum proteasome inhibitors, epoxomicin (**Epx**) and dihydroeponemycin substitute (**Epn**) were used as mobility shift controls because they have been shown to induce mobility shift via covalent modification of proteasome catalytic subunits [168, 211].

As expected, when cells were treated with the broad spectrum proteasome inhibitors, all three catalytic subunits were shown to display a slower mobility shifts due to increased molecular weight by approximately 0.5 kDa (554.7 for Epx and 386.5 for **Epn**) when compared to their respective unbound subunits (lanes 1-4, Figure 3-3). On the other hand, while analog **AM** was able to induce a mobility shift in the LMP2 catalytic subunit (484.74 for **AM**), mobility shifts in the LMP7 and X subunits were not observed (lane 7, Figure 3-3). These results indicate that analog **AM** selectively targets the LMP2 subunit with high efficiency. Even though analog **SM** also displayed some selectivity towards LMP2, two distinct bands can be observed, which indicates the presence of free LMP2 (lower band) and modified LMP2 (upper band). On the other hand, only a single upper band was observed for cells treated with **AM**, which clearly showed that the LMP2 subunit was completely modified because no free LMP2 was observed. Based on these collective results, the analog **AM** was selected as the lead compound and will be subjected to further biological studies described in the next chapters.



D. Conclusions

A small library of seven dihydroeponemycin analogs were designed and synthesized following the first generation in the pursuit of a selective immunoproteasome catalytic subunit LMP2 inhibitor. A screening assay and mobility shift assay were also performed to determine the ability of these analogs to selectively target the LMP2 catalytic subunit. Preliminary studies have suggested that the P2 moiety might play a role in determining subunit specificity. Therefore, the optimization of the lead compound **AM** was focused on the derivatization of P2 site using a variety of amino acid residues. These analogs were also subjected to a similar screening assay as the one used for the first library. Surprisingly, the results indicated that **AM** is still the most selective LMP2 inhibitor in the library. The alanine residue is crucial in directing the LMP2 subunit specificity because when the P2 site was replaced with glycine, which is one carbon less, or aminobutyric acid, which is one carbon more, the LMP2 specificity was dramatically reduced. In addition, a mobility shift assay was carried out to confirm the results obtained from the competition assay. As shown in Figure 3.3, analog **AM** covalently modifies the LMP2 catalytic subunit with the highest efficiency compared to the other dihydroeponemycin analogs.

In conclusion, the P1' and P2 sites of the dihydroeponemycin analogs were critical in determining the immunoproteasome catalytic subunit specificity. Specifically, a dihydroeponemycin analog **AM** with a small bulky protective group and alanine residue at the P1' and P2 sites, respectively, yielded a highly selective LMP2 inhibitor. This analog will be subjected to further biological studies in order to characterize its immunoproteasome subunit binding specificity in prostate cancer cell lines as well as to determine its biological functions and modes of action.

For future optimization and derivatization of **AM**, an alternative linkage that is not easily hydrolyzed may be necessary to replace the amide bonds found in **AM**. This derivatization may help improve stability, solubility as well as selectivity of the compound. The pharmacophore epoxide ketone of **AM** may also be replaced with epoxide amide. The epoxide is a chemical group that has often been shown to have alkylating activity and DNA binding properties; hence, by having an amide group instead of a ketone next to the epoxide ring may help render the ring less reactive and possibly

reducing the toxicity of the compound. While structure-based drug design would be more beneficial to this synthetic work, the crystal structure of immunoproteasome is yet to be completed. However, serendipity alone for such synthetic work to be successful is insufficient; a well thought out and rationalized drug design is the key.

E. Methods and Materials

The following includes the experimental protocols and structural characterization of the second generation dihydroeponemycin analogs. In addition, the experimental procedure of the mobility shift assay is further elaborated.

General Remarks: Unless otherwise stated, all reactions were carried out under Nitrogen with dry freshly distilled solvents, over-dried glassware, and magnetic stirring. All solvents were reagent graded. THF was distilled from sodium/benzophenone. CH₂Cl₂ was distilled from calcium hydride. Diethyl ether anhydrous was purchased from EMD Chemicals and used without further purification. All reagents were purchased from Sigma-Aldrich and used without further purification. All reactions were monitored by TLC using E. Merk 60^{F254} pre-coated silica gel plates. Flash column chromatography was performed using E. Merk silica gel 60 (particle size 0.040-0.063mm) and with the indicated solvents. ¹H and ¹³C NMR spectra were recorded in CDCl₃ using a Varian 300MHz spectrometer at ambient temperature using an internal deuterium lock unless stated otherwise. Chemical shift are referenced to residual chloroform ($\delta = 7.27$ ppm for ¹H and $\delta = 77.0$ ppm for ¹³C). Mass spectra were performed by the University of Kentucky Mass Spectrometry Facility.

(2R,4S)-2-tert-Butyldimethylsiloxymethyl-4-[(S)-N-heptanoyl-glycylamino]-6-

methyl-1,2-oxiranylheptane (GM). O-(7-Azabenzotriazole-1-yl)-N, N,N,N'-tetramethyluronium hexafluorophosphate (HATU) (81mg, 0.213mmol), 1-Hydroxy-7-Azabenzotriazole (HoAt) (23mg, 0.168mmol), and lastly, DIPEA (0.12mL, 0.712mmol) were added to a solution of (2R,4S)-4-amino-2-tert-butyldimethylsiloxymethyl-6-methyl-1,2-oxiranylheptane (35mg, 0.116mmol) and (S)-N-heptanoyl-glycine (27mg, 0.144mmol) in CH₂Cl₂ (3mL). The reaction solution was stirred at room temperature for 3h. The resulting mixture was concentrated under reduced pressure and subject to flash column chromatography (Hex:EtOAc, 3:1) which yielded **GM** as a colorless oil (29mg, 59%). ¹H NMR: $\delta = 6.7$ (d, $J = 7.8$ Hz, 1H, 4-NH), 6.30 (d, $J = 7.8$ Hz, 1H, 2'-NH), 4.61 (m, 1H, 4-H), 4.41 (d, $J = 11.1$ Hz, 1H, 2-CH^a₂), 3.96 (m, 2H, 2'-CH₂), 3.54 (d, $J = 12$ Hz, 1H, 2-CH^b₂), 3.17 (d, $J = 4.5$ Hz, 1H, 1-H^a), 3.01 (d, $J = 4.5$ Hz, 1H, 1-H^b), 2.21 (t, $J =$

7.5 Hz, 2H, 2''-H), 1.63 (m, 4H, 6-H, 5-H^a, H_{Hep}), 1.26 (m, 6H, H_{Hep}), 0.92 (m, 6H, CH₃CHCH₃), 0.86 [s, 12H, (C-2)*t*Bu-H, 7''-CH₃], 0.04 [d, *J* = 4.5Hz, 6 H, (C-2)CH₃SiCH₃] ppm.

(2*R*,4*S*)-2-*tert*-Butyldimethylsiloxymethyl-4-[(*S*)-*N*-heptanoyl-aminobutylamino]-6-methyl-1,2-oxiranylheptane (ABM). HATU (62mg, 0.163mmol), HoAt (17mg, 0.124mmol), and lastly, DIPEA (95μL, 0.545mmol) were added to a solution of (2*R*,4*S*)-4-amino-2-*tert*-butyldimethylsiloxymethyl-6-methyl-1,2-oxiranylheptane (33mg, 0.109mmol) and (*S*)-*N*-heptanoyl-aminobutyric acid (15mg, 0.069mmol) in CH₂Cl₂ (3mL). The reaction solution was stirred at room temperature for 3h. The resulting mixture was concentrated under reduced pressure and subject to flash column chromatography (Hex:EtOAc, 3:1) which yielded **ABM** as a colorless oil (21mg, 60%). ¹H NMR: δ = 6.47 (d, *J* = 7.8 Hz, 1H, 4-NH), 6.04 (m, 1H, 2'-NH), 4.58 (m, 1H, 4-H), 4.42 (m, 2H, 2'-H, 2-CH^a₂), 3.54 (d, *J* = 12.3 Hz, 1H, 2-CH^b₂), 3.20 (d, *J* = 5.4 Hz, 1H, 1-H^a), 3.01 (d, *J* = 5.7 Hz, 1H, 1-H^b), 2.19 (m, 2H, 2''-H), 1.83 (m, 2H, 2'-CH₂), 1.64 (m, 4H, 6-H, 5-H^a, H_{Hep}), 1.28 (m, 6H, H_{Hep}), 0.94 (m, 6H, CH₃CHCH₃), 0.87 [s, 12H, (C-2)*t*Bu-H, 7''-CH₃], 0.05 [d, *J* = 3.3Hz, 6 H, (C-2)CH₃SiCH₃] ppm.

(2*R*,4*S*)-2-*tert*-Butyldimethylsiloxymethyl-4-[(*S*)-*N*-heptanoyl-valylamino]-6-methyl-1,2-oxiranylheptane (VM). HATU (85mg, 0.223mmol), HoAt (24mg, 0.176mmol), and lastly, DIPEA (0.13mL, 0.746mmol) were added to a solution of (2*R*,4*S*)-4-amino-2-*tert*-butyldimethylsiloxymethyl-6-methyl-1,2-oxiranylheptane (45mg, 0.149mmol) and (*S*)-*N*-heptanoyl-valine (36mg, 0.156mmol) in CH₂Cl₂ (3mL). The reaction solution was stirred at room temperature for 3h. The resulting mixture was concentrated under reduced pressure and subject to flash column chromatography (Hex:EtOAc, 3:1) which yielded **VM** as a colorless oil (25mg, 32%). ¹H NMR: δ = 6.39 (m, 1H, 4-NH), 6.05 (m, 1H, 2'-NH), 4.59 (m, 1H, 4-H), 4.41 (m, 1H, 2'-H), 4.31 (m, 1H, 2-CH^a₂), 3.55 (d, *J* = 11.1 Hz, 1H, 2-CH^b₂), 3.19 (d, *J* = 4.5 Hz, 1H, 1-H^a), 3.01 (m, 1H, 1-H^b), 2.20 (m, 2H, 2''-H), 2.06 (m, 1H, 3'-H), 1.65 (m, 4H, 6-H, 5-H^a, H_{Hep}), 1.28 (m, 6H, H_{Hep}), 0.93 (m, 6H, CH₃CHCH₃), 0.86 [s, 12H, (C-2)*t*Bu-H, 7''-CH₃], 0.05 [d, *J* = 4.5Hz, 6 H, (C-2)CH₃SiCH₃] ppm.

(2R,4S)-2-tert-Butyldimethylsiloxymethyl-4-[(S)-N-heptanoyl-isoleucylamino]-6-methyl-1,2-oxiranylheptane (IM). HATU (47mg, 0.123mmol), HoAt (13.4mg, 0.0984mmol), and lastly, DIPEA (71 μ L, 0.407mmol) were added to a solution of (2R,4S)-4-amino-2-tert-butyl dimethylsiloxymethyl-6-methyl-1,2-oxiranylheptane (24.8mg, 0.0822mmol) and (S)-N-heptanoyl-valine (40mg, 0.164mmol) in CH₂Cl₂ (3mL). The reaction solution was stirred at room temperature for 3h. The resulting mixture was concentrated under reduced pressure and subject to flash column chromatography (Hex:EtOAc, 3:1) which yielded **IM** as a colorless oil (24mg, 54%). ¹H NMR: δ = 6.17 (d, *J* = 7.8 Hz, 1H, 4-NH), 6.01 (d, *J* = 8.7 Hz, 1H, 2'-NH), 4.60 (m, 1H, 4-H), 4.42 (d, *J* = 12 Hz, 1H, 2-CH^a₂), 4.29 (m, 1H, 2'-H), 3.55 (d, *J* = 11.1 Hz, 1H, 2-CH^b₂), 3.19 (d, *J* = 4.5 Hz, 1H, 1-H^a), 3.02 (d, *J* = 4.5 Hz, 1H, 1-H^b), 2.19 (t, *J* = 7.0 Hz, 2H, 2''-H), 1.79 (m, 1H, 3'-H), 1.64 (m, 4H, 6-H, 5-H^a, H_{Hep}), 1.44 (m, 2H, 3'-CH₂), 1.28 (m, 6H, H_{Hep}), 0.92 (m, 6H, CH₃CHCH₃), 0.87 [s, 18H, (C-2)*t*Bu-H, 7''-CH₃, 3'-CH₃, 4'-CH₃] 0.05 [d, *J* = 4.5Hz, 6 H, (C-2)CH₃SiCH₃] ppm.

(2R,4S)-2-tert-Butyldimethylsiloxymethyl-4-[(S)-N-heptanoyl-phenylalanyl-amino]-6-methyl-1,2-oxiranylheptane (PM). 1-Ethyl-3-(3-dimethylaminopropyl)carbodiimide (EDC) hydrochloride (21.5mg, 0.112mmol), and lastly, DIPEA (65 μ L, 0.373mmol) were added to a solution of (2R,4S)-4-amino-2-tert-butyl dimethylsiloxymethyl-6-methyl-1,2-oxiranylheptane (22.5mg, 0.0746mmol) and (S)-N-heptanoyl-phenylalanine (28mg, 0.100mmol) in CH₂Cl₂ (3mL). The reaction solution was stirred at room temperature for 3h. The resulting mixture was concentrated under reduced pressure and subject to flash column chromatography (Hex:EtOAc, 5:1) which yielded **PM** as a colorless oil (9mg, 21%). ¹H NMR: δ = 7.24 (m, 5H, Ar), 6.01 (m, 2H, 4-NH, 2'-NH), 4.67 (m, 1H, 4-H), 4.51 (m, 1H, 2'-H), 4.39 (m, 1H, 2-CH^a₂), 3.54 (m, 1H, 2-CH^b₂), 3.06 (m, 4H, 1-H₂, 2'-CH₂), 2.14 (m, 2H, 2''-H), 1.54 (m, 4H, 6-H, 5-H^a, H_{Hep}), 1.24 (m, 6H, H_{Hep}), 1.00 (m, 6H, CH₃CHCH₃), 0.87 [s, 12H, (C-2)*t*Bu-H, 7''-CH₃] 0.09 [m, 6 H, (C-2)CH₃SiCH₃] ppm.

(2R,4S)-2-tert-Butyldimethylsiloxymethyl-4-[(S)-N-heptanoyl-norvalylamino]-6-methyl-1,2-oxiranylheptane (nVM). HATU (22mg, 0.0578mmol), HoAt (6.4mg, 0.0470mmol), and lastly, DIPEA (34 μ L, 0.195mmol) were added to a solution of (2R,4S)-4-amino-2-tert-butyl dimethylsiloxymethyl-6-methyl-1,2-oxiranylheptane (14.6mg, 0.0484mmol) and (S)-N-heptanoyl-norvaline (9mg, 0.0392mmol) in CH₂Cl₂ (3mL). The reaction solution was stirred at room temperature for 3h. The resulting mixture was concentrated under reduced pressure and subject to flash column chromatography (Hex:EtOAc, 3:1) which yielded **nVM** as a colorless oil (7.6mg, 37%). ¹H NMR: δ = 6.29 (d, J = 7.8 Hz, 1H, 4-NH), 5.92 (d, J = 7.8 Hz, 1H, 2'-NH), 4.58 (m, 1H, 4-H), 4.43 (m, 2H, 2'-H, 2-CH^a₂), 3.55 (d, 1H, J = 12 Hz, 2-CH^b₂), 3.19 (d, J = 4.2 Hz, 1H, 1-H^a), 3.01 (d, J = 5.4 Hz, 1H, 1-H^b), 2.17 (m, 2H, 2''-H), 1.65 (m, 6H, 3'-H₂, 6-H, 5-H^a, H_{Hep}), 1.25 (m, 8H, 4'-H₂, H_{Hep}), 0.93 (m, 6H, CH₃CHCH₃), 0.87 [s, 12H, (C-2)*t*Bu-H, 7''-CH₃], 0.05 [d, J = 3.3 Hz, 6H, (C-2)CH₃SiCH₃] ppm.

(2R,4S)-2-tert-Butyldimethylsiloxymethyl-4-[(S)-N-heptanoyl-methionylamino]-6-methyl-1,2-oxiranylheptane (MM). HATU (92mg, 0.241mmol), HoAt (26mg, 0.191mmol), and lastly, DIPEA (0.14mL, 0.804mmol) were added to a solution of (2R,4S)-4-amino-2-tert-butyl dimethylsiloxymethyl-6-methyl-1,2-oxiranylheptane (35mg, 0.116mmol) and (S)-N-heptanoyl-valine (42mg, 0.160mmol) in CH₂Cl₂ (3mL). The reaction solution was stirred at room temperature for 3h. The resulting mixture was concentrated under reduced pressure and subject to flash column chromatography (Hex:EtOAc, 5:1) which yielded **MM** as a colorless oil (36mg, 42%). ¹H NMR: δ = 6.69 (d, J = 7.5 Hz, 1H, 4-NH), 6.26 (d, J = 7.8 Hz, 1H, 2'-NH), 4.65 (m, 1H, 4-H), 4.55 (m, 2H, 2'-H), 4.42 (d, 1H, J = 10.8 Hz, 2-CH^a₂), 3.54 (d, 1H, J = 10.8 Hz, 2-CH^b₂), 3.19 (d, J = 4.5 Hz, 1H, 1-H^a), 3.01 (d, J = 5.4 Hz, 1H, 1-H^b), 2.17 (m, 2H, 2''-H), 2.13 (s, 3H, S-CH₃), 1.98 (m, 2H, 3'-H₂), 1.63 (m, 4H, 6-H, 5-H^a, H_{Hep}), 1.27 (m, 8H, 4'-H₂, H_{Hep}), 0.94 (m, 6H, CH₃CHCH₃), 0.86 [s, 12H, (C-2)*t*Bu-H, 7''-CH₃], 0.04 [d, J = 4.5 Hz, 6H, (C-2)CH₃SiCH₃] ppm.

Cell Culture and Competition Assay. Experiments were performed as previously described in Chapter Two (see p.73).

Mobility Shift Assay. Murine lymphoma EL4 cells were treated with the indicated concentration of controls and dihydroponemycin analogs for 1.5 hours, which were then harvested and lysed. Cells lysates were analyzed with 12% SDS-PAGE, transferred to a PVDF membranes and probed with anti-LMP2, -LMP7, and -X antibodies. The membranes were subsequently visualized by ECL and Biomax X-ray film (Kodak).

CHAPTER FOUR: BIOLOGICAL STUDIES OF THE AM ANALOG IN HUMAN CANCER CELLS

A. Introduction

Given that the ubiquitin proteasome pathway has emerged as a key player in the regulation of numerous short-lived and regulatory proteins in cells, it has become a very attractive target for cancer therapeutics. The first proteasome inhibitor found to possess anti-tumor properties was lactacystin, which was shown to induce DNA fragmentation and apoptosis [212]. More recently, the approval of bortezomib as the first proteasome inhibitor for the treatment of relapsed multiple myeloma by FDA also helped cement the status of the ubiquitin proteasome pathway as a valid chemotherapeutic target. However, broad spectrum proteasome inhibitors are not exceedingly specific as they indiscriminately target all proteasomes in the body, which can lead to severe toxicity. As a result, the development of immunoproteasome specific inhibitors has begun to gain considerable attention. One of the few immunoproteasome inhibitors developed thus far was the analog **AM**, which was described in the previous chapters. Also known as UK-101, **AM** is the first reported immunoproteasome inhibitor that specifically targets the LMP2 catalytic subunit [126, 213].

This promising compound will be a valuable tool for the pathological studies of diseases, especially cancer. Specifically, some cancers, such as multiple myeloma, are known to highly express immunoproteasomes. This form of the proteasome is generally not constitutively expressed in non-immune related tissues and cells, such as the spleen and white blood cells. This evidence has prompted interest in the investigation of differential expression levels of immunoproteasome catalytic subunits in human cancers. Therefore, the subunit binding specificity of **AM** will be investigated in cancers that highly express immunoproteasomes. The cytotoxicity of the analog in cancers will also be examined as well as its possible mode of actions. These biological studies will provide the proof of concept necessary to move **AM** towards *in vivo* studies. These series of experiments will show that the LMP2 subunit is a valid target for chemotherapeutics.

B. LMP2/LMP7 Subunit Profiling in Human Cancers

Given that one of the goals of this project is to explore the pathophysiological functions of LMP2 in diseases, it would be of great interest to determine whether the LMP2 inhibitor developed has any impact on normal biological processes of cancer cells that show increased expression of the LMP2 catalytic subunit. Consequently, a total of 11 human cancer cell lines were investigated for the differential expression levels of the immunoproteasome catalytic subunits LMP2 and LMP7. They include prostate cancer (PC3, LN3, LNCaP and DU145), breast cancer (MCF7, MDA-MB-231 and Hs578T), multiple myeloma (RPMI 8226 and U266), cervical cancer (HeLa), colon cancer (HT-29), and normal lung fibroblast (WI-38) cell lines. These cells were lysed and analyzed via western blot. Subsequently, they were visualized using anti-LMP2 and –LMP7 antibodies. These cancer cell lines were shown to display various expression levels of LMP2 and LMP7 subunits regardless of their tissues of origin (Figure 4.1). In addition, the non-cancerous lung fibroblast cells WI-38 express relatively insignificant levels of immunoproteasome catalytic subunits.

These exciting results indicate that cancer cell lines that were derived from the same tissue of origin do not necessary possess similar proteasome catalytic subunit composition. For example, the androgen-independent PC3 prostate cancer cells displayed higher LMP2 and LMP7 catalytic subunit expression levels compared to the androgen-dependent LNCaP prostate cancer cells. Also, the estrogen receptor (ER) negative MDA-MB-231 breast cancer cell line is shown to express significantly higher levels of LMP2 and LM7 than the ER positive MCF7 breast cancer cell line. While these results may seem random, the expression levels of immunoproteasome catalytic subunits may be in correlation with the metastasis of the cancer cell lines. The PC3 and MDA-MB-231 cell lines are known to possess a higher metastatic ability than the LNCaP and MCF7 cell lines. In fact, the analysis of prostate cancer tissue array revealed that samples with higher tumor grades were found to express higher levels of LMP2 catalytic subunit (data not shown). However, it remains to be determined whether the increased expression level of LMP2 is a causative factor or a secondary effect of the cancer metastasis.

These results also suggest the possibility of personalized cancer therapy in which treatments are specialized for patients based on their cancer's genetic makeup. In addition,

most of the normal cells in the body express minimal levels of the immunoproteasome except for the immune-related tissues and cells; hence, this allows the targeting of immunoproteasome subunits in cancer cells without affecting normal cells, which will help lower the incidence of severe side effects. Therefore, the development of a LMP2 specific immunoproteasome inhibitor will be of tremendous advantage to the cancer chemotherapy.

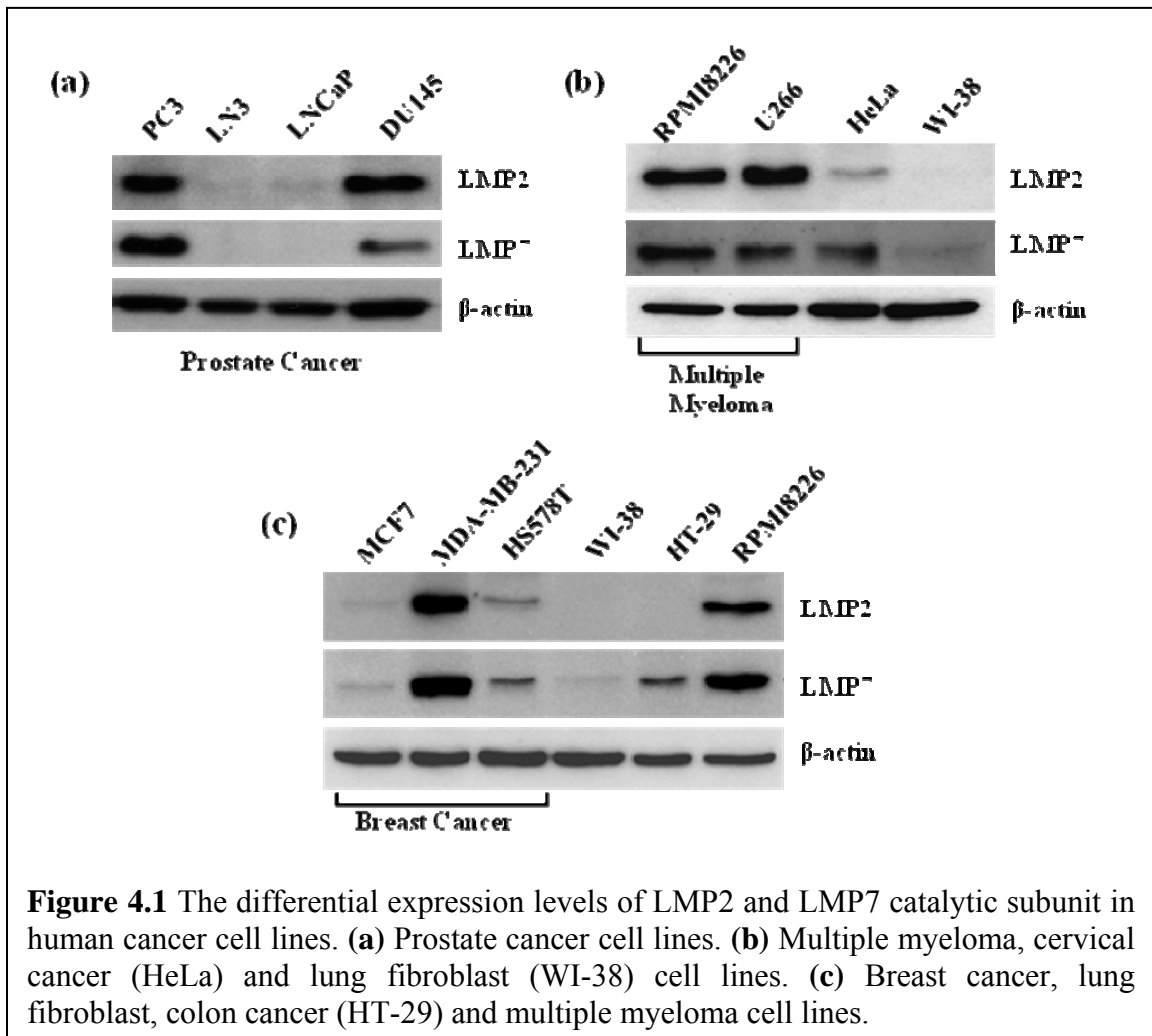


Figure 4.1 The differential expression levels of LMP2 and LMP7 catalytic subunit in human cancer cell lines. **(a)** Prostate cancer cell lines. **(b)** Multiple myeloma, cervical cancer (HeLa) and lung fibroblast (WI-38) cell lines. **(c)** Breast cancer, lung fibroblast, colon cancer (HT-29) and multiple myeloma cell lines.

C. Characterization of Subunit Binding Specificity of AM in Human Prostate Cancer Cells

The immunoproteasome subunit binding specificity of the analog **AM** was previously determined in a murine lymphoma cell line (EL4). In order to begin investigating the immunoproteasome subunit binding specificity of **AM** in human cancer, an ideal human cancer cell model would be needed. This model would include human cancer cell lines that possess an identical tissue of origin with differential expression levels of LMP2 and LMP7 subunits. Cell lines that express high levels of LMP2 would be expected to be sensitive towards **AM** and vice versa. This model would allow for a more accurate assessment of the correlation between LMP2 expression levels and the efficacy of **AM**.

Prostate cancer cell lines were subsequently selected because they fit the criteria for our ideal cancer cell model (Figure 4.1). The comparison between cancer cell lines of different tissues of origins is also possible but it is not desirable due to their inherent differences in many aspects of cellular functions. Although breast cancer cell lines were also considered due to their differential expression levels of LMP2/LMP7 as well as identical tissue of origin, the cell line that expresses lower LMP2 subunit, MCF7, was previously reported to be inherently resistant to proteasome inhibition due to elevated levels of proteasome activity [214]. Therefore, without a creditable LMP2 negative cell line, the breast cancer cell lines would not be an ideal model for the purpose of this project.

The PC3 cell line will be the major focus in this project, as it highly expresses both the LMP2 and LMP7 catalytic subunits as shown in Figure 4.1. Even though the DU145 cell line also expresses high levels of the LMP2 subunit, it appears that it did not express an equal amount of the LMP7 subunit, which may adversely affect the proper assembly of the immunoproteasome structure [111]. A whole immunoproteasome is preferable for a more accurate assessment of the effect of LMP2 subunit inhibition in cancers utilizing the analog **AM**. On the other hand, LN3 cell line was a less attractive choice compared to LNCaP cell line for negative control because LN3 is originally derived from the LNCaP cell line and it is the highly metastatic variant of LNCaP. As a result, LN3 was not even an established cell line at the American Type Culture Collection

(ATCC). Therefore, the LNCaP cell line is believed to be a more suitable cell line to serve as negative control.

Similar to the previously described EL4 cell experiments, the competition and mobility shift assays were repeated in PC3 cells to determine the immunoproteasome subunit binding specificity of **AM**. As shown in Figure 4.2a, the observation that the LMP2 subunit band was attenuated on western blot indicates a high specificity towards the LMP2 subunit by the compound **AM** when competing with the probe, biotin-tagged dihydroeponemycin. Furthermore, the mobility shift assay performed in PC3 cells clearly showed that **AM** covalently modifies the LMP2 subunit, but not the other proteasome catalytic subunits (Figure 4.2b). The **AM**-LMP2 conjugate was observed at a concentration as low as 1 μ M (lane 4) whereas the probe-LMP2 conjugates were not observed at 1 μ M (lane 2-3). On the other hand, the LMP7, X, and Y catalytic subunits did not display any mobility shift even at concentration as high as 10 μ M of **AM** (lane 6). These results indicate that **AM** selectively modifies the LMP2 catalytic subunit that is highly expressed in PC3 prostate cancer cells.

The western blot results also revealed that **AM** is a more potent LMP2 inhibitor than the biotin-tagged probes, biotin-epoxomicin and biotin-dihydroeponemycin. While the biotin-tagged probes were shown to label LMP2 at 1 μ M (Figure 4.2a), a LMP2 mobility shift was not observed from either biotin-tagged probe at 1 μ M (Figure 4.2b). On the other hand, **AM** was able to induce a mobility shift in the LMP2 band starting at 1 μ M (Figure 4.2b); however, the LMP2 band on the competition assay western blot (Figure 4.2a) can still be clearly observed at 1 μ M. These contradicting results could be explained by the exceedingly stronger western blot signal inherent to the streptavidin-biotin interaction compared to the anti-LMP2 antibody. While **AM** may have bound to the majority of the LMP2 subunit at 1 μ M during the competition assay, it may not be sufficient to attenuate the streptavidin signal derived from the minor interaction between the biotin-tagged probe and the remaining LMP2 subunits; hence, the LMP2 band on the competition assay western blot was still clearly visible at 1 μ M.

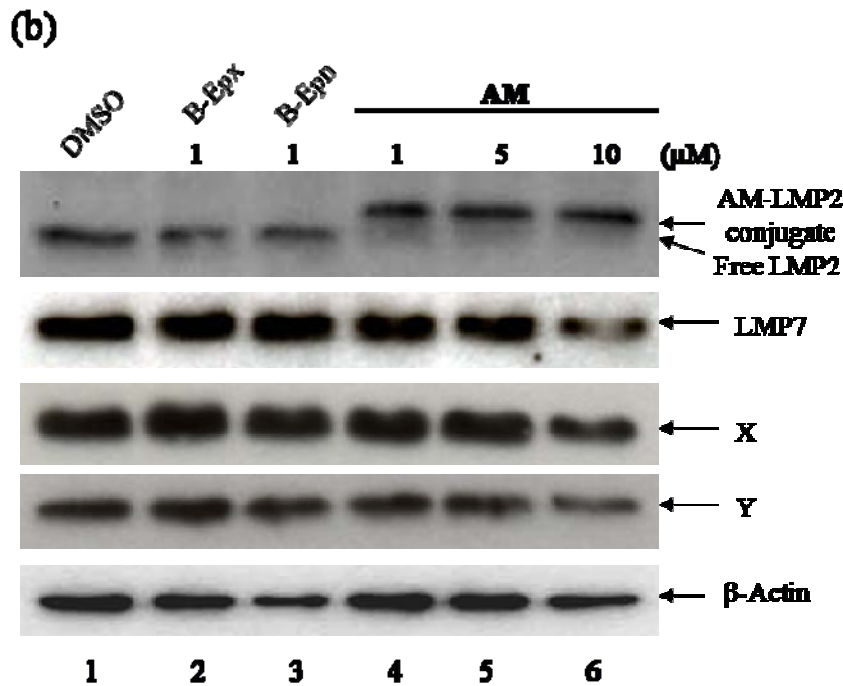
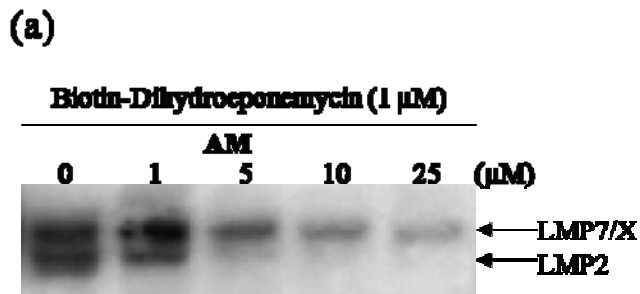


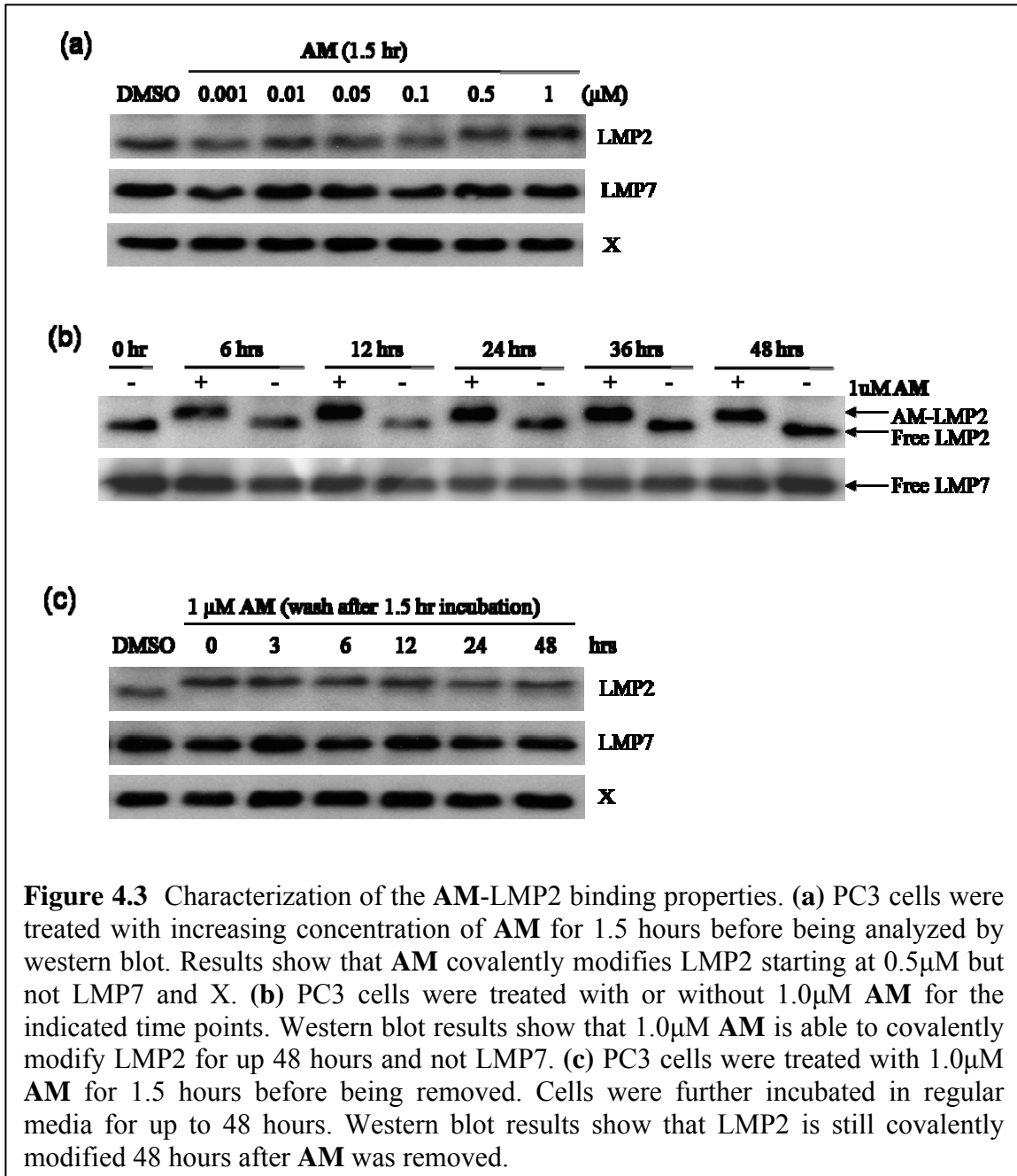
Figure 4.2 Selective modification of LMP2 in PC3 cell line. **(a)** Competition assay. PC3 cells were pre-treated with **AM** before the addition of biotin-tagged dihydroeponemycin to visualize the catalytic subunits that were not targeted by **AM**. **(b)** Mobility shift assay. PC3 cells were treated with the indicated concentrations of **AM**, biotin-epoxomicin (B-Epx) and biotin-dihydroeponemycin (B-Epn) for 1.5 hours. The mobility shift of the catalytic subunits were then analyzed by western blot using anti-LMP2, -LMP7, -X and -Y antibodies.

Furthermore, the covalent binding properties of **AM** to the proteasome catalytic subunits were also investigated in prostate cancer cells. Specifically, PC3 cells were treated with increasing concentrations of **AM** for 1.5 hours as indicated in Figure 4.3a. Similar to the mobility shift assay, they were then analyzed by western blot using anti-LMP2, -LMP7 and -X antibodies to determine the dose dependent covalent modification of these catalytic subunits by **AM**. Results showed that **AM** was able to covalently modify the LMP2 subunit starting at a concentration as low as 0.5 μ M whereas LMP7 and X subunits were not modified even with 1 μ M **AM** (Figure 4.3a). Not only does this experiment reconfirm that **AM** selectively targets LMP2 subunits, but it also indicates that 1 μ M is a selective concentration for **AM** treatments in future experiments.

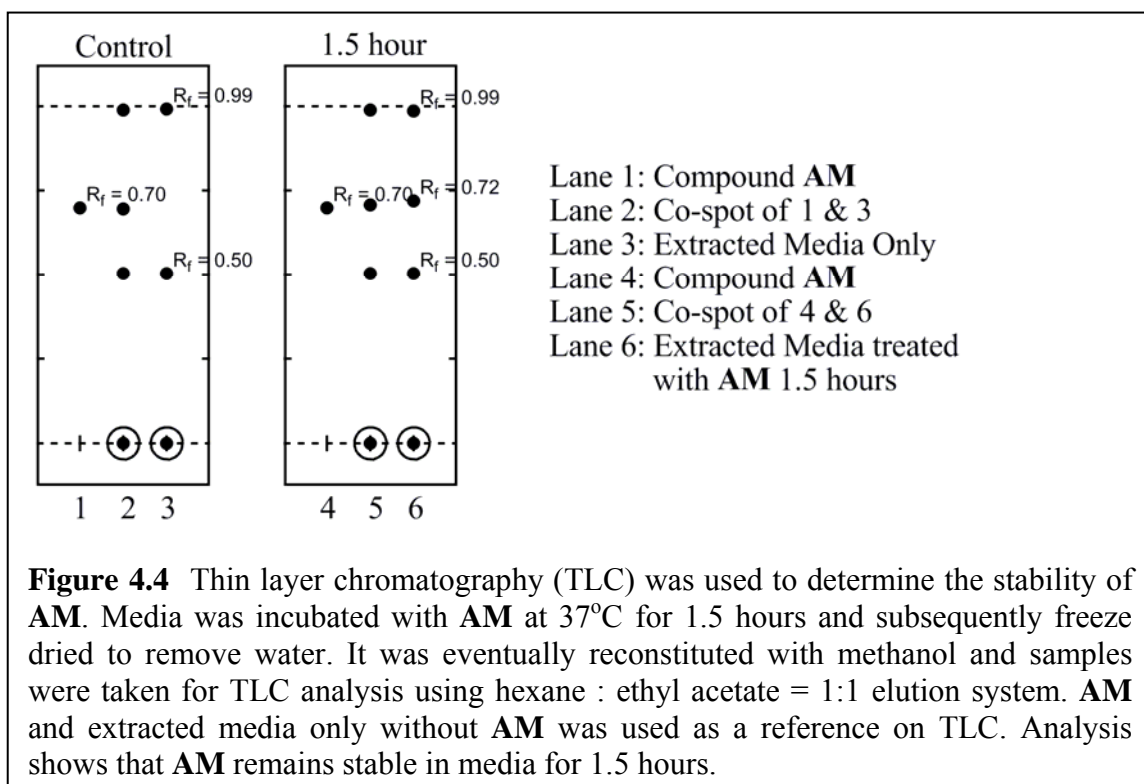
Subsequently, the stability of the compound **AM** in prostate cancer cells was determined. PC3 cells were treated with or without **AM** for up to 48 hours as shown in Figure 4.3b. Western blot results indicate that **AM** was able to maintain a consistent covalent modification of LMP2 for up to 48 hours as no free LMP2 band was observed in the treated cells (Figure 4.3b). On the other hand, **AM** did not modify the LMP7 subunit even after 48 hours incubation. This suggests that the compound is biologically active in prostate cancer cells for at least 48 hours and that the LMP7 subunit is not affected by the 48 hour treatment.

Finally, the binding activity of **AM** was investigated. PC3 cells were treated with 1 μ M **AM** for 1.5 hours. Subsequently, the media was replaced with fresh untreated media, removing the compound from the solution. Cells were then harvested at the indicated time points. As shown in Figure 4.3c, LMP2 is still covalently modified 48 hours after **AM** was removed from the media. This suggests that the interaction between **AM** and LMP2 is irreversible. While a strong interaction between a compound and its target is desirable, covalent binding that lasts more than 48 hours may have adverse consequences. These consequences are often associated with the systemic toxicity of the compound, which will be further investigated in the near future. Considering that no unmodified LMP2 subunit was observed in PC3 cells during the 48 hour time period after the **AM** was removed (figure 4.3c), the turnover rate of the immunoproteasome catalytic subunit LMP2 could be more than 48 hours. However, it is uncertain whether the intrinsic turnover rate of LMP2 in PC3 cells is more than 48 hours or the pre-treatment of **AM** has

delayed the turnover rate of LMP2; hence, additional experiments to elucidate the mechanism in which the LMP2 protein levels is regulated will be needed. In conclusion, 1 μ M **AM** binds to LMP2 in PC3 cells irreversibly and the turnover rate of LMP2 may be more than 48 hours.



In order to further investigate the stability of **AM** in media, the compound **AM** was dissolved in isopropanol and diluted in media to a final concentration of 1mM. **AM** was then incubated at 37°C in the media for 1.5 hours and subsequently freeze dried to remove water. The precipitates obtained were then dissolved in methanol and thin layer chromatography (TLC) using an elution system of hexane : ethyl acetate = 1:1 was performed to determine whether **AM** is still present in the mixture. For control purposes, TLC was first performed to determine the R_f value of pure **AM** and extracted media on TLC for comparison purposes (Figure 4.4, lane 1-3). When TLC was performed with pure **AM** and the sample that was extracted from the treated media, a spot displaying a very close R_f value to pure **AM** was observed with the **AM** treated media sample (Figure 4.4, lane 4-6). This data suggests that the compound **AM** is stable when incubated in media for 1.5 hours, which is the amount of time needed for **AM** to covalently modify the LMP2 subunit. Nevertheless, the TLC is only able to determine the stability of **AM** qualitatively. High technology instrument system such as the high performance liquid chromatography mass spectrometry (HPLC/MS), however, will not only be able to determine the stability of **AM** in a quantitative manner, but also can be used to help

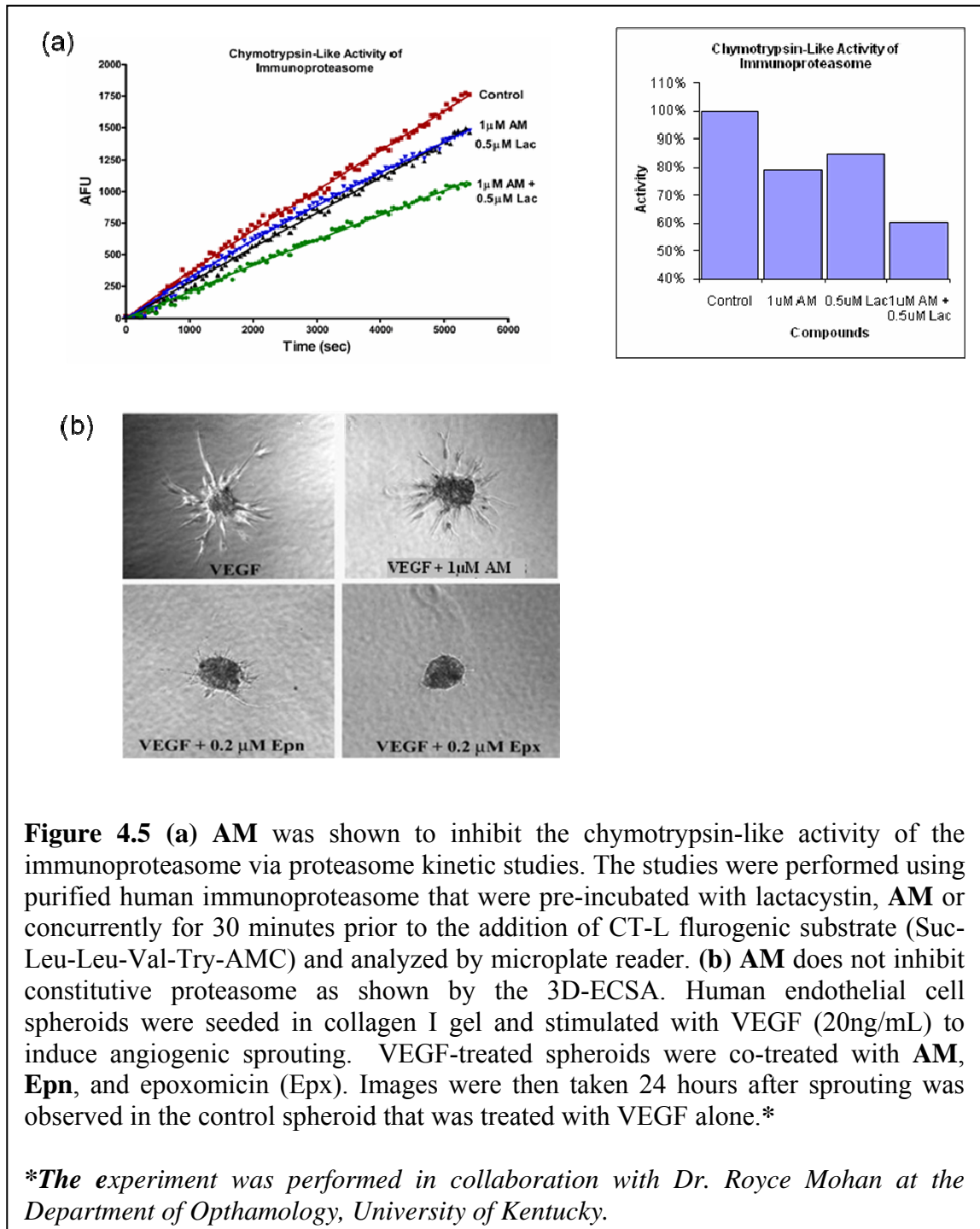


determine the fragments of **AM** if it were to metabolize. Even though the compound **AM** is not expected to metabolize in an *in vivo* setting, the metabolites of the compound could result from the hydrolysis of the two amide bonds, therefore generating three metabolites. In conclusion, while this preliminary data implies that **AM** is stable in media, the true half life and stability of **AM** can only be accurately determined in an *in vivo* experimental setting. Specifically, future animal studies will be required to obtain the complete pharmacokinetic profile of **AM**.

D. Selective Inhibition of Proteolytic Activity and Cytotoxicity of Compound AM

While LMP7 and MECL-1 catalytic subunits of the immunoproteasome have been shown to exhibit CT-L and T-L activity respectively [209, 215], the proteolytic activity of the LMP2 subunit has not been clearly established. It has been previously suggested that LMP2 preferably cleaves after hydrophobic amino acid residues to generate short peptides favoring MHC class I presentation, but the supporting experimental data was lacking [216]. Therefore, there is an interest in determining whether LMP2 is responsible for CT-L activity. In order to carry out this investigation, the natural product lactacystin was used, which primarily binds to the LMP7 and, to a lesser extent, MECL1 subunits [217] and subsequently inhibits their respective catalytic activities. This would facilitate the proteolytic activity assignment of the LMP2 subunit as well as determining the inhibitory activity of compound **AM**.

Specifically, purified 20S human immunoproteasomes from Biomol were used in these experiments for a more accurate assessment of immunoproteasome catalytic subunit activity. The immunoproteasomes were preincubated with lactacystin at a concentration with which a significant amount of the CT-L activity is inhibited in the constitutive proteasome. Kinetic studies showed that approximately 20% of the CT-L activity of the immunoproteasomes was inhibited by lactacystin compared to control (Figure 4.5a). Similarly, when the immunoproteasomes were preincubated with **AM** at a concentration that only covalently modifies LMP2, approximately 20% of the CT-L activity of the immunoproteasome was inhibited compared to control (Figure 4-5a). However, when immunoproteasomes were preincubated with both lactacystin and **AM**, approximately 45% of the CT-L activity of the immunoproteasome was inhibited compared to control (Figure 4.5a). The combination of **AM** and lactacystin produced an inhibitory effect comparable to the sum of the inhibitory effects produced by the compounds individually. Therefore, these results suggest that the inhibitors have an additive inhibitory activity on the CT-L activity of the immunoproteasome. Collectively, they also suggest that the LMP2 catalytic subunit is, at least in part, responsible for the CT-L activity of the immunoproteasome [126].



Despite the finding that **AM** selectively modifies the LMP2 subunit as well as inhibits its CT-L activity, it is still unclear whether the inhibitor also targets the CT-L activity of the constitutive proteasome. Therefore, **AM** was further assessed for its ability to disrupt cellular events that are regulated by the constitutive proteasome, specifically angiogenesis. It has been previously reported that broad spectrum proteasome inhibitors are particularly effective in inhibiting the angiogenic growth of blood vessels, which suggests that the constitutive proteasome is important in angiogenesis [218]. Furthermore, the endothelial cells involved in the angiogenesis process do not generally express immunoproteasomes. Therefore, the application of a LMP2-specific inhibitor to angiogenic endothelial cells would help determine whether the inhibitor targets constitutive proteasome by looking at how it affects angiogenesis. The compound **AM** is not expected to inhibit the angiogenic sprouting process.

The three-dimensional endothelial cell sprouting assay (3D-ECSA) was believed to be a suitable *in vitro* angiogenesis model because it closely mimics the *in vivo* angiogenesis processes. The differentiation of endothelial cells into sprouting structures was stimulated by vascular endothelial growth factor (VEGF) and observed within a 3D matrix of fibrin or collagen I [219]. This was then followed by the treatments of **AM** or broad spectrum proteasome inhibitors. As expected, the sprouting of endothelial cells was completely inhibited when the cells were treated with epoxomicin (Epx) and dihydroeponemycin substitute (**Epn**), as shown in Figure 4.5b. On the other hand, the LMP2-specific inhibitor, **AM**, was not shown to inhibit the endothelial cell sprouting at 1 μ M concentration (Figure 4.5b). Furthermore, a 10 fold increase in the concentration of **AM** only marginally disrupted sprouting (data not shown), which strongly suggest that the LMP2 inhibitor does not target constitutive proteasome. These results indicate that the LMP2 inhibitor does not disrupt the angiogenesis process mediated by the constitutive proteasome in living cells. Also, the results help confirm previous results that **AM** selectively targets the immunoproteasome catalytic subunit LMP2 [126].

Table 1. MTS assays were performed after 48 h incubation with AM or broad spectrum proteasome inhibitors, **Epn** and epoxomicin.

Cell Lines	IC ₅₀ (μM) ^a		Relative Sensitivity ^b
	PC3	LNCaP	
LMP2 Level	High	Low	-
Epoxomicin	0.020	0.022	1
Epn	0.43	0.59	1
AM	4.18	28.27	7
Bortezomib	0.02 ^c	0.007 ^d	0.35

^a Experiments were repeated at least 3-times or more.

^b Relative sensitivity of PC3 cells to inhibitors compared to the LNCaP cell line = $IC_{50}^{LNCaP}/IC_{50}^{PC3}$.

^{c,d} Results were previously reported [1, 2].

In addition to determining the selective inhibition of the proteolytic activity of the immunoproteasome, the cytotoxic effects of **AM** in prostate cancer was also investigated. Given that LMP2 is a major catalytic subunit of the immunoproteasome and that proteasomes play a vital role in the cell cycle as well as cell growth, it is anticipated that cancers that express high level of immunoproteasomes will be more sensitive towards LMP2 inhibition than cancers that express minimal levels of immunoproteasomes. In contrast, broad spectrum proteasome inhibitors, such as epoxomicin and **Epn**, will not have differential cytotoxicity towards cancers regardless of their immunoproteasome expression profile. Specifically, the IC₅₀ of **AM**, epoxomicin, and **Epn** was determined in prostate cancer cell lines by the MTS assay. Remarkably, prostate cancer cells that express a higher level of LMP2 (PC3) are approximately 7-fold more sensitive to the LMP2-specific inhibitor, **AM**, compared to prostate cancer cells that express a lower level of LMP2 (LNCaP). These results suggest that there is a possible correlation between LMP2 expression level and the sensitivity of cancer cells to **AM**. On the contrary, both PC3 and LNCaP cells were equally sensitive to the broad spectrum proteasome inhibitors epoxomicin and **Epn**. Similarly, both cell lines were also equally

sensitive to bortezomib, based on previously reported IC_{50} values as shown in Table 1. In fact, LNCaP cells were observed to be 3-fold more sensitive to the treatment of bortezomib than PC3 cells, which represents the opposite effect of **AM** treatment. These results indicate that the broad spectrum proteasome inhibitors do not discriminate among cancer cells that do and do not express high level of LMP2 but the LMP2-specific inhibitor does.

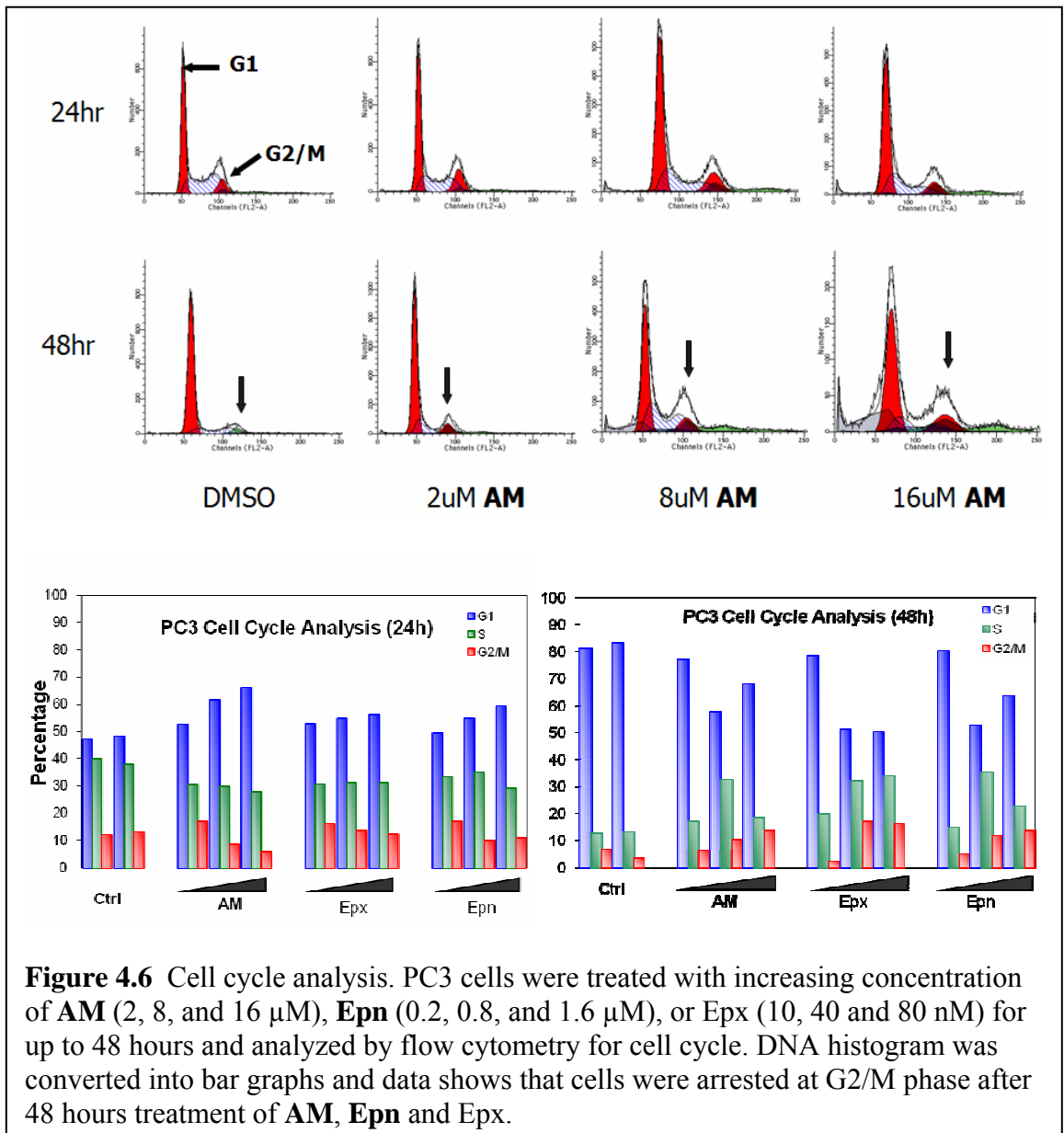
While these MTS results are insufficient to come to a definite conclusion, they strongly suggest that a line of prostate cancer cells that highly express the LMP2 catalytic subunit (PC3) are more sensitive to the compound **AM** than a line of prostate cancer cells that express lower levels of the LMP2 subunit (LNCaP). On the other hand, bortezomib as well as epoxomicin and dihydroeponemycin substitute (**Epn**) inhibit the proliferation of both prostate cancer cell lines with similar IC_{50} values regardless of their LMP2 subunit expression profile. Even though these inhibitors have a much lower IC_{50} value than **AM**, they were unable to selectively target the cancer cell line that express high levels of LMP2. In other words, bortezomib, epoxomicin and **Epn** are more potent proteasome inhibitors but display poor selectivity towards immunoproteasome catalytic subunit. While the compound **AM** has undeniably lost its potency when compared to the other non-specific proteasome inhibitors, the LMP2 selectivity of **AM** was shown to be much greater; hence, it is believed that this selectivity will help alleviate the general toxicity that can be caused by the non-specific proteasome inhibitors.

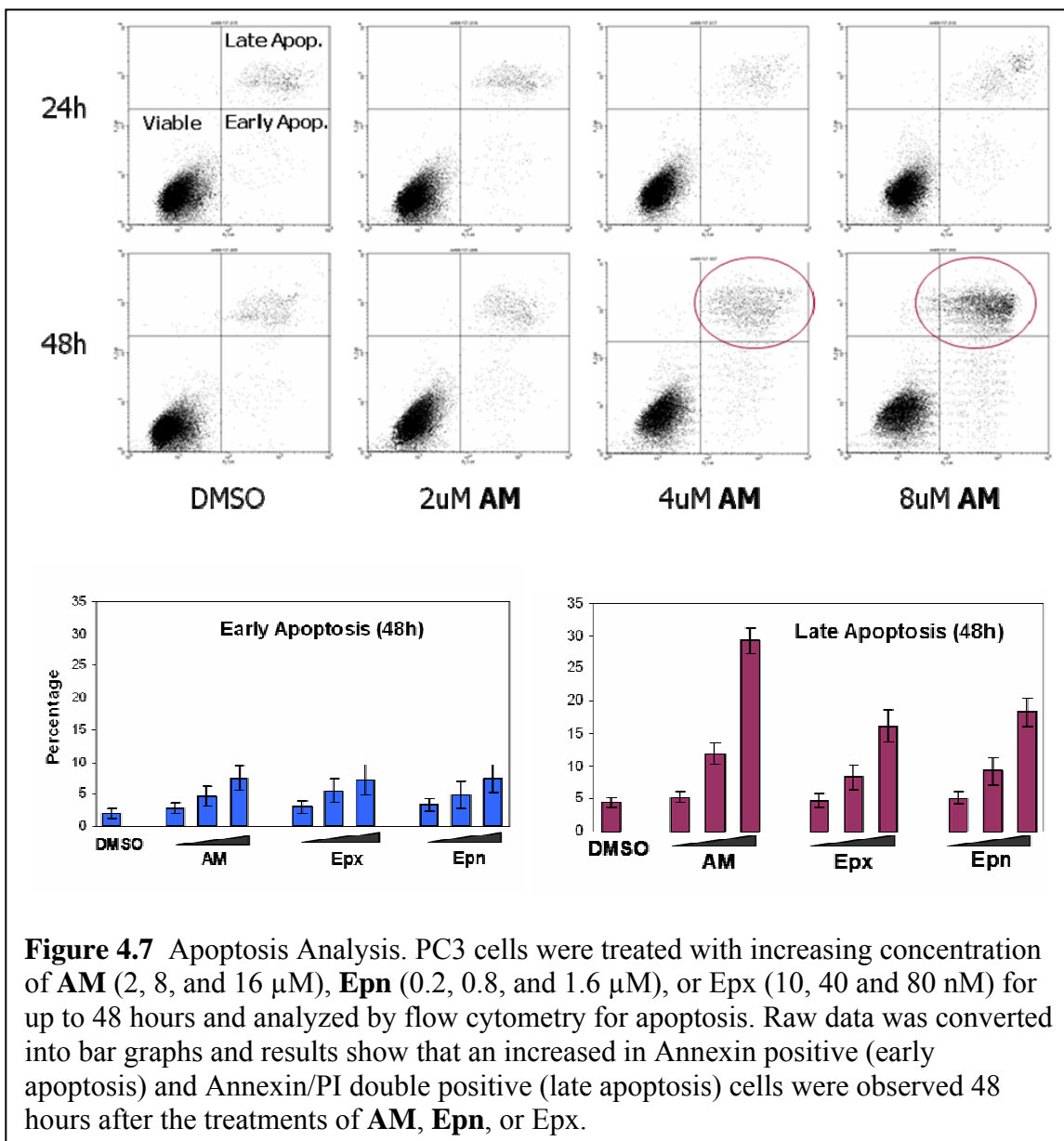
E. Modes of Action of AM

While it has been determined that the proliferation of cancer cells that express high levels of the LMP2 subunit is more sensitive to **AM** than cancer cells that express lower levels of LMP2, it is essential to establish the mode of action of **AM** on a cellular and molecular level. In addition, it remains to be determined whether **AM** exhibits modes of action similar to the other broad spectrum proteasome inhibitors. Therefore, all subsequent experiments will be performed in parallel with the treatments of epoxomicin and the dihydroeponepimycin substitute (**Epn**) for comparison purposes.

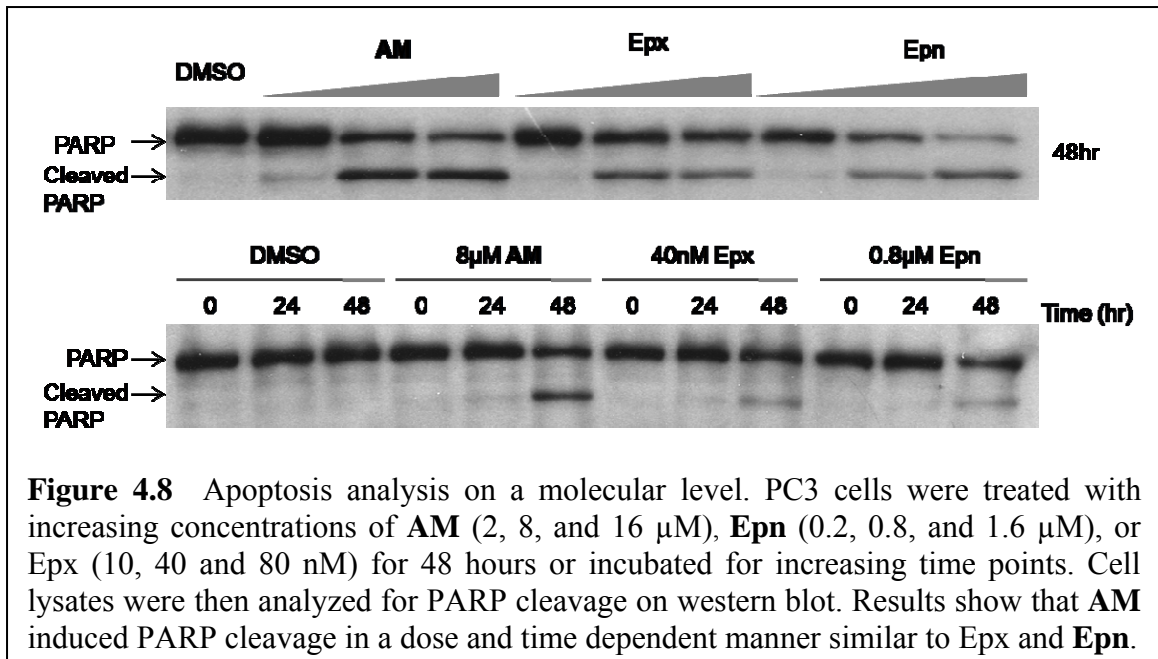
Since **AM** was shown to be cytotoxic to PC3 cells, cell cycle and apoptosis assays were performed to determine whether **AM** induces cell cycle arrest and/or apoptosis in cancer cells that express high levels of LMP2. PC3 cells were incubated with increasing concentrations of **AM** (2, 8, and 16 μM), **Epn** (0.2, 0.8, and 1.6 μM), and epoxomicin (10, 40 and 80 nM) for 24 or 48 hours. The dosages used among these three compounds are values from the same area of the IC_{50} curve for relative comparison purposes. While the IC_{50} values are different for all three compounds, they are shown to exhibit similar efficacy. These dosages allow for a significant amount of cells to undergo the process of cell death without being dead, which will facilitate the better understanding of the cytotoxicity of **AM** on a cellular level.

The cells were subsequently harvested and stained accordingly for cell cycle and apoptosis analyses utilizing flow cytometry. In the cell cycle analysis, the DNA histogram raw data showed that the cells were arrested at G2/M phase after 48 hours treatment of **AM** as well as epoxomicin and **Epn**. The induction of G2/M phase arrest is known to be indicative of apoptosis (Figure 4.6). Subsequently, the cells were also analyzed for apoptosis via Annexin and Propidium Iodide (PI) staining. The results obtained from flow cytometry analysis showed that there was an increased in both Annexin positive as well as Annexin and PI double positive cells after 48 hours treatment of **AM**, epoxomicin and **Epn**. Cells that were Annexin positive represents early apoptosis and cells that were Annexin and PI double positive represents late apoptosis (Figure 4.7). These results suggest that **AM** may induce apoptosis in a similar manner as epoxomicin and **Epn**.



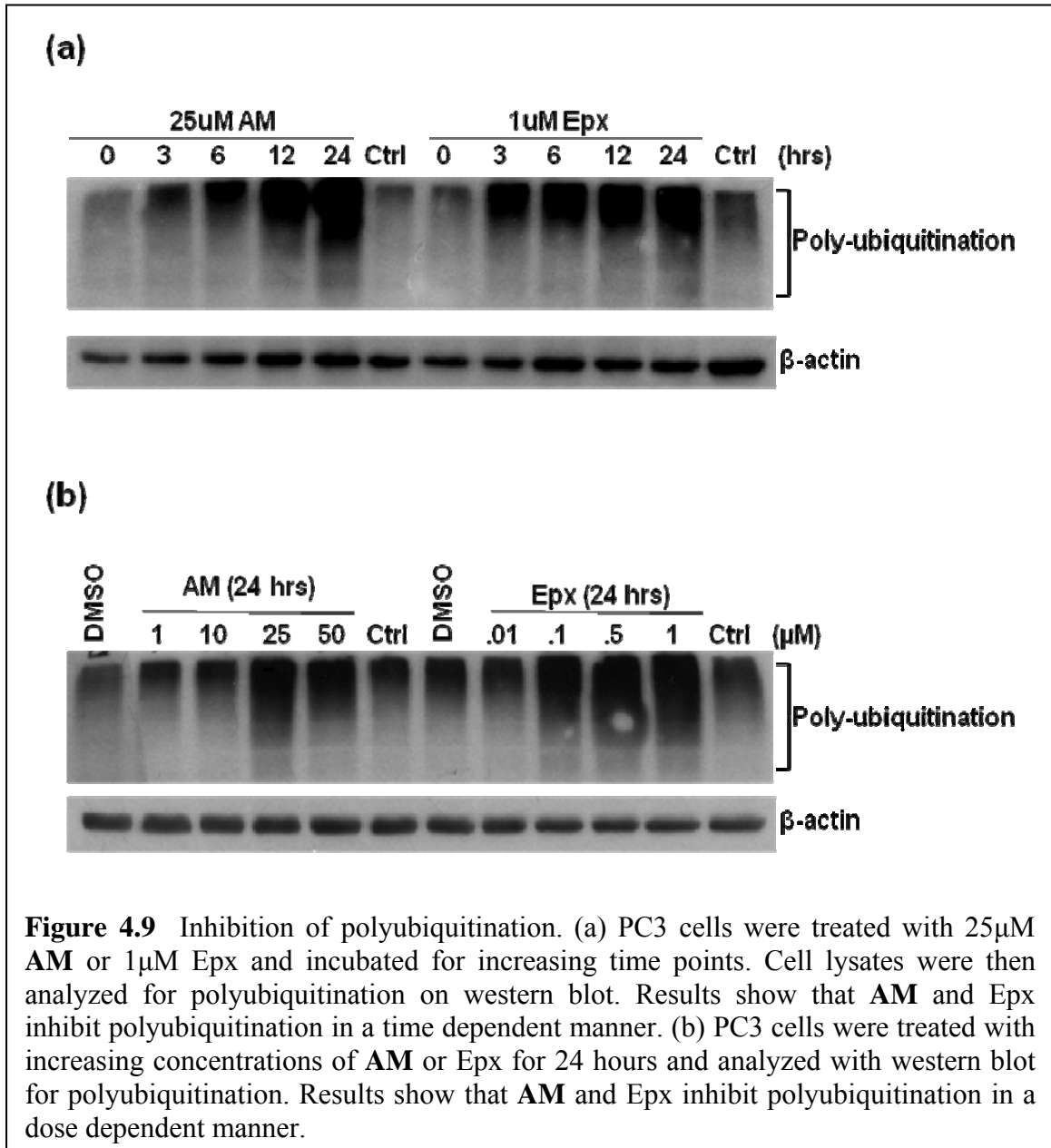


Apoptosis plays an essential role in development, immunological competence, and homeostasis [220]. It is not only characterized by morphological changes that can be recognized by flow cytometry but also by many cellular events such as the cleavage of poly (ADP-ribose) polymerase (PARP). PARP is an enzyme involved in DNA repair and it is also one of the main substrates of caspase 3, which is actively involved in the execution of apoptosis. Specifically, caspase 3 is responsible for the cleavage of PARP during the onset of apoptosis. Therefore, PARP cleavage was also determined in addition to the flow cytometry apoptosis assay in order to investigate apoptosis on a molecular level. PC3 cells were treated with increasing concentration **AM** (2, 8, and 16 μM), epoxomicin (10, 40 and 80 nM), and **Epn** (0.2, 0.8, and 1.6 μM) for 24 or 48 hours. Cells were then lysed and analyzed with western blot using an antibody that targets both full length and cleaved PARP. Western blot results clearly show that **AM** induces apoptosis in PC3 cells in a dose and time dependent manner, similar to the results seen with epoxomicin and **Epn** (Figure 4.8).



Given that the epoxomicin was previously shown to inhibit proteolysis as well as exhibit anti-inflammatory activity [211], it is of great interest to investigate the effects of **AM** on proteolysis and inflammation in cells. The inhibition of proteolysis is generally characterized by the accumulation of poly-ubiquitinated proteins, because the proteasome is unable to process and degrade ubiquitinated proteins. On the other hand, it is well known that the inflammation pathway is mediated by the ubiquitin proteasome pathway. Therefore, it is not unexpected that proteasome inhibitors exhibit anti-inflammatory activity. The inhibition of inflammation is largely characterized by the accumulation of phosphorylated I κ B because again, the inhibited proteasome is unable to degrade the inhibitory protein of NF κ B for the activation of inflammation to commence. NF κ B is a transcription factor that is involved in a myriad of cellular signaling pathways. Some of the well known pathways mediated by NF κ B include inflammation, apoptosis, stress and immune responses. In addition, the malfunctioning of NF κ B has also been linked to cancer. In fact, one of the major pathways reported to be inhibited by bortezomib is the NF κ B pathway [221].

As shown in Figure 4.9a, PC3 cells were treated with 25 μ M **AM** or 1 μ M epoxomicin (Epx) for increasing time points as indicated. This resulted in the accumulation of poly-ubiquitinated proteins compared to controls. On the other hand, when PC3 cells were treated with increasing concentrations of **AM** or epoxomicin (Epx) for 24 hours, an accumulation of poly-ubiquitinated proteins was observed as well (Figure 4.9b). These results indicate that the compound **AM** inhibits proteolysis in a time and dose dependent manner, similar to epoxomicin.



In order to begin exploring the effects of **AM** on inflammatory activity in cells, artificial activation of NFκB by TNF-α was performed to serve as a control (Figure 4.10a). PC3 cells were treated with 20ng/mL of TNF-α for up to 30 minutes and harvested at different time points as indicated. Cell lysates were analyzed and visualized using a phosphorylated IκB antibody as well as an IκB antibody. Western blot results indicate that the treatment TNF-α induced the phosphorylation of IκB by 3 minutes and reached its peak at 5 minutes. The IκB protein remained phosphorylated until 12 minutes, when it was degraded by the proteasome. On the other hand, IκB was only observed on the western blot at zero minutes and 3 minutes. The protein was then no longer observed because it was completely phosphorylated and subsequently degraded by the proteasome. In other words, NFκB was activated within 15 minutes following treatment with TNF-α.

Subsequently, the cells were treated with 1μM epoxomicin for 2 hours prior to the treatment of TNF-α as indicated in Figure 4.10b. Results showed that the treatment of epoxomicin prevented the degradation of phosphorylated IκB. This indicates that the proteasome inhibitor epoxomicin was able to block the activation of NFκB. On the other hand, when cells were pre-treated with 50μM **AM** for 2 hours prior to the treatment of TNF-α, accumulation of phosphorylated IκB was not observed (Figure 4.10c). This result indicates that the LMP2 inhibitor **AM** did not block the activation of NFκB because, unlike the epoxomicin pre-treatment, the phosphorylated IκB was degraded after 15 minutes of TNF-α treatment. Therefore, it can be concluded that, while epoxomicin inhibits both proteolysis and the activation of NFκB, **AM** was shown to only inhibit proteolysis but not the activation of NFκB in PC3 cells.

The activation of NFκB has been thought to be mediated by constitutive proteasomes, not immunoproteasomes. Controversial evidence supporting a role for the immunoproteasome in this process has been reported recently [222]. Nevertheless, the results presented here strongly support the common belief that the activation of inflammation is mediated by constitutive proteasomes. While the LMP2 inhibitor **AM** was shown to inhibit proteolysis, it did not exhibit anti-inflammatory activity in PC3 cells. These results strongly suggest that the immunoproteasome catalytic subunit LMP2 is not responsible for the degradation of IκB and subsequently the activation of NFκB in PC3 cells. Furthermore, it also indicates that **AM** may have a different mode of actions than

the broad spectrum proteasome inhibitor epoxomicin. However, these results alone are insufficient to conclude with confidence that the compound **AM** is an anti-inflammatory agent. As mentioned earlier, all cancer cell lines are inherently different regardless of their tissue of origin; hence, it is inaccurate to make a generalized conclusion from experiments performed in a single cancer cell line. Supplementary experiments to make these findings more conclusive are needed. For example, immune cells may be used to investigate the claimed anti-inflammatory activity of **AM** because it could closely mimics the *in vivo* inflammatory responses. As immunoproteasome has been associated with immune responses, the effect of **AM** on the immune system can also be investigated by using immune cells in the experiments.

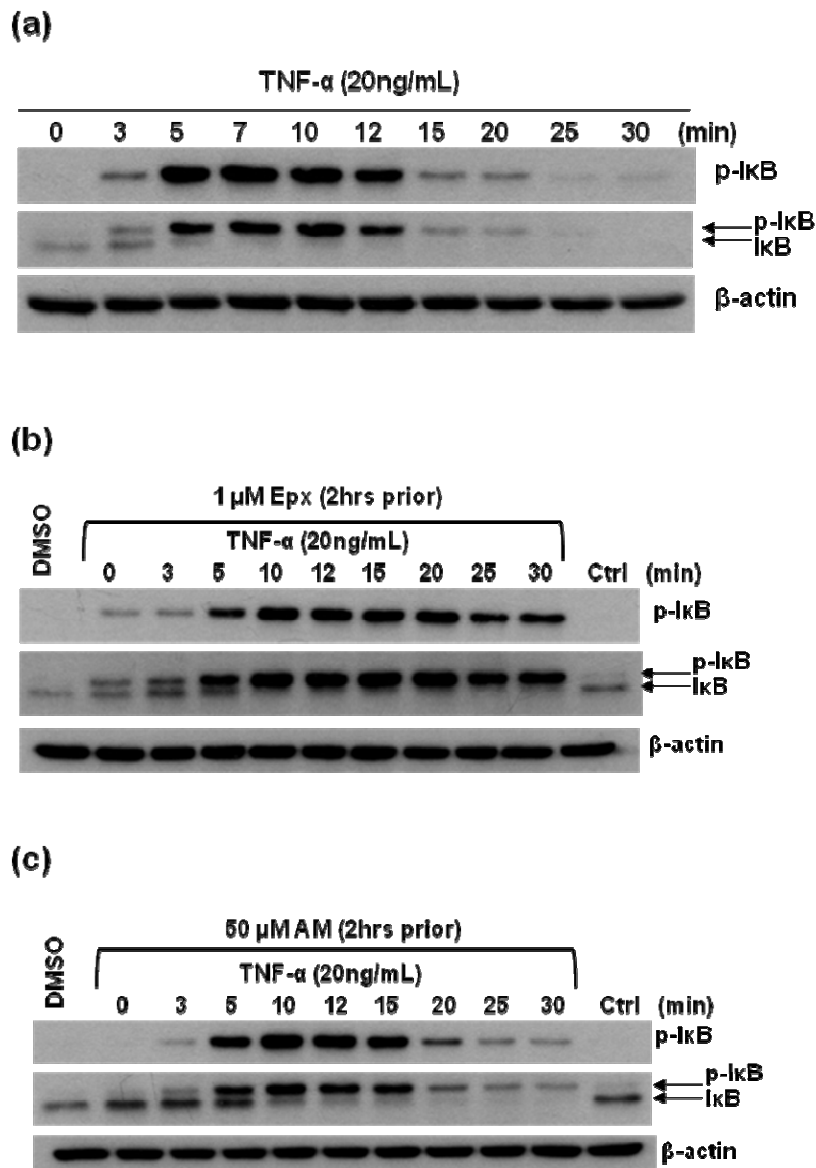


Figure 4.10 The effect of AM on NF κ B activation. **(a)** PC3 cells were treated with TNF- α (20ng/mL) for up to 30 minutes and harvested at the indicated time points. Cell lysates were analyzed for phosphorylated I κ B and I κ B on western blot. Results indicated that the treatment of TNF- α induced the phosphorylation of I κ B in less than 5 minutes and peaked at approximately 10 minutes. The protein is then rapidly degraded by 15 minutes and returned to basal level by 25 minutes. This serves as a control for the following experiments. **(b,c)** PC3 cells were treated with 1 μ M Epx or 50 μ M AM 2 hours prior to the treatment of TNF- α similar to **(a)**. Western blot results indicate that epoxomicin was able to inhibit the phosphorylation of I κ B as shown by the accumulation of phosphorylated I κ B up to 30 minutes. However, AM did not appear to effectively inhibit I κ B phosphorylation as the degradation of phosphorylated I κ B can still be observed starting at 20 minutes of the TNF- α treatment.

F. Conclusions

The investigation of the modes of action of **AM** was essential because not only does it facilitate a better understanding of the biological function of the LMP2 catalytic subunit, but it also help pave the way for validating the potential therapeutic properties of **AM** in the treatment of cancer. The finding that cancers express differential levels of LMP2 and LMP7 catalytic subunits regardless of their tissue of origin was unprecedented (Figure 4.1). It allows for the possibility of developing a personalized cancer treatment utilizing a LMP2-specific inhibitor. Furthermore, this phenomenon and the availability of a LMP2 specific inhibitor can be exploited for the further biological studies of the immunoproteasome.

The compound **AM** was found to selectively target LMP2 not only in the murine lymphoma cell line EL4 (Figure 2.4) but also in the prostate cancer cell line PC3 (Figure 4.2a). **AM** was shown to maintain its LMP2 selectivity in PC3 cells even at concentrations as high as 25 μ M. This high selectivity was further confirmed by the mobility shift assay that also demonstrated the potency of **AM** (Figure 4.2b). In other words, the results suggest that **AM** is not only selective towards the LMP2 subunit but also a more potent LMP2 inhibitor than the biotin-tagged probes in PC3 cells. Furthermore, characterization of the binding properties of **AM** with LMP2 revealed that a dose as low as 0.5 μ M **AM** was sufficient to covalently modify all LMP2 subunits (Figure 4.3a) and the covalent modification of LMP2 by **AM** was maintained for at least 48 hours (Figure 4.3b). It was later demonstrated that the interaction between **AM** and LMP2 is irreversible in PC3 cells, which also revealed that the turnover rate of LMP2 could be more than 48 hours after treatment with **AM**. Finally, the compound **AM** was also shown to be stable in cell culture media, which provided preliminary evidence for the *in vitro* stability of **AM** (Figure 4.4).

While western blot data have clearly demonstrated that the compound **AM** covalently binds to LMP2 irreversibly for up to 48 hours, it is of great interest to determine whether **AM** inhibits the catalytic activity of LMP2 as well. Proteasome kinetic studies was able to verify that the compound **AM** indeed possesses inhibitory activity against the CT-L activity of the LMP2 subunit (Figure 4.5a). Furthermore, the results obtained from the 3D-ECSA confirms that **AM** selectively inhibits the CT-L

activity of the immunoproteasome and not that of the constitutive proteasome. While it is tempting to conclude that **AM** is not cytotoxic to normal cells because it does not target constitutive proteasome, more definitive experiments to directly measure systemic cytotoxicity will be needed. As mentioned earlier, the proteasome inhibitor bortezomib causes severe system cytotoxicity, mainly peripheral neuropathy. For an *in vitro* studies approach, a motor neuronal cell line could be used to evaluate the cytotoxic effects of **AM** treatment on these cells. Some possible experiments to measure *in vivo* systemic cytotoxicity include animal studies by which body weight of mice treated with **AM** is monitored as well as histopathological and genotoxic analysis of multiple organs removed from the animals.

Conversely, **AM** was shown to exhibit a higher anti-proliferative activity in prostate cancer cell lines that highly express the LMP2 subunit (PC3) than prostate cancer cell lines with lower expression levels of LMP2 (LNCaP) (Table 1.). This finding may suggest that **AM** has potential therapeutic properties in prostate cancer cells, but more experiments to render these findings more definitive will be needed. Additional prostate cancer cell lines can be screened for LMP2 expression levels and subjected to similar MTS assays to determine their relative sensitivity towards the anti-proliferative activity of **AM**. Normal non-cancerous prostate cancer cell lines can also be used as another source of LMP2 negative prostate cell lines. The utilization of multiple cell lines will definitely render the results statistically more significant. The correlation between LMP2 levels and the anti-proliferative activity of **AM** can also be investigated using artificial systems. For example, the LMP2 subunit can be artificially knocked down in PC3 cells using siRNAs or induced in LNCaP cells by IFN- γ . These systems may allow for the assessment of the cytotoxicity of **AM** in a different aspect as they eliminate the external influences that can potentially arise from using multiple cancer cell lines. These experiments will definitely facilitate the target validation of the compound **AM**.

In the modes of action studies, the compound **AM** was found to induce G2/M cell cycle arrest after 48 hours in a dose dependent manner (Figure 4.6); it also caused apoptosis in a time and dose dependent manner (Figure 4.7). Similarly, **AM** was also observed to induce apoptosis on a molecular level, causing PARP cleavage in a time and dose dependent manner (Figure 4.8). These results were in agreement with those of the

broad spectrum proteasome inhibitors epoxomicin and **Epn**. Epoxomicin has also been shown previously to inhibit proteolysis and inflammation, but the LMP2 inhibitor **AM** was found to only inhibit proteolysis (Figure 4.9) and not inflammation (Figure 4.10) in PC3 cells. These results indicate that while **AM** inhibits general proteolysis, it does not inhibit the proteolysis that is involved in the activation of NF κ B in PC3 cells. In conclusion, the modes of action studies imply that the immunoproteasome may possess many similar properties as the constitutive proteasome but it may not be involved in the regulation of the NF κ B activation pathway in PC3 cells.

Being the only proteasome inhibitor on the market for chemotherapy, bortezomib is very potent and effective. After five years since it was first approved by FDA for the treatment of relapsed multiple myeloma, it was finally approved as a first line of treatment for multiple myeloma in June 2008. Nevertheless, systemic toxicities remain an issue. While the LMP2 inhibitor has greatly lost its potency compared to bortezomib, it has gained tremendous selectivity towards the LMP2 subunit. The essence of this research project was to develop an immunoproteasome inhibitor that could target cancer that highly express immunoproteasome, resulting in lower toxicities in normal tissues. Nevertheless, the immunoproteasome is still a baffling area in the field of biology. The availability of a LMP2 inhibitor would also help fuel biological studies of the immunoproteasome by serving as a molecular probe. Diseases that were previously shown to over-express immunoproteasomes will benefit as well because **AM** could function as a tool for pathological studies. While it is overreaching to state that **AM** has potential therapeutic properties based on current results, it is definitely a possibility to consider. This novel class of immunoproteasome catalytic subunit inhibitor has been proven to be of significant importance and it is undoubtedly worth exploring further.

G. Future Directions

Given the promising preliminary data obtained thus far, the further development of the LMP2 inhibitor **AM** is inevitable. In fact, *in vivo* studies using prostate cancer mouse models are currently ongoing to determine the tumor growth inhibition as well as toxicities towards normal tissues of **AM** treatment. Preliminary results obtained from the *in vivo* studies suggested that **AM** reduces tumor volume and weight without severe systemic cytotoxicity. This promising data opens up the possibility of allowing the LMP2 inhibitor to be considered as a potential chemotherapeutic agent. Another ongoing project includes the investigation of the immunoproteasome catalytic subunit selectivity of **AM**. Given that the crystal structure of immunoproteasome has yet to be completed, 3D computational molecular modeling was used to examining the selective interaction between LMP2 subunit and **AM**. Preliminary results strongly indicated that the molecular structure of LMP2 favors the binding of **AM** and it is not favorable to the binding of epoxomicin and dihydroeponemycin. In other words, the LMP2 selectivity of **AM** is further substantiated.

Another important future direction of this project is the further target validation of **AM**. While **AM** has been shown to covalently modify LMP2 with high selectivity in comparison to the other proteasome catalytic subunits, its effect on other cellular proteins remains to be determined. Therefore, in order to attempt to establish a causal relationship between **AM** treatment and LMP2 inhibition, multiple orthogonal tools will be utilized to modify the expression level as well as the activity of LMP2 in cancer cells. Specifically, by using LMP2 overexpression and knockdown systems, the relative sensitivity to **AM** can be determined in various cancer cell lines that either expresses high or low levels of LMP2 subunit. Similarly, chemical proteomic approach will be considered as well for the investigation of the downstream effects of LMP2 inhibition by **AM**. Biotinylated **AM** will be synthesized to determine the possible interaction of **AM** with proteins other than LMP2. In addition, chemical proteomic approach such as two dimensional gels will also facilitate the investigation of the effects of **AM** treatment on cellular proteins and their pathways. The accomplishment of these goals will provide substantial confidence in the employment of **AM** in the future investigations that utilize LMP2 inhibition.

H. Methods and Materials

Cell Culture. The human prostate cancer cells, PC3, DU145, and LNCaP; human breast cancer cells, MCF7, MDA-MD-231, and Hs578T; human multiple myeloma cancer cells, RPMI8226 and U266; human non small cell lung cancer cells, H358, H460, and A549; human colon cancer cells, HT29; human cervical cancer cells, HeLa; normal human lung fibroblast, WI-38; and murine lymphoma cells, EL4; were purchased from American Type Culture Collection (Rockville, MD). PC3, MCF7, MDA-MB-231, Hs578T, RPMI8226, U266, H358, H460, A549, HeLa and EL4 cells were cultured in RPMI Media 1640 (Gibco BRL, USA). DU145 was cultured in Dulbecco's Modified Eagle Media (Gibco BRL, USA). HT29 was cultured in McCoy's 5a Media (Gibco BRL, USA). WI-38 was cultured in Minimum Essential Media (Gibco BRL, USA). All media contained 10% heat inactivated fetal bovine serum, 100 U/ml penicillin and 100 mg/ml streptomycin (Gibco BRL, USA) except for U266 cells in which media contained 15% heat inactivated fetal bovine serum. LNCaP was cultured in RPMI Media 1640 containing 10% non heat inactivated fetal bovine serum (ATCC, Manassa, VA) and no antibiotics. All cells were maintained at 37°C in a humidified atmosphere containing 5% CO₂. Inhibitors were dissolved in dimethyl sulfoxide (DMSO) and made into a stock solution of 10mM concentration.

Western Blotting. Whole cell lysates were prepared by incubating cells in non-denaturing lysis buffer (50mM Tris-Cl, 150mM NaCl, 1% NP40, 1% Triton X-100, and 1% protease inhibitor cocktail (Sigma-Aldrich, St. Louis, MO)) on ice for 1 hour. Cells were then centrifuged at 14,000 rpm for 10 min at 4°C (Sorvall Biofuge Primo R, Kendro Laboratory Products, Newtown, CT). Supernatants were collected and subjected to protein assay via method of Bradford using Protein Assay Dye Reagent Concentrate (Bio-Rad, Hercules, CA). Protein concentrations were determined by a GENESYS 10 spectrophotometer, Thermo Spectronic (VWR, Arlington Heights, IL). The supernatants were then added 2x Laemmli Sample Buffer (Sigma-Aldrich) and heated in boiling water for 10 min. Subsequently, the denatured whole cell lysates were resolved by 8%-12% SDS-PAGE and transferred to PVDF membranes (Bio-Rad). Membranes were blocked

with 5% skim milk (Bio-Rad) or BSA (Sigma-Aldrich) for 1 hour at room temperature on the rotator. Appropriate primary and secondary antibodies were used to incubate the membranes for 1 hour at room temperature on the rotator or overnight at 4°C. Finally, Amersham ECL Western Blotting Detection Reagents (GE Healthcare Life Sciences, Pittsburgh, PA) were used to visualize protein of interests on Kodak BioMax XAR Films (Sigma-Aldrich).

Enzyme Kinetic Assay. $k_{\text{association}}$ values were determined as follows. Inhibitors were mixed with a fluorogenic peptide substrate and assay buffer (20 mM Tris (pH 8.0), 0.5 mM EDTA, and 0.035% SDS) in a 96-well plate. The chymotrypsin-like activity was assayed using the fluorogenic peptide substrates Suc-Leu-Leu-Val-Tyr-AMC (Sigma-Aldrich). Hydrolysis was initiated by the addition of bovine 20S proteasomes or immunoproteasomes (Biomol International, Plymouth Meeting, PA), and the reaction was followed by fluorescence detection (360-nm excitation/460-nm detection) using a Microplate Fluorescence Reader (FL600; Bio-Tek Instruments, Inc., Winoski, VT) employing the software KC4 v.2.5 (Bio-Tek Instruments, Inc., Winooski, VT). Reactions were allowed to proceed for 60 - 90 min, and fluorescence data was collected every minute. Fluorescence was quantified as arbitrary units and progression curves were plotted for each reaction as a function of time. $k_{\text{observed}}/[I]$ values were obtained using PRISM software by nonlinear least squares fit of the data to the following equation: $\text{fluorescence} = v_s t + [(v_0 - v_s)/k_{\text{observed}}][1 - \exp(-k_{\text{observed}} t)]$, where v_0 and v_s are the initial and final velocities, respectively, and k_{observed} is the reaction rate constant [189]. The range of inhibitor concentrations tested was chosen so that several half-lives could be observed during the course of the measurement. Reactions were performed using inhibitor concentrations that were <100-fold than that of the proteasome assayed.

3D Endothelial Cell Sprouting Assay. Endothelial cell spheroids were generated from human umbilical vein endothelial cells (HUVECs; Cascade Biologicals, Portland, OR) as described [223]. The spheroids (4-6/well) were distributed in 96-well plates in collagen I matrix for the 3D-ECSA. Cell culture medium was added to each well along with 20 ng/ml VEGF in the presence and absence of the individual inhibitor. The 3D cultures

were incubated in tissue culture chambers at 37°C in 5% CO₂ for 24 h. Photographic images of spheroids were obtained at 10X objective using a Nikon TE2000 microscope. Sprouting was quantified from digital images according to our previously published method [218].

MTS Assay. Cells were seeded on 96-well plates and incubated at 37°C with 5% CO₂ until 70% confluent. The indicated inhibitors were added in increasing concentration and cells were treated for 48 hours. The percentage of cell survival was determined using the MTS reagent, CellTiter 96[®] AQueous One Solution Cell Proliferation Assay (Promega, Madison, WI) following the manufacturer's protocol. Briefly, 20µL of MTS reagent were added to cell samples in 100µl of culture media and incubated for 1 hour at 37°C. Absorbance was recorded at 490nm wavelength on a microplate reader (FL600; Bio-Tek Instruments, Inc., Winooski, VT) using the software KC4 v.2.5 (Bio-Tek Instruments, Inc., Winooski, VT). Cell proliferation was determined as a percentage relative to vehicle treated cells. IC₅₀ values were calculated from sigmoid dose response curves by the method of nonlinear regression to a logarithmic function using PRISM. These data represent the average of three or more experiments.

Flow Cytometry. In order to assess the induction of apoptosis, the Annexin V-FITC Apoptosis Detection Kit (Sigma-Aldrich) was used following the manufacturer's protocol. Briefly, cells were treated with the indicated concentrations of the inhibitors for 24-48 hours. Floating cells were first collected and then combined with adhered cells that were trypsinized and pelleted by centrifuging at 600 g⁻¹ for 10 minutes at 4°C. The cell pellets were washed twice with cold phosphate buffered saline (PBS) and resuspended in 1X Binding Buffer at a concentration of 1 x 10⁶ cells/mL. 500µL of the cell suspension of each sample was transferred into a 12 x 75 mm test tube and 5µL of Annexin V-FITC and 10µL propidium iodide (PI) was added. The cells were then incubated at room temperature for 10 minutes, protected from light, before analysis by flow cytometry (Becton-Dickinson FACScalibur). A minimum of 2x10⁴ cells were analyzed per sample for Annexin V and Propidium Iodide. Viable cells were defined as Annexin-V and PI double negative, while Annexin-V positive and PI negative was defined as apoptotic cells.

Necrotic or late apoptotic cells were defined Annexin-V and PI double positive. These data represent the average of three or more experiments.

Cell cycle analysis was also determined using flow cytometry. Samples were prepared following the protocol in *Current Protocols in Cytometry* [224]. Briefly, cells were treated with the indicated concentrations of the inhibitor for 24-48 hours. Fixatives were prepared by keeping 12 X 75 mm test tubes that contained 4.5 mL of 70% ethanol on ice. Floating cells were first collected and then combined with adhered cells that were trypsinized and pelleted by centrifuging at 200 g^{-1} for 6 minutes at 4°C . Cells were washed with 1mL cold PBS before resuspending in 0.5 mL cold PBS. The single cell suspensions were transferred into the cold 70% ethanol fixatives and incubated for at least 2 hours. Cell suspensions can also be stored in -20°C until ready to be stained. Ethanol suspended cells were centrifuged at 200 g^{-1} for 5 minutes at 4°C and the supernatant was decanted carefully. Cell pellets were resuspended in 1mL cold PBS and centrifuged at 200 g^{-1} for 5 minutes at 4°C a minute later. The final cell pellets were resuspended in 1mL PI/Triton X-100 staining solution with RNase A (2mg DNase-free RNase A (Sigma-Aldrich) and $200\mu\text{L}$ of 1mg/mL PI in 100mL of 0.1% (v/v) Triton X-100 in PBS). The cells were incubated at room temperature for 30 minutes before being analyzed by flow cytometry. A minimum of 1×10^4 cells were analyzed per sample and the DNA histogram was further analyzed using integration software (ModFit LT V2.0, Topsham, MN, USA) for cell cycle analysis.

References:

1. Adams, J., Palombella, V.J., Sausville, E.A., Johnson, J., Destree, A., Lazarus, D.D., Maas, J., Pien, C.S., Prakash, S., and Elliott, P.J. (1999). Proteasome inhibitors: a novel class of potent and effective antitumor agents. *Cancer Res* 59, 2615-2622.
2. An, J., Sun, Y.P., Adams, J., Fisher, M., Belldegrun, A., and Rettig, M.B. (2003). Drug interactions between the proteasome inhibitor bortezomib and cytotoxic chemotherapy, tumor necrosis factor (TNF) alpha, and TNF-related apoptosis-inducing ligand in prostate cancer. *Clin Cancer Res* 9, 4537-4545.
3. Vijay-Kumar, S., Bugg, C.E., Wilkinson, K.D., and Cook, W.J. (1985). Three-dimensional structure of ubiquitin at 2.8 Å resolution. *Proc Natl Acad Sci U S A* 82, 3582-3585.
4. Mani, A., and Gelmann, E.P. (2005). The ubiquitin-proteasome pathway and its role in cancer. *J Clin Oncol* 23, 4776-4789.
5. Chau, V., Tobias, J.W., Bachmair, A., Marriott, D., Ecker, D.J., Gonda, D.K., and Varshavsky, A. (1989). A multiubiquitin chain is confined to specific lysine in a targeted short-lived protein. *Science* 243, 1576-1583.
6. Wilkinson, K.D., and Audhya, T.K. (1981). Stimulation of ATP-dependent proteolysis requires ubiquitin with the COOH-terminal sequence Arg-Gly-Gly. *J Biol Chem* 256, 9235-9241.
7. Pickart, C.M. (1997). Targeting of substrates to the 26S proteasome. *FASEB J* 11, 1055-1066.
8. Pickart, C.M. (2000). Ubiquitin in chains. *Trends Biochem Sci* 25, 544-548.
9. Chastagner, P., Israel, A., and Brou, C. (2006). Itch/AIP4 mediates Deltex degradation through the formation of K29-linked polyubiquitin chains. *EMBO Rep* 7, 1147-1153.
10. Lim, K.L., Dawson, V.L., and Dawson, T.M. (2006). Parkin-mediated lysine 63-linked polyubiquitination: a link to protein inclusions formation in Parkinson's and other conformational diseases? *Neurobiol Aging* 27, 524-529.
11. Pickart, C.M., and Eddins, M.J. (2004). Ubiquitin: structures, functions, mechanisms. *Biochim Biophys Acta* 1695, 55-72.
12. Muller, S., Hoegel, C., Pyrowolakis, G., and Jentsch, S. (2001). SUMO, ubiquitin's mysterious cousin. *Nat Rev Mol Cell Biol* 2, 202-210.
13. Pan, Z.Q., Kentsis, A., Dias, D.C., Yamoah, K., and Wu, K. (2004). Nedd8 on cullin: building an expressway to protein destruction. *Oncogene* 23, 1985-1997.
14. Thrower, J.S., Hoffman, L., Rechsteiner, M., and Pickart, C.M. (2000). Recognition of the polyubiquitin proteolytic signal. *EMBO J* 19, 94-102.
15. Hershko, A., and Ciechanover, A. (1998). The ubiquitin system. *Annu Rev Biochem* 67, 425-479.
16. Haglund, K., and Dikic, I. (2005). Ubiquitylation and cell signaling. *EMBO J* 24, 3353-3359.
17. Di Fiore, P.P., Polo, S., and Hofmann, K. (2003). When ubiquitin meets ubiquitin receptors: a signalling connection. *Nat Rev Mol Cell Biol* 4, 491-497.

18. Hicke, L. (2001). Protein regulation by monoubiquitin. *Nat Rev Mol Cell Biol* 2, 195-201.
19. Passmore, L.A., and Barford, D. (2004). Getting into position: the catalytic mechanisms of protein ubiquitylation. *Biochem J* 379, 513-525.
20. Huang, T.T., and D'Andrea, A.D. (2006). Regulation of DNA repair by ubiquitylation. *Nat Rev Mol Cell Biol* 7, 323-334.
21. Jin, J., Li, X., Gygi, S.P., and Harper, J.W. (2007). Dual E1 activation systems for ubiquitin differentially regulate E2 enzyme charging. *Nature* 447, 1135-1138.
22. Pelzer, C., Kassner, I., Matentzoglou, K., Singh, R.K., Wollscheid, H.P., Scheffner, M., Schmidtke, G., and Groettrup, M. (2007). UBE1L2, a novel E1 enzyme specific for ubiquitin. *J Biol Chem* 282, 23010-23014.
23. McGrath, J.P., Jentsch, S., and Varshavsky, A. (1991). UBA 1: an essential yeast gene encoding ubiquitin-activating enzyme. *EMBO J* 10, 227-236.
24. Hatfield, P.M., and Vierstra, R.D. (1992). Multiple forms of ubiquitin-activating enzyme E1 from wheat. Identification of an essential cysteine by in vitro mutagenesis. *J Biol Chem* 267, 14799-14803.
25. Finley, D., Ciechanover, A., and Varshavsky, A. (1984). Thermolability of ubiquitin-activating enzyme from the mammalian cell cycle mutant ts85. *Cell* 37, 43-55.
26. Ciechanover, A., Finley, D., and Varshavsky, A. (1984). Ubiquitin dependence of selective protein degradation demonstrated in the mammalian cell cycle mutant ts85. *Cell* 37, 57-66.
27. Pickart, C.M. (2004). Back to the future with ubiquitin. *Cell* 116, 181-190.
28. Hochstrasser, M. (1996). Ubiquitin-dependent protein degradation. *Annu Rev Genet* 30, 405-439.
29. von Arnim, A.G. (2001). A hitchhiker's guide to the proteasome. *Sci STKE* 2001, PE2.
30. Sung, P., Prakash, S., and Prakash, L. (1990). Mutation of cysteine-88 in the *Saccharomyces cerevisiae* RAD6 protein abolishes its ubiquitin-conjugating activity and its various biological functions. *Proc Natl Acad Sci U S A* 87, 2695-2699.
31. Wu, P.Y., Hanlon, M., Eddins, M., Tsui, C., Rogers, R.S., Jensen, J.P., Matunis, M.J., Weissman, A.M., Wolberger, C., and Pickart, C.M. (2003). A conserved catalytic residue in the ubiquitin-conjugating enzyme family. *EMBO J* 22, 5241-5250.
32. Pickart, C.M. (2001). Mechanisms underlying ubiquitination. *Annu Rev Biochem* 70, 503-533.
33. Myung, J., Kim, K.B., and Crews, C.M. (2001). The ubiquitin-proteasome pathway and proteasome inhibitors. *Med Res Rev* 21, 245-273.
34. Bachmair, A., Finley, D., and Varshavsky, A. (1986). In vivo half-life of a protein is a function of its amino-terminal residue. *Science* 234, 179-186.
35. Scheffner, M., Huibregtse, J.M., Vierstra, R.D., and Howley, P.M. (1993). The HPV-16 E6 and E6-AP complex functions as a ubiquitin-protein ligase in the ubiquitination of p53. *Cell* 75, 495-505.

36. Huibregtse, J.M., Scheffner, M., Beaudenon, S., and Howley, P.M. (1995). A family of proteins structurally and functionally related to the E6-AP ubiquitin-protein ligase. *Proc Natl Acad Sci U S A* *92*, 2563-2567.
37. Huibregtse, J.M., Yang, J.C., and Beaudenon, S.L. (1997). The large subunit of RNA polymerase II is a substrate of the Rsp5 ubiquitin-protein ligase. *Proc Natl Acad Sci U S A* *94*, 3656-3661.
38. Freemont, P.S. (2000). RING for destruction? *Curr Biol* *10*, R84-87.
39. Honda, R., and Yasuda, H. (2000). Activity of MDM2, a ubiquitin ligase, toward p53 or itself is dependent on the RING finger domain of the ligase. *Oncogene* *19*, 1473-1476.
40. Waterman, H., Levkowitz, G., Alroy, I., and Yarden, Y. (1999). The RING finger of c-Cbl mediates desensitization of the epidermal growth factor receptor. *J Biol Chem* *274*, 22151-22154.
41. Fang, S., Jensen, J.P., Ludwig, R.L., Vousden, K.H., and Weissman, A.M. (2000). Mdm2 is a RING finger-dependent ubiquitin protein ligase for itself and p53. *J Biol Chem* *275*, 8945-8951.
42. Weissman, A.M. (2001). Themes and variations on ubiquitylation. *Nat Rev Mol Cell Biol* *2*, 169-178.
43. Capili, A.D., Schultz, D.C., Rauscher, I.F., and Borden, K.L. (2001). Solution structure of the PHD domain from the KAP-1 corepressor: structural determinants for PHD, RING and LIM zinc-binding domains. *EMBO J* *20*, 165-177.
44. Lu, Z., Xu, S., Joazeiro, C., Cobb, M.H., and Hunter, T. (2002). The PHD domain of MEKK1 acts as an E3 ubiquitin ligase and mediates ubiquitination and degradation of ERK1/2. *Mol Cell* *9*, 945-956.
45. Fang, S., and Weissman, A.M. (2004). A field guide to ubiquitylation. *Cell Mol Life Sci* *61*, 1546-1561.
46. Aravind, L., and Koonin, E.V. (2000). The U box is a modified RING finger - a common domain in ubiquitination. *Curr Biol* *10*, R132-134.
47. Hatakeyama, S., and Nakayama, K.I. (2003). U-box proteins as a new family of ubiquitin ligases. *Biochem Biophys Res Commun* *302*, 635-645.
48. Nijman, S.M., Luna-Vargas, M.P., Velds, A., Brummelkamp, T.R., Dirac, A.M., Sixma, T.K., and Bernards, R. (2005). A genomic and functional inventory of deubiquitinating enzymes. *Cell* *123*, 773-786.
49. Amerik, A., Swaminathan, S., Krantz, B.A., Wilkinson, K.D., and Hochstrasser, M. (1997). In vivo disassembly of free polyubiquitin chains by yeast Ubp14 modulates rates of protein degradation by the proteasome. *EMBO J* *16*, 4826-4838.
50. Peters, J.M., Franke, W.W., and Kleinschmidt, J.A. (1994). Distinct 19 S and 20 S subcomplexes of the 26 S proteasome and their distribution in the nucleus and the cytoplasm. *J Biol Chem* *269*, 7709-7718.
51. Groll, M., Bajorek, M., Kohler, A., Moroder, L., Rubin, D.M., Huber, R., Glickman, M.H., and Finley, D. (2000). A gated channel into the proteasome core particle. *Nat Struct Biol* *7*, 1062-1067.
52. Lam, Y.A., Lawson, T.G., Velayutham, M., Zweier, J.L., and Pickart, C.M. (2002). A proteasomal ATPase subunit recognizes the polyubiquitin degradation signal. *Nature* *416*, 763-767.

53. Deveraux, Q., Ustrell, V., Pickart, C., and Rechsteiner, M. (1994). A 26 S protease subunit that binds ubiquitin conjugates. *J Biol Chem* 269, 7059-7061.
54. Yao, T., and Cohen, R.E. (2002). A cryptic protease couples deubiquitination and degradation by the proteasome. *Nature* 419, 403-407.
55. Koulich, E., Li, X., and Demartino, G.N. (2008). Relative Structural and Functional Roles of Multiple Deubiquitylating Proteins Associated with Mammalian 26S Proteasome. *Mol Biol Cell* 19, 1072-1082.
56. Kohler, A., Cascio, P., Leggett, D.S., Woo, K.M., Goldberg, A.L., and Finley, D. (2001). The axial channel of the proteasome core particle is gated by the Rpt2 ATPase and controls both substrate entry and product release. *Mol Cell* 7, 1143-1152.
57. Smith, D.M., Chang, S.C., Park, S., Finley, D., Cheng, Y., and Goldberg, A.L. (2007). Docking of the proteasomal ATPases' carboxyl termini in the 20S proteasome's alpha ring opens the gate for substrate entry. *Mol Cell* 27, 731-744.
58. Rabl, J., Smith, D.M., Yu, Y., Chang, S.C., Goldberg, A.L., and Cheng, Y. (2008). Mechanism of gate opening in the 20S proteasome by the proteasomal ATPases. *Mol Cell* 30, 360-368.
59. Braun, B.C., Glickman, M., Kraft, R., Dahlmann, B., Kloetzel, P.M., Finley, D., and Schmidt, M. (1999). The base of the proteasome regulatory particle exhibits chaperone-like activity. *Nat Cell Biol* 1, 221-226.
60. Schmidt, M., Hanna, J., Elsasser, S., and Finley, D. (2005). Proteasome-associated proteins: regulation of a proteolytic machine. *Biol Chem* 386, 725-737.
61. Sijts, A., Sun, Y., Janek, K., Kral, S., Paschen, A., Schadendorf, D., and Kloetzel, P.M. (2002). The role of the proteasome activator PA28 in MHC class I antigen processing. *Mol Immunol* 39, 165-169.
62. Rechsteiner, M., and Hill, C.P. (2005). Mobilizing the proteolytic machine: cell biological roles of proteasome activators and inhibitors. *Trends Cell Biol* 15, 27-33.
63. Demartino, G.N., and Gillette, T.G. (2007). Proteasomes: machines for all reasons. *Cell* 129, 659-662.
64. Jager, S., Groll, M., Huber, R., Wolf, D.H., and Heinemeyer, W. (1999). Proteasome beta-type subunits: unequal roles of propeptides in core particle maturation and a hierarchy of active site function. *J Mol Biol* 291, 997-1013.
65. Orłowski, M., Cardozo, C., and Michaud, C. (1993). Evidence for the presence of five distinct proteolytic components in the pituitary multicatalytic proteinase complex. Properties of two components cleaving bonds on the carboxyl side of branched chain and small neutral amino acids. *Biochemistry* 32, 1563-1572.
66. Unno, M., Mizushima, T., Morimoto, Y., Tomisugi, Y., Tanaka, K., Yasuoka, N., and Tsukihara, T. (2002). The structure of the mammalian 20S proteasome at 2.75 Å resolution. *Structure* 10, 609-618.
67. Oinonen, C., and Rouvinen, J. (2000). Structural comparison of Ntn-hydrolases. *Protein Sci* 9, 2329-2337.
68. Seemuller, E., Lupas, A., Stock, D., Lowe, J., Huber, R., and Baumeister, W. (1995). Proteasome from *Thermoplasma acidophilum*: a threonine protease. *Science* 268, 579-582.

69. Lowe, J., Stock, D., Jap, B., Zwickl, P., Baumeister, W., and Huber, R. (1995). Crystal structure of the 20S proteasome from the archaeon *T. acidophilum* at 3.4 Å resolution. *Science* 268, 533-539.
70. Groll, M., Ditzel, L., Lowe, J., Stock, D., Bochtler, M., Bartunik, H.D., and Huber, R. (1997). Structure of 20S proteasome from yeast at 2.4 Å resolution. *Nature* 386, 463-471.
71. Groll, M., Huber, R., and Potts, B.C. (2006). Crystal structures of Salinosporamide A (NPI-0052) and B (NPI-0047) in complex with the 20S proteasome reveal important consequences of beta-lactone ring opening and a mechanism for irreversible binding. *J Am Chem Soc* 128, 5136-5141.
72. Borissenko, L., and Groll, M. (2007). Diversity of proteasomal missions: fine tuning of the immune response. *Biol Chem* 388, 947-955.
73. Akopian, T.N., Kisselev, A.F., and Goldberg, A.L. (1997). Processive degradation of proteins and other catalytic properties of the proteasome from *Thermoplasma acidophilum*. *J Biol Chem* 272, 1791-1798.
74. Kisselev, A.F., Akopian, T.N., Woo, K.M., and Goldberg, A.L. (1999). The sizes of peptides generated from protein by mammalian 26 and 20 S proteasomes. Implications for understanding the degradative mechanism and antigen presentation. *J Biol Chem* 274, 3363-3371.
75. Beninga, J., Rock, K.L., and Goldberg, A.L. (1998). Interferon-gamma can stimulate post-proteasomal trimming of the N terminus of an antigenic peptide by inducing leucine aminopeptidase. *J Biol Chem* 273, 18734-18742.
76. Emmerich, N.P., Nussbaum, A.K., Stevanovic, S., Priemer, M., Toes, R.E., Rammensee, H.G., and Schild, H. (2000). The human 26 S and 20 S proteasomes generate overlapping but different sets of peptide fragments from a model protein substrate. *J Biol Chem* 275, 21140-21148.
77. Dhananjayan, S.C., Ismail, A., and Nawaz, Z. (2005). Ubiquitin and control of transcription. *Essays Biochem* 41, 69-80.
78. Melino, G. (2005). Discovery of the ubiquitin proteasome system and its involvement in apoptosis. *Cell Death Differ* 12, 1155-1157.
79. Lin, A., and Karin, M. (2003). NF-kappaB in cancer: a marked target. *Semin Cancer Biol* 13, 107-114.
80. Rogers, S., Wells, R., and Rechsteiner, M. (1986). Amino acid sequences common to rapidly degraded proteins: the PEST hypothesis. *Science* 234, 364-368.
81. Palombella, V.J., Rando, O.J., Goldberg, A.L., and Maniatis, T. (1994). The ubiquitin-proteasome pathway is required for processing the NF-kappa B1 precursor protein and the activation of NF-kappa B. *Cell* 78, 773-785.
82. Lin, L., and Ghosh, S. (1996). A glycine-rich region in NF-kappaB p105 functions as a processing signal for the generation of the p50 subunit. *Mol Cell Biol* 16, 2248-2254.
83. Liu, C.W., Corboy, M.J., DeMartino, G.N., and Thomas, P.J. (2003). Endoproteolytic activity of the proteasome. *Science* 299, 408-411.
84. Glickman, M.H., and Ciechanover, A. (2002). The ubiquitin-proteasome proteolytic pathway: destruction for the sake of construction. *Physiol Rev* 82, 373-428.

85. Janse, D.M., Crosas, B., Finley, D., and Church, G.M. (2004). Localization to the proteasome is sufficient for degradation. *J Biol Chem* 279, 21415-21420.
86. Murakami, Y., Matsufuji, S., Hayashi, S., Tanahashi, N., and Tanaka, K. (2000). Degradation of ornithine decarboxylase by the 26S proteasome. *Biochem Biophys Res Commun* 267, 1-6.
87. Rock, K.L., Gramm, C., Rothstein, L., Clark, K., Stein, R., Dick, L., Hwang, D., and Goldberg, A.L. (1994). Inhibitors of the proteasome block the degradation of most cell proteins and the generation of peptides presented on MHC class I molecules. *Cell* 78, 761-771.
88. Akiyama, K., Kagawa, S., Tamura, T., Shimbara, N., Takashina, M., Kristensen, P., Hendil, K.B., Tanaka, K., and Ichihara, A. (1994). Replacement of proteasome subunits X and Y by LMP7 and LMP2 induced by interferon-gamma for acquirement of the functional diversity responsible for antigen processing. *FEBS Lett* 343, 85-88.
89. Rammensee, H.G. (1995). Chemistry of peptides associated with MHC class I and class II molecules. *Curr Opin Immunol* 7, 85-96.
90. Rivett, A.J., Bose, S., Brooks, P., and Broadfoot, K.I. (2001). Regulation of proteasome complexes by gamma-interferon and phosphorylation. *Biochimie* 83, 363-366.
91. Murata, S., Udono, H., Tanahashi, N., Hamada, N., Watanabe, K., Adachi, K., Yamano, T., Yui, K., Kobayashi, N., Kasahara, M., Tanaka, K., and Chiba, T. (2001). Immunoproteasome assembly and antigen presentation in mice lacking both PA28alpha and PA28beta. *EMBO J* 20, 5898-5907.
92. Preckel, T., Fung-Leung, W.P., Cai, Z., Vitiello, A., Salter-Cid, L., Winqvist, O., Wolfe, T.G., Von Herrath, M., Angulo, A., Ghazal, P., Lee, J.D., Fourie, A.M., Wu, Y., Pang, J., Ngo, K., Peterson, P.A., Fruh, K., and Yang, Y. (1999). Impaired immunoproteasome assembly and immune responses in PA28^{-/-} mice. *Science* 286, 2162-2165.
93. Van Kaer, L., Ashton-Rickardt, P.G., Eichelberger, M., Gaczynska, M., Nagashima, K., Rock, K.L., Goldberg, A.L., Doherty, P.C., and Tonegawa, S. (1994). Altered peptidase and viral-specific T cell response in LMP2 mutant mice. *Immunity* 1, 533-541.
94. Fehling, H.J., Swat, W., Laplace, C., Kuhn, R., Rajewsky, K., Muller, U., and von Boehmer, H. (1994). MHC class I expression in mice lacking the proteasome subunit LMP-7. *Science* 265, 1234-1237.
95. Basler, M., Moebius, J., Elenich, L., Groettrup, M., and Monaco, J.J. (2006). An altered T cell repertoire in MECL-1-deficient mice. *J Immunol* 176, 6665-6672.
96. Murata, S., Sasaki, K., Kishimoto, T., Niwa, S., Hayashi, H., Takahama, Y., and Tanaka, K. (2007). Regulation of CD8⁺ T cell development by thymus-specific proteasomes. *Science* 316, 1349-1353.
97. Caudill, C.M., Jayarapu, K., Elenich, L., Monaco, J.J., Colbert, R.A., and Griffin, T.A. (2006). T cells lacking immunoproteasome subunits MECL-1 and LMP7 hyperproliferate in response to polyclonal mitogens. *J Immunol* 176, 4075-4082.
98. Hayashi, T., and Faustman, D. (1999). NOD mice are defective in proteasome production and activation of NF-kappaB. *Mol Cell Biol* 19, 8646-8659.

99. Hisamatsu, H., Shimbara, N., Saito, Y., Kristensen, P., Hendil, K.B., Fujiwara, T., Takahashi, E., Tanahashi, N., Tamura, T., Ichihara, A., and Tanaka, K. (1996). Newly identified pair of proteasomal subunits regulated reciprocally by interferon gamma. *J Exp Med* *183*, 1807-1816.
100. Schmidtke, G., Kraft, R., Kostka, S., Henklein, P., Frommel, C., Lowe, J., Huber, R., Kloetzel, P.M., and Schmidt, M. (1996). Analysis of mammalian 20S proteasome biogenesis: the maturation of beta-subunits is an ordered two-step mechanism involving autocatalysis. *EMBO J* *15*, 6887-6898.
101. Chen, P., and Hochstrasser, M. (1996). Autocatalytic subunit processing couples active site formation in the 20S proteasome to completion of assembly. *Cell* *86*, 961-972.
102. Schmidtke, G., Schmidt, M., and Kloetzel, P.M. (1997). Maturation of mammalian 20 S proteasome: purification and characterization of 13 S and 16 S proteasome precursor complexes. *J Mol Biol* *268*, 95-106.
103. Hirano, Y., Hendil, K.B., Yashiroda, H., Iemura, S., Nagane, R., Hioki, Y., Natsume, T., Tanaka, K., and Murata, S. (2005). A heterodimeric complex that promotes the assembly of mammalian 20S proteasomes. *Nature* *437*, 1381-1385.
104. Hirano, Y., Hayashi, H., Iemura, S., Hendil, K.B., Niwa, S., Kishimoto, T., Kasahara, M., Natsume, T., Tanaka, K., and Murata, S. (2006). Cooperation of multiple chaperones required for the assembly of mammalian 20S proteasomes. *Mol Cell* *24*, 977-984.
105. Le Tallec, B., Barrault, M.B., Courbeyrette, R., Guerois, R., Marsolier-Kergoat, M.C., and Peyroche, A. (2007). 20S proteasome assembly is orchestrated by two distinct pairs of chaperones in yeast and in mammals. *Mol Cell* *27*, 660-674.
106. Li, X., Kusmierczyk, A.R., Wong, P., Emili, A., and Hochstrasser, M. (2007). beta-Subunit appendages promote 20S proteasome assembly by overcoming an Ump1-dependent checkpoint. *EMBO J* *26*, 2339-2349.
107. Jayarapu, K., and Griffin, T.A. (2004). Protein-protein interactions among human 20S proteasome subunits and proteasemblin. *Biochem Biophys Res Commun* *314*, 523-528.
108. Frentzel, S., Pesold-Hurt, B., Seelig, A., and Kloetzel, P.M. (1994). 20 S proteasomes are assembled via distinct precursor complexes. Processing of LMP2 and LMP7 proproteins takes place in 13-16 S preproteasome complexes. *J Mol Biol* *236*, 975-981.
109. Fricke, B., Heink, S., Steffen, J., Kloetzel, P.M., and Kruger, E. (2007). The proteasome maturation protein POMP facilitates major steps of 20S proteasome formation at the endoplasmic reticulum. *EMBO Rep* *8*, 1170-1175.
110. Heink, S., Ludwig, D., Kloetzel, P.M., and Kruger, E. (2005). IFN-gamma-induced immune adaptation of the proteasome system is an accelerated and transient response. *Proc Natl Acad Sci U S A* *102*, 9241-9246.
111. Griffin, T.A., Nandi, D., Cruz, M., Fehling, H.J., Kaer, L.V., Monaco, J.J., and Colbert, R.A. (1998). Immunoproteasome assembly: cooperative incorporation of interferon gamma (IFN-gamma)-inducible subunits. *J Exp Med* *187*, 97-104.
112. De, M., Jayarapu, K., Elenich, L., Monaco, J.J., Colbert, R.A., and Griffin, T.A. (2003). Beta 2 subunit propeptides influence cooperative proteasome assembly. *J Biol Chem* *278*, 6153-6159.

113. Kingsbury, D.J., Griffin, T.A., and Colbert, R.A. (2000). Novel propeptide function in 20 S proteasome assembly influences beta subunit composition. *J Biol Chem* 275, 24156-24162.
114. Williams, C.A., Angelman, H., Clayton-Smith, J., Driscoll, D.J., Hendrickson, J.E., Knoll, J.H., Magenis, R.E., Schinzel, A., Wagstaff, J., Whidden, E.M., and et al. (1995). Angelman syndrome: consensus for diagnostic criteria. Angelman Syndrome Foundation. *Am J Med Genet* 56, 237-238.
115. Dindot, S.V., Antalffy, B.A., Bhattacharjee, M.B., and Beaudet, A.L. (2008). The Angelman syndrome ubiquitin ligase localizes to the synapse and nucleus, and maternal deficiency results in abnormal dendritic spine morphology. *Hum Mol Genet* 17, 111-118.
116. Ivan, M., Kondo, K., Yang, H., Kim, W., Valiando, J., Ohh, M., Salic, A., Asara, J.M., Lane, W.S., and Kaelin, W.G., Jr. (2001). HIF α targeted for VHL-mediated destruction by proline hydroxylation: implications for O₂ sensing. *Science* 292, 464-468.
117. Maxwell, P.H., Wiesener, M.S., Chang, G.W., Clifford, S.C., Vaux, E.C., Cockman, M.E., Wykoff, C.C., Pugh, C.W., Maher, E.R., and Ratcliffe, P.J. (1999). The tumour suppressor protein VHL targets hypoxia-inducible factors for oxygen-dependent proteolysis. *Nature* 399, 271-275.
118. Seizinger, B.R., Rouleau, G.A., Ozelius, L.J., Lane, A.H., Farmer, G.E., Lamiell, J.M., Haines, J., Yuen, J.W., Collins, D., Majoor-Krakauer, D., and et al. (1988). Von Hippel-Lindau disease maps to the region of chromosome 3 associated with renal cell carcinoma. *Nature* 332, 268-269.
119. Keinan, E., Schechter, I., and Sela, M. (2004). *Life sciences for the 21st century* (Weinheim: Wiley-VCH).
120. Leach, F.S., Tokino, T., Meltzer, P., Burrell, M., Oliner, J.D., Smith, S., Hill, D.E., Sidransky, D., Kinzler, K.W., and Vogelstein, B. (1993). p53 Mutation and MDM2 amplification in human soft tissue sarcomas. *Cancer Res* 53, 2231-2234.
121. Loda, M., Cukor, B., Tam, S.W., Lavin, P., Fiorentino, M., Draetta, G.F., Jessup, J.M., and Pagano, M. (1997). Increased proteasome-dependent degradation of the cyclin-dependent kinase inhibitor p27 in aggressive colorectal carcinomas. *Nat Med* 3, 231-234.
122. Gstaiger, M., Jordan, R., Lim, M., Catzavelos, C., Mestan, J., Slingerland, J., and Krek, W. (2001). Skp2 is oncogenic and overexpressed in human cancers. *Proc Natl Acad Sci U S A* 98, 5043-5048.
123. Slingerland, J., and Pagano, M. (2000). Regulation of the cdk inhibitor p27 and its deregulation in cancer. *J Cell Physiol* 183, 10-17.
124. Donnellan, R., and Chetty, R. (1999). Cyclin E in human cancers. *FASEB J* 13, 773-780.
125. Strohmaier, H., Spruck, C.H., Kaiser, P., Won, K.A., Sangfelt, O., and Reed, S.I. (2001). Human F-box protein hCdc4 targets cyclin E for proteolysis and is mutated in a breast cancer cell line. *Nature* 413, 316-322.
126. Ho, Y.K., Bargagna-Mohan, P., Wehenkel, M., Mohan, R., Kim, K. B. (2007). LMP2-specific inhibitors: Novel chemical genetic tools for proteasome biology. *Chem Biol* 14, 419-430.

127. Miyoshi, Y., Nagase, H., Ando, H., Horii, A., Ichii, S., Nakatsuru, S., Aoki, T., Miki, Y., Mori, T., and Nakamura, Y. (1992). Somatic mutations of the APC gene in colorectal tumors: mutation cluster region in the APC gene. *Hum Mol Genet* *1*, 229-233.
128. Rubinfeld, B., Souza, B., Albert, I., Muller, O., Chamberlain, S.H., Masiarz, F.R., Munemitsu, S., and Polakis, P. (1993). Association of the APC gene product with beta-catenin. *Science* *262*, 1731-1734.
129. Munemitsu, S., Albert, I., Souza, B., Rubinfeld, B., and Polakis, P. (1995). Regulation of intracellular beta-catenin levels by the adenomatous polyposis coli (APC) tumor-suppressor protein. *Proc Natl Acad Sci U S A* *92*, 3046-3050.
130. Aberle, H., Bauer, A., Stappert, J., Kispert, A., and Kemler, R. (1997). beta-catenin is a target for the ubiquitin-proteasome pathway. *EMBO J* *16*, 3797-3804.
131. Bence, N.F., Sampat, R.M., and Kopito, R.R. (2001). Impairment of the ubiquitin-proteasome system by protein aggregation. *Science* *292*, 1552-1555.
132. Bingol, B., and Schuman, E.M. (2005). Synaptic protein degradation by the ubiquitin proteasome system. *Curr Opin Neurobiol* *15*, 536-541.
133. Mishto, M., Bellavista, E., Santoro, A., Stolzing, A., Ligorio, C., Nacmias, B., Spazzafumo, L., Chiappelli, M., Licastro, F., Sorbi, S., Pession, A., Ohm, T., Grune, T., and Franceschi, C. (2006). Immunoproteasome and LMP2 polymorphism in aged and Alzheimer's disease brains. *Neurobiol Aging* *27*, 54-66.
134. Diaz-Hernandez, M., Hernandez, F., Martin-Aparicio, E., Gomez-Ramos, P., Moran, M.A., Castano, J.G., Ferrer, I., Avila, J., and Lucas, J.J. (2003). Neuronal induction of the immunoproteasome in Huntington's disease. *J Neurosci* *23*, 11653-11661.
135. Zhang, J., Bardos, T., Li, D., Gal, I., Vermes, C., Xu, J., Mikecz, K., Finnegan, A., Lipkowitz, S., and Glant, T.T. (2002). Cutting edge: regulation of T cell activation threshold by CD28 costimulation through targeting Cbl-b for ubiquitination. *J Immunol* *169*, 2236-2240.
136. Wang, J., and Maldonado, M.A. (2006). The ubiquitin-proteasome system and its role in inflammatory and autoimmune diseases. *Cell Mol Immunol* *3*, 255-261.
137. Egerer, T., Martinez-Gamboa, L., Dankof, A., Stuhlmuller, B., Dorner, T., Krenn, V., Egerer, K., Rudolph, P.E., Burmester, G.R., and Feist, E. (2006). Tissue-specific up-regulation of the proteasome subunit beta5i (LMP7) in Sjogren's syndrome. *Arthritis Rheum* *54*, 1501-1508.
138. Sia, C., and Weinem, M. (2005). Genetic susceptibility to type 1 diabetes in the intracellular pathway of antigen processing - a subject review and cross-study comparison. *Rev Diabet Stud* *2*, 40-52.
139. Twombly, R. (2003). First proteasome inhibitor approved for multiple myeloma. *J Natl Cancer Inst* *95*, 845.
140. Kim, K.B., and Crews, C.M. (2004). *Natural Product and Synthetic Proteasome Inhibitors* (Totowa, N.J.: Humana Press).
141. Wilk, S., and Orłowski, M. (1983). Evidence that pituitary cation-sensitive neutral endopeptidase is a multicatalytic protease complex. *J Neurochem* *40*, 842-849.
142. Orłowski, M. (1990). The multicatalytic proteinase complex, a major extralysosomal proteolytic system. *Biochemistry* *29*, 10289-10297.

143. Wilk, S., and Figueiredo-Pereira, M.E. (1993). Synthetic inhibitors of the multicatalytic proteinase complex (proteasome). *Enzyme Protein* 47, 306-313.
144. Bogyo, M., McMaster, J.S., Gaczynska, M., Tortorella, D., Goldberg, A.L., and Ploegh, H. (1997). Covalent modification of the active site threonine of proteasomal beta subunits and the Escherichia coli homolog HslV by a new class of inhibitors. *Proc Natl Acad Sci U S A* 94, 6629-6634.
145. Bromme, D., Klaus, J.L., Okamoto, K., Rasnick, D., and Palmer, J.T. (1996). Peptidyl vinyl sulphones: a new class of potent and selective cysteine protease inhibitors: S2P2 specificity of human cathepsin O2 in comparison with cathepsins S and L. *Biochem J* 315 (Pt 1), 85-89.
146. Palmer, J.T., Rasnick, D., Klaus, J.L., and Bromme, D. (1995). Vinyl sulfones as mechanism-based cysteine protease inhibitors. *J Med Chem* 38, 3193-3196.
147. Kessler, B.M., Tortorella, D., Altun, M., Kisselev, A.F., Fiebiger, E., Hekking, B.G., Ploegh, H.L., and Overkleeft, H.S. (2001). Extended peptide-based inhibitors efficiently target the proteasome and reveal overlapping specificities of the catalytic beta-subunits. *Chem Biol* 8, 913-929.
148. Fevig, J.M., Buriak, J., Jr., Cacciola, J., Alexander, R.S., Kettner, C.A., Knabb, R.M., Pruitt, J.R., Weber, P.C., and Wexler, R.R. (1998). Rational design of boropeptide thrombin inhibitors: beta, beta-dialkyl-phenethylglycine P2 analogs of DuP 714 with greater selectivity over complement factor I and an improved safety profile. *Bioorg Med Chem Lett* 8, 301-306.
149. Adams, J., Behnke, M., Chen, S., Cruickshank, A.A., Dick, L.R., Grenier, L., Klunder, J.M., Ma, Y.T., Plamondon, L., and Stein, R.L. (1998). Potent and selective inhibitors of the proteasome: dipeptidyl boronic acids. *Bioorg Med Chem Lett* 8, 333-338.
150. Adams, J. (2002). Development of the proteasome inhibitor PS-341. *Oncologist* 7, 9-16.
151. Roccaro, A.M., Vacca, A., and Ribatti, D. (2006). Bortezomib in the treatment of cancer. *Recent Patents Anticancer Drug Discov* 1, 397-403.
152. (2005). Bortezomib: new drug. A last resort in myeloma: modest efficacy, major risks. *Prescrire Int* 14, 94-98.
153. (2006). Bortezomib: new indication. Second-line treatment of myeloma: limited efficacy, major risks. *Prescrire Int* 15, 98-100.
154. Chauhan, D., Li, G., Podar, K., Hideshima, T., Mitsiades, C., Schlossman, R., Munshi, N., Richardson, P., Cotter, F.E., and Anderson, K.C. (2004). Targeting mitochondria to overcome conventional and bortezomib/proteasome inhibitor PS-341 resistance in multiple myeloma (MM) cells. *Blood* 104, 2458-2466.
155. Dorsey, B.D., Iqbal, M., Chatterjee, S., Menta, E., Bernardini, R., Bernareggi, A., Cassara, P.G., D'Arasmo, G., Ferretti, E., De Munari, S., Oliva, A., Pezzoni, G., Allievi, C., Streponi, I., Ruggeri, B., Ator, M.A., Williams, M., and Mallamo, J.P. (2008). Discovery of a potent, selective, and orally active proteasome inhibitor for the treatment of cancer. *J Med Chem* 51, 1068-1072.
156. Piva, R., Ruggeri, B., Williams, M., Costa, G., Tamagno, I., Ferrero, D., Gai, V., Coscia, M., Peola, S., Massaia, M., Pezzoni, G., Allievi, C., Pescalli, N., Cassin, M., di Giovine, S., Nicoli, P., de Feudis, P., Streponi, I., Roato, I., Ferracini, R., Bussolati, B., Camussi, G., Jones-Bolin, S., Hunter, K., Zhao, H., Neri, A.,

- Palumbo, A., Berkers, C., Ovaa, H., Bernareggi, A., and Inghirami, G. (2008). CEP-18770: A novel, orally active proteasome inhibitor with a tumor-selective pharmacologic profile competitive with bortezomib. *Blood* *111*, 2765-2775.
157. Omura, S., Fujimoto, T., Otoguro, K., Matsuzaki, K., Moriguchi, R., Tanaka, H., and Sasaki, Y. (1991). Lactacystin, a novel microbial metabolite, induces neuritogenesis of neuroblastoma cells. *J Antibiot (Tokyo)* *44*, 113-116.
158. Dick, L.R., Cruikshank, A.A., Destree, A.T., Grenier, L., McCormack, T.A., Melandri, F.D., Nunes, S.L., Palombella, V.J., Parent, L.A., Plamondon, L., and Stein, R.L. (1997). Mechanistic studies on the inactivation of the proteasome by lactacystin in cultured cells. *J Biol Chem* *272*, 182-188.
159. Dick, L.R., Cruikshank, A.A., Grenier, L., Melandri, F.D., Nunes, S.L., and Stein, R.L. (1996). Mechanistic studies on the inactivation of the proteasome by lactacystin: a central role for clasto-lactacystin beta-lactone. *J Biol Chem* *271*, 7273-7276.
160. Fenteany, G., Standaert, R.F., Lane, W.S., Choi, S., Corey, E.J., and Schreiber, S.L. (1995). Inhibition of proteasome activities and subunit-specific amino-terminal threonine modification by lactacystin. *Science* *268*, 726-731.
161. Ostrowska, H., Wojcik, C., Omura, S., and Worowski, K. (1997). Lactacystin, a specific inhibitor of the proteasome, inhibits human platelet lysosomal cathepsin A-like enzyme. *Biochem Biophys Res Commun* *234*, 729-732.
162. Ostrowska, H., Wojcik, C., Wilk, S., Omura, S., Kozlowski, L., Stoklosa, T., Worowski, K., and Radziwon, P. (2000). Separation of cathepsin A-like enzyme and the proteasome: evidence that lactacystin/beta-lactone is not a specific inhibitor of the proteasome. *Int J Biochem Cell Biol* *32*, 747-757.
163. Feling, R.H., Buchanan, G.O., Mincer, T.J., Kauffman, C.A., Jensen, P.R., and Fenical, W. (2003). Salinosporamide A: a highly cytotoxic proteasome inhibitor from a novel microbial source, a marine bacterium of the new genus salinospira. *Angew Chem Int Ed Engl* *42*, 355-357.
164. Macherla, V.R., Mitchell, S.S., Manam, R.R., Reed, K.A., Chao, T.H., Nicholson, B., Deyanat-Yazdi, G., Mai, B., Jensen, P.R., Fenical, W.F., Neuteboom, S.T., Lam, K.S., Palladino, M.A., and Potts, B.C. (2005). Structure-activity relationship studies of salinosporamide A (NPI-0052), a novel marine derived proteasome inhibitor. *J Med Chem* *48*, 3684-3687.
165. Chauhan, D., Singh, A., Brahmandam, M., Podar, K., Hideshima, T., Richardson, P., Munshi, N., Palladino, M.A., and Anderson, K.C. (2008). Combination of proteasome inhibitors bortezomib and NPI-0052 trigger in vivo synergistic cytotoxicity in multiple myeloma. *Blood* *111*, 1654-1664.
166. Hanada, M., Sugawara, K., Kaneta, K., Toda, S., Nishiyama, Y., Tomita, K., Yamamoto, H., Konishi, M., and Oki, T. (1992). Epoxomicin, a new antitumor agent of microbial origin. *J Antibiot (Tokyo)* *45*, 1746-1752.
167. Sugawara, K., Hatori, M., Nishiyama, Y., Tomita, K., Kamei, H., Konishi, M., and Oki, T. (1990). Eponemycin, a new antibiotic active against B16 melanoma. I. Production, isolation, structure and biological activity. *J Antibiot (Tokyo)* *43*, 8-18.

168. Meng, L., Kwok, B.H., Sin, N., and Crews, C.M. (1999). Eponemycin exerts its antitumor effect through the inhibition of proteasome function. *Cancer Res* 59, 2798-2801.
169. Sin, N., Kim, K.B., Eloffsson, M., Meng, L., Auth, H., Kwok, B.H., and Crews, C.M. (1999). Total synthesis of the potent proteasome inhibitor epoxomicin: a useful tool for understanding proteasome biology. *Bioorg Med Chem Lett* 9, 2283-2288.
170. Groll, M., Kim, K.B., Kairies, N., Huber, R., and Crews, C.M. (2000). Crystal Structure of Epoxomicin:20S Proteasome Reveals a Molecular Basis for Selectivity of alpha',beta'-Epoxyketone Proteasome Inhibitors. *J. Am. Chem. Soc.* 122, 1237-1238.
171. Koguchi, Y., Kohno, J., Suzuki, S., Nishio, M., Takahashi, K., Ohnuki, T., and Komatsubara, S. (2000). TMC-86A, B and TMC-96, new proteasome inhibitors from *Streptomyces* sp. TC 1084 and *Saccharothrix* sp. TC 1094. II. Physico-chemical properties and structure determination. *J Antibiot (Tokyo)* 53, 63-65.
172. Demo, S.D., Kirk, C.J., Aujay, M.A., Buchholz, T.J., Dajee, M., Ho, M.N., Jiang, J., Laidig, G.J., Lewis, E.R., Parlati, F., Shenk, K.D., Smyth, M.S., Sun, C.M., Vallone, M.K., Woo, T.M., Molineaux, C.J., and Bennett, M.K. (2007). Antitumor activity of PR-171, a novel irreversible inhibitor of the proteasome. *Cancer Res* 67, 6383-6391.
173. Koguchi, Y., Kohno, J., Nishio, M., Takahashi, K., Okuda, T., Ohnuki, T., and Komatsubara, S. (2000). TMC-95A, B, C, and D, novel proteasome inhibitors produced by *Apiospora montagnei* Sacc. TC 1093. Taxonomy, production, isolation, and biological activities. *J Antibiot (Tokyo)* 53, 105-109.
174. Kohno, J., Koguchi, Y., Nishio, M., Nakao, K., Kuroda, M., Shimizu, R., Ohnuki, T., and Komatsubara, S. (2000). Structures of TMC-95A-D: novel proteasome inhibitors from *Apiospora montagnei* sacc. TC 1093. *J Org Chem* 65, 990-995.
175. Groll, M., Koguchi, Y., Huber, R., and Kohno, J. (2001). Crystal structure of the 20 S proteasome:TMC-95A complex: a non-covalent proteasome inhibitor. *J Mol Biol* 311, 543-548.
176. Basse, N., Piguel, S., Papapostolou, D., Ferrier-Berthelot, A., Richy, N., Pagano, M., Sarthou, P., Sobczak-Thepot, J., Reboud-Ravaux, M., and Vidal, J. (2007). Linear TMC-95-based proteasome inhibitors. *J Med Chem* 50, 2842-2850.
177. Sekizawa, R., Momose, I., Kinoshita, N., Naganawa, H., Hamada, M., Muraoka, Y., Iinuma, H., and Takeuchi, T. (2001). Isolation and structural determination of phepropeptins A, B, C, and D, new proteasome inhibitors, produced by *Streptomyces* sp. *J Antibiot (Tokyo)* 54, 874-881.
178. Chen, D., Daniel, K.G., Kuhn, D.J., Kazi, A., Bhuiyan, M., Li, L., Wang, Z., Wan, S.B., Lam, W.H., Chan, T.H., and Dou, Q.P. (2004). Green tea and tea polyphenols in cancer prevention. *Front Biosci* 9, 2618-2631.
179. Nam, S., Smith, D.M., and Dou, Q.P. (2001). Ester bond-containing tea polyphenols potently inhibit proteasome activity in vitro and in vivo. *J Biol Chem* 276, 13322-13330.
180. Chen, D., Daniel, K.G., Chen, M.S., Kuhn, D.J., Landis-Piwowar, K.R., and Dou, Q.P. (2005). Dietary flavonoids as proteasome inhibitors and apoptosis inducers in human leukemia cells. *Biochem Pharmacol* 69, 1421-1432.

181. Kazi, A., Daniel, K.G., Smith, D.M., Kumar, N.B., and Dou, Q.P. (2003). Inhibition of the proteasome activity, a novel mechanism associated with the tumor cell apoptosis-inducing ability of genistein. *Biochem Pharmacol* 66, 965-976.
182. Yang, H., Chen, D., Cui, Q.C., Yuan, X., and Dou, Q.P. (2006). Celastrol, a triterpene extracted from the Chinese "Thunder of God Vine," is a potent proteasome inhibitor and suppresses human prostate cancer growth in nude mice. *Cancer Res* 66, 4758-4765.
183. Yang, H., Shi, G., and Dou, Q.P. (2007). The tumor proteasome is a primary target for the natural anticancer compound Withaferin A isolated from "Indian winter cherry". *Mol Pharmacol* 71, 426-437.
184. Loidl, G., Groll, M., Musiol, H.J., Ditzel, L., Huber, R., and Moroder, L. (1999). Bifunctional inhibitors of the trypsin-like activity of eukaryotic proteasomes. *Chem Biol* 6, 197-204.
185. Loidl, G., Groll, M., Musiol, H.J., Huber, R., and Moroder, L. (1999). Bivalency as a principle for proteasome inhibition. *Proc Natl Acad Sci U S A* 96, 5418-5422.
186. Nazif, T., and Bogyo, M. (2001). Global analysis of proteasomal substrate specificity using positional-scanning libraries of covalent inhibitors. *Proc Natl Acad Sci U S A* 98, 2967-2972.
187. Baldisserotto, A., Marastoni, M., Trapella, C., Gavioli, R., Ferretti, V., Pretto, L., and Tomatis, R. (2007). Glutamine vinyl ester proteasome inhibitors selective for trypsin-like (beta2) subunit. *Eur J Med Chem* 42, 586-592.
188. Marastoni, M., Baldisserotto, A., Cellini, S., Gavioli, R., and Tomatis, R. (2005). Peptidyl vinyl ester derivatives: new class of selective inhibitors of proteasome trypsin-like activity. *J Med Chem* 48, 5038-5042.
189. Myung, J., Kim, K.B., Lindsten, K., Dantuma, N.P., and Crews, C.M. (2001). Lack of proteasome active site allostery as revealed by subunit-specific inhibitors. *Mol Cell* 7, 411-420.
190. van Swieten, P.F., Samuel, E., Hernandez, R.O., van den Nieuwendijk, A.M., Leeuwenburgh, M.A., van der Marel, G.A., Kessler, B.M., Overkleeft, H.S., and Kisselev, A.F. (2007). A cell-permeable inhibitor and activity-based probe for the caspase-like activity of the proteasome. *Bioorg Med Chem Lett* 17, 3402-3405.
191. Lim, H.S., Archer, C.T., and Kodadek, T. (2007). Identification of a peptoid inhibitor of the proteasome 19S regulatory particle. *J Am Chem Soc* 129, 7750-7751.
192. Lim, H.S., Cai, D., Archer, C.T., and Kodadek, T. (2007). Periodate-triggered cross-linking reveals Sug2/Rpt4 as the molecular target of a peptoid inhibitor of the 19S proteasome regulatory particle. *J Am Chem Soc* 129, 12936-12937.
193. Lim, H.S., Archer, C.T., Kim, Y.C., Hutchens, T., and Kodadek, T. (2008). Rapid identification of the pharmacophore in a peptoid inhibitor of the proteasome regulatory particle. *Chem Commun (Camb)*, 1064-1066.
194. Schulze, K., Mulder, A., Tinazli, A., and Tampe, R. (2006). Controlling the activity of the 20S proteasome complex by synthetic gatekeepers. *Angew Chem Int Ed Engl* 45, 5702-5705.

195. Sprangers, R., Li, X., Mao, X., Rubinstein, J.L., Schimmer, A.D., and Kay, L.E. (2008). TROSY-based NMR evidence for a novel class of 20S proteasome inhibitors. *Biochemistry* *47*, 6727-6734.
196. Verma, R., Peters, N.R., D'Onofrio, M., Tochtrop, G.P., Sakamoto, K.M., Varadan, R., Zhang, M., Coffino, P., Fushman, D., Deshaies, R.J., and King, R.W. (2004). Ubistatins inhibit proteasome-dependent degradation by binding the ubiquitin chain. *Science* *306*, 117-120.
197. Vassilev, L.T. (2004). Small-molecule antagonists of p53-MDM2 binding: research tools and potential therapeutics. *Cell Cycle* *3*, 419-421.
198. Vassilev, L.T., Vu, B.T., Graves, B., Carvajal, D., Podlaski, F., Filipovic, Z., Kong, N., Kammlott, U., Lukacs, C., Klein, C., Fotouhi, N., and Liu, E.A. (2004). In vivo activation of the p53 pathway by small-molecule antagonists of MDM2. *Science* *303*, 844-848.
199. Shangary, S., Qin, D., McEachern, D., Liu, M., Miller, R.S., Qiu, S., Nikolovska-Coleska, Z., Ding, K., Wang, G., Chen, J., Bernard, D., Zhang, J., Lu, Y., Gu, Q., Shah, R.B., Pienta, K.J., Ling, X., Kang, S., Guo, M., Sun, Y., Yang, D., and Wang, S. (2008). Temporal activation of p53 by a specific MDM2 inhibitor is selectively toxic to tumors and leads to complete tumor growth inhibition. *Proc Natl Acad Sci U S A* *105*, 3933-3938.
200. Yang, Y., Kitagaki, J., Dai, R.M., Tsai, Y.C., Lorick, K.L., Ludwig, R.L., Pierre, S.A., Jensen, J.P., Davydov, I.V., Oberoi, P., Li, C.C., Kenten, J.H., Beutler, J.A., Vousden, K.H., and Weissman, A.M. (2007). Inhibitors of ubiquitin-activating enzyme (E1), a new class of potential cancer therapeutics. *Cancer Res* *67*, 9472-9481.
201. Orłowski, R., and Orłowski, M. (2006). Potent and specific immunoproteasome inhibitors (U.S.P. Application, ed.).
202. Sadaghiani, A.M., Verhelst, S.H., and Bogoy, M. (2007). Tagging and detection strategies for activity-based proteomics. *Curr Opin Chem Biol* *11*, 20-28.
203. Berkers, C.R., van Leeuwen, F.W., Groothuis, T.A., Peperzak, V., van Tilburg, E.W., Borst, J., Neeffjes, J.J., and Ovaa, H. (2007). Profiling proteasome activity in tissue with fluorescent probes. *Mol Pharm* *4*, 739-748.
204. Verdoes, M., Florea, B.I., Menendez-Benito, V., Maynard, C.J., Witte, M.D., van der Linden, W.A., van den Nieuwendijk, A.M., Hofmann, T., Berkers, C.R., van Leeuwen, F.W., Groothuis, T.A., Leeuwenburgh, M.A., Ovaa, H., Neeffjes, J.J., Filippov, D.V., van der Marel, G.A., Dantuma, N.P., and Overkleeft, H.S. (2006). A fluorescent broad-spectrum proteasome inhibitor for labeling proteasomes in vitro and in vivo. *Chem Biol* *13*, 1217-1226.
205. Verdoes, M., Hillaert, U., Florea, B.I., Sae-Heng, M., Risseuw, M.D., Filippov, D.V., van der Marel, G.A., and Overkleeft, H.S. (2007). Acetylene functionalized BODIPY dyes and their application in the synthesis of activity based proteasome probes. *Bioorg Med Chem Lett* *17*, 6169-6171.
206. Berkers, C.R., Verdoes, M., Lichtman, E., Fiebiger, E., Kessler, B.M., Anderson, K.C., Ploegh, H.L., Ovaa, H., and Galardy, P.J. (2005). Activity probe for in vivo profiling of the specificity of proteasome inhibitor bortezomib. *Nat Methods* *2*, 357-362.

207. Sin, N., Meng, L., Auth, H., and Crews, C.M. (1998). Eponemycin analogues: syntheses and use as probes of angiogenesis. *Bioorg Med Chem* 6, 1209-1217.
208. Kim, K.B., Myung, J., Sin, N., and Crews, C.M. (1999). Proteasome inhibition by the natural products epoxomicin and dihydroeponemycin: insights into specificity and potency. *Bioorg Med Chem Lett* 9, 3335-3340.
209. Bogoyo, M., Shin, S., McMaster, J.S., and Ploegh, H.L. (1998). Substrate binding and sequence preference of the proteasome revealed by active-site-directed affinity probes. *Chem Biol* 5, 307-320.
210. Ho, A., Cyrus, K., Kim, K. B. (2005). Towards Immunoproteasome-Specific Inhibitors: An Improved Synthesis of Dihydroeponemycin. *Eur. J. Org. Chem.*, 4829-4834.
211. Meng, L., Mohan, R., Kwok, B.H., Elofsson, M., Sin, N., and Crews, C.M. (1999). Epoxomicin, a potent and selective proteasome inhibitor, exhibits in vivo antiinflammatory activity. *Proc Natl Acad Sci U S A* 96, 10403-10408.
212. Imajoh-Ohmi, S., Kawaguchi, T., Sugiyama, S., Tanaka, K., Omura, S., and Kikuchi, H. (1995). Lactacystin, a specific inhibitor of the proteasome, induces apoptosis in human monoblast U937 cells. *Biochem Biophys Res Commun* 217, 1070-1077.
213. Kim, K.B., and Ho, Y.K. (2008). Epoxyketone-Based Immunoproteasome Inhibitors. In <http://patft.uspto.gov/> (U.P.T. Office, ed.).
214. Codony-Servat, J., Tapia, M.A., Bosch, M., Oliva, C., Domingo-Domenech, J., Mellado, B., Rolfe, M., Ross, J.S., Gascon, P., Rovira, A., and Albanell, J. (2006). Differential cellular and molecular effects of bortezomib, a proteasome inhibitor, in human breast cancer cells. *Mol Cancer Ther* 5, 665-675.
215. Salzmann, U., Kral, S., Braun, B., Standera, S., Schmidt, M., Kloetzel, P.M., and Sijts, A. (1999). Mutational analysis of subunit i beta2 (MECL-1) demonstrates conservation of cleavage specificity between yeast and mammalian proteasomes. *FEBS Lett* 454, 11-15.
216. Cardozo, C., and Kohanski, R.A. (1998). Altered properties of the branched chain amino acid-preferring activity contribute to increased cleavages after branched chain residues by the "immunoproteasome". *J Biol Chem* 273, 16764-16770.
217. Craiu, A., Gaczynska, M., Akopian, T., Gramm, C.F., Fenteany, G., Goldberg, A.L., and Rock, K.L. (1997). Lactacystin and clasto-lactacystin beta-lactone modify multiple proteasome beta-subunits and inhibit intracellular protein degradation and major histocompatibility complex class I antigen presentation. *J Biol Chem* 272, 13437-13445.
218. Mohan, R., Hammers, H. J., Bargagna-Mohan, P., Zhan, X. H., Herbstritt, C. J., Ruiz, A., Zhang, L., Hanson, A. D., Conner, B. P., Rougas, J., Pribluda, V. S. (2004). Withaferin A is a potent inhibitor of angiogenesis. *Angiogenesis* 7, 115-122.
219. Korff, T., and Augustin, H.G. (1998). Integration of endothelial cells in multicellular spheroids prevents apoptosis and induces differentiation. *J Cell Biol* 143, 1341-1352.
220. Boulares, A.H., Yakovlev, A.G., Ivanova, V., Stoica, B.A., Wang, G., Iyer, S., and Smulson, M. (1999). Role of poly(ADP-ribose) polymerase (PARP) cleavage

- in apoptosis. Caspase 3-resistant PARP mutant increases rates of apoptosis in transfected cells. *J Biol Chem* 274, 22932-22940.
221. McConkey, D.J., and Zhu, K. (2008). Mechanisms of proteasome inhibitor action and resistance in cancer. *Drug Resist Updat*.
 222. Hayashi, T., and Faustman, D. (2000). The role of the proteasome in autoimmunity. *Diabetes Metab Res Rev* 16, 325-337.
 223. Bargagna-Mohan, P., Ravindranath, P.P., Mohan, R. (2006). Small molecule anti-angiogenic probes of the ubiquitin proteasome pathway: potential application to choroidal neovascularization. *Invest Ophthalmol Vis Sci* 47, 4138-4145.
 224. (2007). *Current Protocols in Cytometry* (John Wiley and Sons, Inc).

VITA
Yik Khuan Ho

Birth

September 29, 1981
Petaling Jaya, Selangor. Malaysia.

Education

University of Kentucky
Bachelor of Science in Biology and minor in Chemistry
2000-2003

Professional Positions

University of Kentucky
Undergraduate Research Assistant
Sept 2002 – July 2003

University of Kentucky
Pharmaceutical Sciences Summer Research Program
Summer Undergraduate Intern
Summer 2002

University of Kentucky
Student research technician
Mar 2001 – May 2002

Scholastic and Professional Honors

Rho Chi Honor Society, Member since 2006

magna cum laude, University of Kentucky, 2003

Biology Departmental Honors, University of Kentucky, 2003

Golden Key International Honor Society, Member since 2002

University of Kentucky Dean Lists, 2000-2003

Metropolitan College Dean's List, Spring 2000

Professional Publications

Wehenkel, M.; **Ho, Y.K.**; and Kim, K.B. Proteasome Inhibitors: Recent Progress and Future Directions, a book chapter for "Modulation of Protein Stability in Cancer Therapy" edited by Dr. Kathleen Sakamoto and Dr. Eric Rubin, Cancer Research, Springer Science. In Press. 2008

Bargagna-Mohan, P.; Hamza, A.; Kim, Y.E.; **Ho, Y.K.**; Mor-vaknin, N.; Wendschlag, N.; Liu, J.; Evans, R.M.; Markovitz, D.M.; Zhan, C.; Kim, K.B. and Mohan, R. The Tumor Inhibitor and Anti-angiogenic Agent Withaferin A Targets the Intermediate Filament Protein Vimentin. *Chem. Biol.* 2007 June; 14 (6):623-634

Ho, Y.K.; Bargagna-Mohan, P.; Wehenkel, M.; Mohan, R. and Kim, K.B. LMP2-Specific Inhibitors: Novel Chemical Genetic Tools for Proteasome Biology. *Chem. Biol.* 2007 Apr; 14 (4):419-430.

Ho, A.; Kim, Y.E.; Lee, H.; Cyrus, K.; Baek, S.H. and Kim, K.B. SAR Studies of 2-Methoxyestradiol and Development of its Analogs as Probes of Anti-tumor Mechanism. *Bioorg. Med. Chem. Lett.* 2006 Jul 1;16 (13):3383-7

Ho, A.; Cyrus, K.; and Kim, K.B. Towards Immunoproteasome-Specific Inhibitors: An Improved Synthesis of Dihydroeponemycin. *Eur. J. Org. Chem.* 2005 22:4829-4832.

Zhang, D.; Baek, S.H.; Ho, A. and Kim, K.B. Degradation of Target Protein in Living Cells by Small-Molecule Proteolysis Inducer. *Bioorg. Med. Chem. Lett.* 2004 Feb 9;14(3):645-8.

Zhang, D.; Baek, S.H.; **Ho, A.**; Lee, H.; Jeong, Y.S. and Kim, K.B. Targeted Degradation of Proteins by Small Molecules: A Novel Tool for Functional Proteomics. *Comb. Chem. High Throughput Screen.* 2004 Nov; 7(7):689-97.